THE EFFECTS OF DIFFERENT FORMS OF PROSTATE-SPECIFIC ANTIGEN ON PROSTATE CANCER CELL INVASION

BY

ANDREW PHILIP CUMMING

A Thesis
Submitted to the Faculty of Biology
in Partial Fulfillment of the Requirements
for the Degree of

MASTER OF SCIENCE

Department of Biology
Lakehead University
Thunder Bay, ON

May, 2005

Your file Votre référence
ISBN: 978-0-494-31823-2
Our file Notre référence
ISBN: 978-0-494-31823-2

Table of Contents

List of Figures

List of Tables

Acknowledgments

I would like to first thank my supervisor, Dr. Helga Duivenvoorden, for her mentorship during the thesis process. Her understanding and patience has allowed me the independence I needed to fully take in the field of prostate cancer biology. She was tolerant of my barrage of questions in the beginning of my studies and was tremendously helpful in the writing of this thesis, even through missed deadlines and "minor" revisions.

The advice and guidance of my co-supervisor Dr. John Th'ng was also vital to my graduate studies at Lakehead University. His understanding of molecular biology and DNA manipulation – as well as his lab supplies! – was indispensable in the creation of the plasmids used in this study. I would also like to thank the counselling from my thesis committee members Dr. Kam Leung and Dr. David Law, especially since the thesis could still have used some work when it was defended.

Everyone in the lab was wonderfully generous with his or her time and help. Thanks to Dr. Mary-Lynn Tassotto (and Bucko!) for lending an ear, Dr. Ingeborg Zehbe for making me feel like part of the team, Rucy Vergidis for helping me work as long as possible, Christina Richard for her friendship and advice, Kyle "Veggie" Cullingham, Lindsay "Linner" Sutherland, Mel "Melaheney" Heney, Correne "Med or bust" DeCarlo, Sean "Maskman" Bryan, Marlon "Smell smell" Hagerty, Roos "Love stricken" Kleinendorst, Taylor "Mr.B" Bureyko, and Donald "Red bull" Matthews.

Most of all, thanks to my fiancé Jen Potter, for simply EVERYTHING, especially putting up with all I could ever ask someone to put up with and still take me in with loving arms. And lastly, to our ecstatic bundle of furry energy, Griffin, who is always happy to see me and brighten my day.

Abstract

Prostate cancer (PCa) is one of the most common cancers in males around the world. Prostate-specific antigen (PSA) is a serine protease that is secreted at high levels by prostate epithelial cells and most prostate cancer cells. It is thought that this enzyme is involved in prostate cancer cell invasion. This study aimed to test the effects of enzymatically active PSA and inactive forms of PSA on prostate cancer cell invasion. PSA is transcribed with a 17 amino acid secretory "pre" sequence and a 7 amino acid latency-conferring "pro" sequence. A deletion mutant lacking the "pro" region of the full-length preproPSA gene was used to create the prePSA gene, in the hopes that enzymatically active PSA would be formed upon cleavage of the "pre" sequence. Full length preproPSA cDNA and prePSA cDNA were each inserted into plasmids that allowed for inducible expression of the PSA genes under the control of the insect hormone derivative, ponasterone A (PonA). DU-145 subclones were created with the ability to inducibly produce preproPSA (DU-pERV3 C3 ppPSA) and prePSA (DU-pERV3 C3 prePSA). The growth properties, migratory abilities, and invasiveness of these cells were assayed. The same properties were tested with exogenous active PSA added to DU-145 cells. Exogenous PSA induced little change in growth, invasion or migration. However, there was a slight decrease in the invasion of DU-145 cells when using commercially isolated enzymatically active PSA. DU-pERV3 C3 ppPSA transfected cells showed increased invasion compared to control cells. Conversely, DU-pERV3 C3 prePSA transfected cells showed decreased invasion and migration compared to control cells. This study suggests that active PSA decreases the invasiveness of DU-145 cells, whereas the inactive zymogen form increases cellular invasion.

Abbreviations

aa	- amino acid
α-Mac	- α2-macroglobulin
ACT	- α_1-antichymotrypsin
ActPSA	- Active PSA
AMF	- Autocrine motility factor
AR	- Androgen receptor
BM	- Basement membrane
BME	- Basement membrane extract
BPH	- Benign prostatic hyperplasia
CAF	- Cancer-associated fibroblast
CD44	- Cluster of differentiation 44
cDNA	- Complimentary DNA
cdk	- Cyclin-dependent kinase
CL	- Cell lysate
CM	- Conditioned medium
CMV	- Cytomegalovirus
DHT	- 5α-dihydrotestosterone
DNA	- Deoxyribonucleic acid
ECM	- Extracellular matrix
EDTA	- Ethylenediaminetetraacetic acid
EGF	- Epidermal growth factor
EHS	- Engelbreth-Holm-Swarm
EMT	- Epithelial to mesenchymal transition
FAK	- Focal adhesion kinase
FBS	- Foetal bovine serum
FGF	- Fibroblast growth factor
GF	- Growth factor
GSTP1	- Glutathione S-transferase P1
HA	- Hyaluronan
HGF	- Hepatocyte growth factor
hK	- Human kallikrein
IGF	- Insulin-like growth factor
IGF-R	- Insulin-like growth factor receptor
IGFBP	- Insulin-like growth factor binding protein
IL	- Interleukin
KGF	- Keratinocyte growth factor
MAPK	- Mitogen activated protein kinase
MCS	- Multiple-cloning site
MEM	- Minimum essential medium
MMP	- Matrix metalloproteinases
NB	- Nuclei buffer
NGF	- Nerve growth factor
PAI	- Plasminogen activator inhibitor
PAR	- Protease-activated receptor

PBS	- Phosphate buffered saline
PCa	- Prostate cancer
PCR	- Polymerase chain reaction
PDT	- Population-doubling time
PIN	- Prostatic intraepithelial neoplasia
PMSF	- Phenylmethylsulphonyl fluoride
PonA	- Ponasterone A
ppPSA	- preproPSA
PSA	- Prostate-specific antigen
PTEN	- Phosphatase and tensin homologue
RFU	- Relative fluorescence units
RLU	- Relative luminescence units
RNA	- Ribonucleic acid
ROCK	- Ras associated kinase
ROS	- Reactive oxygen species
SDS	- Sodium dodecyl sulphate
SEM	- Standard error of the mean
Serpin	- Serine protease inhibitor
SF	- Serum-free
TBE	- Tris, boric acid, EDTA
TBST	- Tris buffered saline with tween 20
TE	- Tris buffered EDTA
TGF-β	- Transforming growth factor β
TGF-βR	- Transforming growth factor β receptor
TIMP	- Tissue inhibitor of metalloproteinases
TNE	- Tris sodium chloride EDTA
TNM	- Tumour, (lymph)nodes, metastases
TPCK	- Tosyl phenylalanyl chloromethyl ketone
uPA	- Urokinase plasminogen activator
uPAR	- Urokinase plasminogen activator receptor

Introduction

1 Prostate cancer

Prostate cancer (PCa) is one of the most frequent cancers to occur in men in North America and is a leading cause of cancer death in the United States[1]. It is estimated that in the US alone, there will be over 230,000 new cases of PCa and over 27,000 people will die due to the disease in 2006[2]. It is a disease of the elderly, and over 70% of PCa diagnosed in the US is in men over the age of sixty-five[3]. By the time it is diagnosed, about three out of every four men positive for PCa show signs of invasive or metastatic disease[4]. Tumour metastasis and invasion is responsible for the majority of morbidity and mortality, and metastatic disease of the prostate is currently incurable[5]. An understanding of the biology of the development and progression of PCa is important in understanding the disease.

1.1 Prostate biology

The prostate is a walnut sized organ in the male through which the urethra passes. It is located inferior to the bladder and anterior to the rectum and is divided into three major zones: the peripheral zone, the central zone, and the transition zone[6]. The vas deferens and the seminal vesicles join the urethra in the prostate and this sexual gland functions to add secretions to seminal plasma to form an ejaculate[7]. These secretions contain acid phosphatases, zinc, magnesium, albumin, and prostate-specific antigen (PSA)[8]. Following ejaculation, the seminal fluid quickly forms a gel encasing the spermatozoa[9]. There is strong evidence that the function of the prostatic secretions is to aid in the lysis of this gel over time through the actions of proteases[9].

The interior structure of the prostate consists of branching acinar ducts that converge towards the urethra. The epithelial cells that line the ducts include secretory cells in contact with the lumen and basal cells which are thought to be precursors of secretory cells[10]. Other cells present may include lymphocytes and stromal cells such as fibroblasts, and muscle cells[10]. Both epithelial and stromal prostate cell growth and function is largely controlled by the androgen testosterone, which is mainly produced by the testis[11]. It is converted intracellularly to 5α-dihydrotestosterone (DHT) by the enzyme 5-α reductase[7,12]. DHT is then available to bind to the cytoplasmic androgen receptor (AR), which translocates into the nucleus, where the complex acts as a transcriptional activator[7]. Other androgens can also bind to the AR and induce similar effects. The AR has been implicated in the upregulation of transcription genes involved in the cell cycle, such as cyclin-dependent kinases 2 (cdk2) and 4 (cdk4) – both involved in advancing the cell cycle – as well as upregulation of growth factors, such as keratinocyte growth factor (KGF)[13]. However, the activated AR complex also promotes differentiation in epithelial cells, and so plays a dual regulatory role on growth activation and inhibition[14]. In addition to the influence of androgens in prostate growth, differentiation and function are the effects of peptide growth factors as well as cytokines. Together they form a complex network of growth/inhibition interactions[13]. For example, epidermal growth factor (EGF) acts as a mitogen for epithelial prostate cells, whereas transforming growth factor β (TGF-β) acts as an antagonist for positive growth factors[15]. Furthermore, there are also complex interactions between different cell types in the prostate, as stromal cells produce androgen-induced growth factors (andromedins) that can affect epithelial cells[14]. During normal prostate growth, androgens such as testosterone function to suppress many andromedin-stimulating effects on epithelial cells, putting androgens at the forefront in control of growth and differentiation of these duct lining cells[14].

1.2 Development of prostate cancer

Over 95% of prostate cancers originate from the epithelial cells that line the acinar ducts of the prostate[1], and can thus be classified as adenocarcinomas[8]. More than 80% of cancers originate in the peripheral zone of the prostate[16], which constitutes about ¾ of the volume of the prostate. This is clinically important, as it is the transition zone where most benign prostatic hyperplasia (BPH)[8] – a common syndrome associated with an enlarged prostate – arise, however, only a small fraction of cancers originate in the transition zone. One of the first signs of PCa is thought to be prostatic intraepithelial neoplasia (PIN)[17]. PIN refers to morphological changes of epithelial cells in the acinar ducts that precede PCa, such as irregular cell spacing and nuclear enlargement[18].

The initial molecular changes that are associated with PCa are less clear and appear to be heterogeneous in origin. Under normal conditions, effects of growth factors produced by the stromal cells on epithelial cells are kept in check by direct androgen stimulation of the epithelial cells. However, this process becomes dysregulated in prostate tumourigenesis, and PCa cell growth can be stimulated by the effects of both androgens and growth factors[14]. Upregulation of growth factor receptors and down regulation of the androgen receptor are common themes in PCa[14]. One common mutation suspected to be carcinogenic in the prostate is "loss-of-function" mutations in the glutathione S-transferase P1 (GSTP1) protein – an enzyme responsible for metabolizing reactive oxygen species[19]. Another genetic alteration that may initiate PCa is a copy number increase of the c-Myc proto-oncoprotein, a transcriptional activator involved in cell proliferation and transformation[19]. Amplification of c-Myc is seen in 40% of primary prostate cancers[19].

1.3 Prostate cancer progression and androgen independence

PCa progresses in similar ways to many other adenocarcinomas. Briefly, the tumour attracts a blood supply, cells detach from the tumour and invade the surrounding tissue, and finally, tumour cells metastasize to distant organs[5]. Many genetic changes in PCa cells have been associated with cancer progression. Functional deletions of the phosphatase and tensin homologue (PTEN) protein – an inhibitor of the phosphatidylinositol-3-kinase signalling pathway – are frequent in late stage and metastatic prostate cancers[14,19], leading to increased invasiveness[20]. Furthermore, deleterious mutations in the p53 sequence – a tumour suppressor protein whose function is lost in numerous cancers – are frequently observed in late stage tumours and in metastases[19], most likely allowing for widespread unregulated changes in genomic DNA.

Androgen independence is another key factor in PCa progression. For PCa cells to extend their growth to regions outside of the prostate with lower concentrations of testosterone, they must reduce their dependence on this hormone for growth. As well, decreasing effects of androgens on PCa cells reduces their inhibitory and differentiation-inducing properties. There are multiple means by which PCa cells can become androgen independent; through hypersensitivity to androgens by increasing the amount of AR, mutations that allow the AR to recognize non-androgen steroids, or by using an alternative growth pathway that bypasses the androgen dependence through signalling cross-talk[12]. As one example, defects in autocrine production or changes in cellular response to TGF-β1 can allow cells to proliferate in an uncontrolled manner regardless of androgen availability[4]. Another specific means for PCa cells to become androgen independent is by upregulating the AR-binding protein CBP, which allows other steroids than androgens the activate the AR[21]. The evolved mechanisms to prevent the need for androgens are numerous and are a large obstacle in the development of new treatment options for PCa patients.

1.4 Screening and staging of prostate cancer

There are several methods to screen patients for PCa. Examination of the prostate can be done either by ultrasound or a digital rectal exam, where prostate enlargement is the main indicator for abnormality[1]. However, this method can confuse PCa with BPH, a non-malignant condition that is also associated with an enlarged prostate. In addition to direct examination, the level of PSA in the patient's serum can be used as a diagnostic indicator. PSA is almost exclusively produced by the prostate, and measuring levels of this protein in the bloodstream can be predictive of cancer[22]. This method will be described at length in section 3.5.

Prostate biopsies are used to diagnose and grade prostate cancer. Tumours are graded using the Gleason score and staged using the TNM levels, each an indication of the progression of the tumour. The Gleason score uses the levels of differentiation of particular glandular patterns with low levels of differentiation correlating with higher Gleason scores and poorer prognosis[1]. TNM stages are common criteria used to stage cancers, and refer to the size, spread and aggressiveness of the tumour[1].

1.5 Treatment of prostate cancer

The treatment of a PCa patient depends largely on the stage, grade, and localization of the cancer. Localized PCa is much easier to treat than metastasized cancer. Prostatectomy is one option where the whole prostate gland is removed by surgery. It is most effective in patients with localized disease[1]. Radiation therapy is also an option, where an external ionizing radiation beam is used to irradiate and kill the cancerous cells without the removal of the prostate gland[23]. However, there is always the risk of adverse effects to non-cancerous cells when using ionizing radiation[24].

Another method of PCa treatment is androgen deprivation. Since the growth of prostate epithelial cells is largely driven by the androgen hormone testosterone, one option is to castrate the patient – removing the main source of testosterone production in the body – and another is to treat with anti-androgens, such as bicalutamide[12]. More advanced cancers will frequently develop androgen independence in which case these methods are ineffective. In hormone-refractory prostate cancer, taxanes (such as docetaxel) may also be used[12]. These drugs are able to promote cell death through microtubule over-stabilization and/or reducing anti-apoptotic abilities of Bcl-2[12]. Bisphosponates (e.g. zoledronic acid) are used to palliatively treat patients with bone metastasis by reducing bone resorption[12]. As there is a lack of effective treatments of PCa in the advanced stages of disease, it is important to understand the mechanisms by which this disease progresses.

2 Cellular invasion in prostate cancer

Cancer cell invasion is an important event in cancer progression. Malignant tumours differ from their benign counterparts in that they are able to override the growth and localization restraints of their environment and disrupt normal tissue[25]. In order for this to occur, cells from the tumour must invade the surrounding tissue, frequently altering normal physiological functions for the benefit of the cancer[26]. The mechanisms of tumour invasion are complex and different pathways of action can lead to the same invasive consequence. Tissue invasion requires cell adhesion, migration and proteolytic activity. For cells to become invasive they can mimic regular physiological functions that normal non-cancerous cells would not have, such as degrading the extracellular matrix (ECM)[27]. Cancer cells must also interact with their surrounding tissue, involving cell-cell contact, cell-ECM contact and secreted molecular factors[27]. Another key change for invasiveness is that the tumour cells must become motile, as they need to physically move into the surrounding tissue to invade it[26]. Many of the molecular factors involved in invasion of prostate cancer have been elucidated.

2.1 Stromal involvement in prostate cancer invasion

Cells located in the tumour stroma can have effects on cancer invasion. Cancer-associated fibroblasts (CAFs) have been shown to be involved in prostate cancer[28], especially myofibroblasts[29]. CAFs can assist PCa invasion by secreting growth factors and in degrading the ECM through the release of extracellular proteases, and the same is true for cancer-associated macrophages[29]. Myofibroblasts, as well as tumour cells, can be activated to become invasive by high levels of fibroblast growth factor-2 (FGF-2) and hepatocyte growth factor (HGF). Both growth factors (GFs) are found at higher levels in

PCa tissue as compared to normal tissue[29]. N-cadherin is also found upregulated in invasive PCa cells, most likely allowing for greater cell-cell interaction between cancer and stromal cells[30].

In PCa with very reactive stroma, the amount of interstitial collagen in the ECM is increased, but the collagen forms less organized structures[29]. PCa tissue has also been found to have high levels of fibronectin, and the PCa cell line DU-145 shows an increase in invasiveness in an *in vitro* invasion assay using plasma fibronectin as a chemoattractant, showing a probable involvement of this protein in promoting invasion[29]. As well, high levels of hyaluronan (HA) have been found in association with advanced prostate cancer[31]. Although PCa cells will normally adhere to HA, decreasing motility by maintaining cellular contact with the ECM, the hyaluronan/matrix metaloproteinase-9 (MMP-9) receptor CD44 is found downregulated in advanced PCa cells[31]. It reasons that this aids the prostate cancer cells in motility. While HA hydrates the stroma, making for a motility-enhancing surface, a decrease in CD44 may mean that the cells do not strongly adhere to HA as they migrate[31].

2.2 The basement membrane and prostate cancer cell attachment

The normal prostate epithelial basement membrane (BM) contains many ubiquitous components, such as collagen IV, laminins, and proteoglycans, but also more specific BM molecules, such as tenascin, laminin-10 and vitronectin[32]. Studies have shown that there appears to be an increasing loss of basal lamina with higher level Gleason grade of the tumour[33]. Not only is the BM decreased in PCa, but also some components that form hemidesmosomes are altered upon PCa cell conversion to an invasive phenotype.

Changes in cell-cell receptors (cadherins) as well as cell-ECM receptors (integrins) are prominent in the progression of PCa cells. As PCa progresses, the contributors to normal hemidesmosome formation, namely $\alpha6\beta4$ integrin (laminin-5 receptor)[33], laminin-5[30,32], collagen VII[32], $\beta1$ integrins[32], and E-cadherin[30], are all found at notably decreased levels. This can lead to a loss of both cell-cell interactions of the epithelia as well as a lower affinity to the BM, allowing cells to escape migratory constraints. Expression of E-cadherin is lost in the metastatic PCa cell lines LNCaP and PC-3[30] and the $\alpha1\beta1$ integrin (a collagen IV receptor) is lost in invasive PCa[32]. This further supports the importance of the loss of these adhesion molecules in PCa progression.

However, not all adhesion proteins are decreased in prostate cancer. It has been shown that the integrins found most often and at the highest levels in PCa are $\alpha3\beta1$ and $\alpha6\beta1$, the major integrin receptors for laminin-10[32]. Although it could be suspected that this would act to hold cells more tightly to the prostate BM, these integrins may also allow PCa cells to adapt to new surroundings. Both the stroma of the surrounding muscle tissue of prostate and of bone marrow matrix (a common site for PCa metastasis) are high in laminin-10[32], which implies that integrins $\alpha3\beta1$ and $\alpha6\beta1$ may help PCa cells survive in these environments.

2.3 The proteases of invasive prostate cancer

PCa cells must degrade their surrounding barriers – especially that of the BM – in order to invade adjacent tissue. Multiple protease systems have been found to be involved in PCa invasion.

2.3.1 The plasminogen activation system

The plasminogen activation system functions as a proteolytic cascade, wherein urokinase plasminogen activator (uPA) cleaves the zymogen plasminogen to obtain the enzymatically active plasmin[34]. Plasmin is a wide specificity protease that can activate many other proteases including MMPs, leading to a process responsible for degrading most components of the ECM, including those of the BM[34]. Other components of the plasminogen activation system include the cell surface uPA receptor (uPAR) and the two uPA serpin inhibitors, plasminogen activator inhibitor-1 (PAI-1) and PAI-2[34,35].

uPA bound to uPAR is involved in PCa cell adhesion and mitogenic signals[36] and both are often found upregulated in PCa[36]. As well, the PCa cell line LNCaP has been shown to bind and activate latent exogenous uPA on its surface, and cell lines that produce their own uPA, such as DU-145 and PC3, are able to use uPA in an autocrine manner[36]. As the surface activity of uPA increases in these cell lines through binding the uPAR, so does the *in vitro* invasive capability to pass through a BM-like barrier[36].

2.3.2 Matrix metalloproteinases

Another family of proteases involved in PCa invasion are the matrix metalloproteinases. There are at least 24 Zn^{+2} dependent MMPs in humans[37] and in total they are capable of degrading nearly all known components of the ECM[38]. The MMPs are a family of Zn^{+2} and/or Ca^{+2}-dependent endopeptidases that are secreted as zymogens[37]. Their activation can occur via auto-proteolysis or by specific proteases such as plasmin[37] as well as other MMPs[39], a process that can progress in cascades. MMP activity is also controlled by the protease inhibitor α-macroglobulin (α-Mac) and tissue inhibitors of metalloproteinases (TIMPs)[40]. The MMP family is transcriptionally regulated by growth factors (GFs), hormones, and cytokines and their production is controlled by cell differentiation and transformation[40]. The main physiological role of MMPs is in tissue morphogenesis, tissue repair and angiogenesis, but they also are involved in diseases, such as rheumatoid arthritis, autoimmune blistering disorders of skin, and cancer[38]. MMPs are able to have a regulatory effect on the tumour's microenvironment, and almost all invasive cancers have some form of upregulated MMP expression and activation[41]. As well as secreted by cancer cells, many MMPs can be synthesized by stromal cells, and cancer cells can secrete factors that enhance stromal cells to transcribe and/or activate MMPs and vice versa[38,39]. *In vivo*, certain MMPs are expressed at the edge of the invasive front of the tumours[39]. However, the functions of MMPs are complex and often redundant, and so their role in tumour progression is not always clear; MMPs may be beneficial to cancers at some stages and detrimental at other times[25].

The main MMPs associated with PCa are MMP-2, -7 and -9[38] which are secreted not only by tumour cells, but also by the monocytes/macrophages present in the stroma and stromal fibroblasts[42]. Increased MMP-2[38,42] and MMP-9[42] protein levels are associated with disease progression in PCa. In breast carcinomas and melanomas, MMP-2 and MMP-9 activity is localized to the periphery of invading tumours at the areas of stromal interaction, while no activity was found in the tumour interior[25]. MMP-2 and MMP-9 are hypothesized to be required for cells to penetrate the BM, as they are efficient at degrading collagens IV and VII[38] as well as laminin and nidogen[39]. In the interstitial ECM, MMPs are essential in degrading gelatin, the product of degraded fibrilar collagens[38]. In support of the involvement of MMPs in PCa invasion, is the finding that TIMP-1 levels are lower in high-grade PCa tissue samples than both normal tissue and more differentiated PCa[42]. There is also a correlation of high uPA levels with those of MMP-2 and MMP-9[43]. In conclusion, one proposed proteolytic mechanism of PCa invasion via uPA is the initial cleavage of latent TGF-β and/or EGF, which in turn can lead to an increase in both uPA and PAI-1 followed by MMP-9 activation with corresponding BM degradation and cell migration[43].

2.3.3 Kallikreins

Another group of proteases that normal prostate epithelial cells secrete and may be involved in cancer are the human kallikrein (hK) serine proteases. hKs are a family of 15 homologous single chain serine endopeptidases, ranging in size from 25 to 30 kDa. They are all located on the same gene locus, and some cancers have been shown to aberrantly express as many as twelve of these hKs at the same time. All hKs are expressed in zymogen form and are activated upon cleavage and removal of their inhibitory pro-peptide. Various serine protease inhibitors, such as serine protease inhibitors (serpins) and α-Mac can inhibit their activity. Glandular epithelial cells mainly express these kallikreins and only a few of their physiological purposes have been elucidated, such as hK3 cleaving semenogelin to increase sperm motility. In cancer, many hKs are improperly regulated; they are increased in some cancers, such as ovarian cancer while downregulated in breast and prostate cancer[44].

In PCa, the kallikreins hK2, hK3 (also known as PSA), hK4 and hK15, are present to varying degrees[44]. PSA is most well known as a serum marker for prostate cancer. Its inhibition in the PCa cell line LNCaP using monoclonal antibodies against the active site[45] or Zn^{+2} as a proteolytic inhibitor[46] yields decreased invasive ability through a simulated BM *in vitro*. Furthermore, PC-3 cells transfected with either PSA or hK4 show a morphological change similar to epithelial to mesenchymal transition (EMT, as discussed in the following section) as shown by molecular signs of the transformation such as loss of E-cadherin and gain of N-cadherin[47]. However, decreases in both hK2 and PSA levels are correlated with malignant tumours[44], so their role is unclear.

2.4 Prostate cancer cell migration

Cell motility is needed by invading cancer cells to physically migrate through tissues. This can include moving from an epithelial layer through to the interstitial ECM, or to migrate into another tissue area. Cell migration happens through four main steps: protrusion, adhesion, translocation and retraction[48]. The molecular pathways controlling cancer cell migration are similar to non-cancer cell migration, as regularly performed by immune cells and fibroblasts[48]. Integrins are important in cell migration, as signalling pathways resulting from integrin binding can lead to increases in cellular migration[49]. Cells are able to move by reorganizing their actin cytoskeleton through polymerization, which helps in forming filopodia by pushing out the membrane, and – by de-polymerization – releasing the cells at their trailing edge[48]. The directionality of migration is often along gradients of certain chemical factors, such as along an ECM component gradient (haptotaxis) or towards soluble components (chemotaxis)[50]. In response to this gradient, actin polymerization occurs in the area where chemo-attractant receptors are activated, polarizing the cells[26]. Some motility-inducing factors present in the ECM include vitronectin, fibronectin, laminin, collagens I and IV[27]. Other motility factors include secreted factors released from stromal cells, such as histamine, insulin-like growth factor-I (IGF-I) and interleukin-8 (IL-8), as well as cancer-cell secreted autocrine motility factors (AMFs), such as IGF-II and autotaxin[27]. To follow these chemical gradients, there are three main mechanisms that cancer cells can use to migrate: mesenchymal, amoeboid, and collective migration. Within a given tumour, any combination of these three types of motilities can be present[48].

Cell migration in PCa can be activated by many soluble factors, such as AMFs, excess EGF receptor, as well as growth factors TGF-β, nerve growth factor (NGF), HGF and IGF[51]. Certain integrins appear to be involved in PCa motility. The PCa cell line DU-H – a DU-145 sub line selected for high α6 integrin expression – show a greater degree of mobility on laminin substrates as well as elevated *in vivo* invasive ability compared to the low α6 integrin expressing sub cell line, DU-L[51]. As well, levels of both Src kinase and focal adhesion kinase (FAK) – proteins involved in relaying integrin signalling from the cell surface – are elevated in more aggressive PCa[49]. Signal transduction activated by these proteins is correlated to an increase in PCa cell migration through Rac/Raf/MAPK signalling[49]. Expression of various *ras* genes – connected to relaying signals from growth factor receptors – have also been linked to advanced prostate cancer, and upon transfection into low-motility PCa cell lines, increase cell migration[51]. As well, inhibitors of Ras-associated kinase (ROCK) – a signalling protein associated with amoeboid motility – are able to decrease the amount of cellular migration in the PC-3 cell line using an *in vivo* migration assay[52]. This is further supported by a decrease in myosin phosphorylation[52]. Higher expression of some cell surface receptors results in lower PCa cell motility. Overexpression of the hyaluronan binding receptor CD44 correlates with decreased motility[51], and decreased expression of the cell-cell binding protein E-cadherin in rat PCa cell lines increases an invasive phenotype[51]. As each CD44 and E-cadherin immobilize cells by attaching to their respective ligands, lower levels of these adhesion proteins could allow for increases in motility.

EMT may also be involved in prostate cancer invasion, as this process provides epithelial cells with a phenotype and mobility similar to that of mobile mesenchymal cells. To initiate EMT, the signalling proteins Rac and Cdc42 – once activated by surface tyrosine kinases such as c-met[26] and various integrins[53] – begin the reorganization of the actin skeleton at the front of cell migration towards a chemotactic gradient[48]. Cells employing a mesenchymal mode of motility use focal adhesion points – with integrins as anchors to the ECM – to lead the migration[26]. One facet of EMT is increased expression of N-cadherin with decreased expression of E-cadherin induced by factors such as TGF-β[54]. Since E-cadherin induces cell-cell interaction with neighbouring epithelial cells and N-cadherin induces cell-cell interaction with stromal cells, this can assist migration of epithelially arisen PCa by allowing cells to decrease epithelial interactions and increase interaction with stromal cells[54]. EMT has also been induced in the PC-3 cell line by transfection with either PSA or hK4[47].

2.5 Growth factor involvement in prostate cancer invasion

GFs can be in an inactive state in the ECM[55] and can be secreted by either cells of the immune system, stroma, or the tumour cells themselves[25]. GFs are important for tumour invasion in many ways. Once a cancer becomes invasive, signals induced by ligand-receptor binding can initiate pathways for cell migration, enzyme degradation, and self-activation. Mutations in the receptors of these ligands can permanently activate positive signalling pathways for invasion[56]. Conversely, other mutations can turn off inhibitory signalling systems that would normally arrest cancer cell invasion[56]. Two important growth factors involved in modulating PCa cell invasiveness are TGF-β and IGF.

2.5.1 TGF-β in prostate cancer invasion

The transforming growth factor-β family consists of TGF-β1, 2 and 3; each elicit similar biological effects, but differ in their tissue-specific expression patterns[57]. The growth factors bind to TGF-β receptor I (TGF-βRI) and TGF-βRII, each of which are serine/threonine kinases that transmit signals into the cell mainly through the downstream Smad family of signalling proteins[57]. TGF-β can be secreted by fibroblasts, immune cells, and cancer cells alike[56]. It can be found in the ECM in an inactive form associated with proteins in a latency-conferring complex, and becomes activated upon proteolytic cleavage[55].

Under normal physiological circumstances, TGF-β is involved in restricting epithelial cell proliferation and differentiation[57], however, malignant cancer cells can become immune to inhibitory effects[53]. In the early stages of cancer progression, TGF-β can inhibit cancer cell growth, induce apoptosis[44], and downregulate MMPs[39]. However, in later stage cancers TGF-β is often upregulated[57]. Tumour promoting mutations in Smad proteins can lead to alterations in receptor-ligand signalling, helping cells to avoid suppressive effects[57]. TGF-β can also assist in stimulating EMT[53], giving cells a migratory phenotype[54]. This change is orchestrated through Ras and Smad signalling via the TGF-β receptor as well as through interactions with some integrins[53]. Furthermore, TGF-β also has the ability to attract fibroblasts[25,53] as well as regulate autotaxin secretion in cancer cells[27]. Additionally, it was found that latent TGF-β can be activated by MMP-

2 and MMP-9[58]. TGF-β can stimulate stromal cells to produce and secrete increased levels of ECM molecules, which could act as a barrier to cancer invasion[57]. However, some MMPs can cleave ECM molecules in such a way that cryptic migratory inducing domains are revealed, thus activating cancer cell migration instead of acting as barrier[57]. TGF-β seems to have a pleiotropic role in cancer invasion, as it is beneficial or detrimental to tumour cells at different times in cancer progression[28].

In PCa invasion, TGF-β appears to play an important role. The loss of the TGF-β type II receptor in tumour fibroblasts – decreasing this receptor's regulatory effects – as well as an increase in TGF-β levels in the prostate have given rise to invasiveness in PCa[25] and correlates with a negative clinical outcome[59]. PCa can become resistant to TGF-β inhibition while still gaining increased invasiveness[59]. PCa cells are able to subvert the inhibitory effects of TGF-β by either altering TGF-β receptor/Smad expression or mutations in signalling partners, including downstream signallers[59]. These mechanisms are also suspected of helping PCa cells to gain androgen independence[59], as stimulating signals from TGF-β may replace those needed for growth in PCa cells as they invade tissues outside of the prostate.

2.5.2 IGF in prostate cancer invasion

There are two types of insulin-like growth factors (IGF-I and IGF-II) with corresponding cellular receptors for each (IGF-IR and IGF-IIR), as well as six extracellular binding proteins (IGFBP-1 to IGFBP-6) which can bind and capture IGF-I and IGF-II extracellularly[60]. IGF-I binding to IGF-IR on the cell surface stimulates PI3K[61], Akt kinase[60], and MAPK[61], promoting survival, migration and invasion[60]. IGF-I binding to IGF-IR can also turn on expression of MMP-2, MMP-9 and MTI-MMP in cell lines developed from lung carcinoma, leading to increased invasive potential by cleaving BM proteins collagen IV and gelatin[60]. IGFBPs, although known mostly for their role in sequestering IGFs, can have other modes of action. IGFBP-2, for example, has been linked to the progression of cancer through upregulation of invasion-related genes, such as MMP-2, although the mechanism by which this happens is unknown[60].

In serum of PCa patients, increased levels of IGF-I are observed[61] and this GF has been shown to be important to PCa invasion in a number of ways. It can induce activation of the androgen receptor in the absence of androgens, thought to occur through a cross-talk between IGF-IR and androgen receptor pathways[61] and may allow PCa cells to become androgen-independent and migrate into areas with lower androgen concentrations. Furthermore, IGF-IR activation leads to an increase in both MMP-2 and uPAR production in PCa cell lines[61]. As well, the IGF-IR is found highly expressed in advanced prostate cancer cells[62]. Regarding the IGF binding proteins, IGFBP-2 is upregulated in over 90% of prostate cancers[60], promoting an invasive phenotype through such means as MMP-2 upregulation. Furthermore, PSA and hK2 are each able to cleave IGFBP-3[44], simultaneously abolishing the intrinsic anti-proliferative and apoptotic effects of this IGF binding protein, while at the same time freeing IGF-I[60]. Finally, IGF produced by stromal cells can act as a chemotactic factor for PCa cells, encouraging the invasion of surrounding tissue[27].

3 Prostate-specific antigen

PSA was originally discovered as a forensic marker for sex crimes as it was a highly produced male-specific protein in seminal plasma[63]. In the 1980's, PSA was confirmed as a serum marker for prostate cancer[64]. Although it is a useful serum marker for prostate cancer, it is not very specific and its role in PCa biology and progression has not been fully elucidated.

3.1 Biology of PSA

PSA is a serine proteinase of the human kallikrein family, with a calculated molecular weight of 28.4 kDa[65]. The gene encoding PSA, *klk3*, is located on chromosome 19q13.4 next to 15 other members of the kallikrein family[66]. The transcription of *klk3* is controlled by the androgen/androgen receptor binding to androgen-responsive elements to activate the promoter of the gene[66]. PSA is translated as 261 amino acid (aa) prepro zymogen with a single N-linked glycosylation on Asp-45[67]. The 17 aa signal peptide (pre-domain) is cleaved off upon transport into the extracellular environment. The resulting pro-PSA is the latent form of the PSA enzyme, which has to be activated extracellularly by proteolytic cleavage of the pro domain to give the 237 aa enzymatically active enzyme[66].

This enzyme is true to its name, as prostate-specific antigen is expressed at levels in the prostate 1,000-fold that of any other bodily fluid[68]. In the prostate lumen, PSA levels are in the 10 – 50 μM (~0.3 – 1.8 mg/ml) range where it occurs mainly in its enzymatically mature form[69]. In seminal plasma, PSA is found at very high concentrations still mainly in the enzymatically active form, in concentrations ranging from 0.5 – 2.0 mg/ml[70]. Human seminal fluid contains at least five different PSA isoforms, including two that are enzymatically active and three that inactive, nicked forms[71].

3.2 Regulation of PSA enzymatic activity

There are four different regulatory mechanisms for proteolytic activity of PSA[69]. First, PSA is secreted as zymogen, and needs cleavage of its N-terminal pro-region for activation. Once activated, binding of divalent cations to allosteric regions, internal proteolytic cleavage of mature PSA, or binding to protease inhibitors can all abate the enzymatic activity of PSA.

3.2.1 Activators of zymogen PSA

Removal of the pro-region of the PSA zymogen can be achieved through trypsin-like proteolytic cleavage. This enzymatic specificity is demonstrated by the fact that trypsin is able to activate PSA[72]. Cleavage of the enzymatically inhibitory pro-peptide of PSA can be also accomplished by at least four other human kallikreins. The trypsin-like serine protease hK2 was the first protease found to cleave the pro-peptide and activate PSA[73]. This enzyme is also able to auto-activate, and is found at an average concentration of 6.4 mg/ml in the prostate, about 100-fold lower than that found for PSA[68]. Because of these features, there is a strong possibility that hK2 is a physiological activator of PSA that leads to the liquefaction of semen. Another human kallikrein expressed almost exclusively in the prostate is hK4, which also displays the ability to activate latent PSA[73]. Using recombinant hK4, strong activation of PSA was observed without any notable internal cleavages[74]. hK5, another trypsin-like serine protease, has been shown to auto-activate as well as activate both hK2 and PSA[75]. Recombinant hK15 (prostin) also can activate PSA, and hK15 is produced primarily in the prostate[76]. However, this enzyme needs trypsin activation before being capable of PSA activation.

3.2.2 PSA inhibition by Zn^{+2}

The main physiological inhibitor of PSA appears to be the divalent cation Zn^{+2}. It is thought to bind to PSA in two separate binding pockets, most likely allosterically, thus reducing the enzymatic activity of PSA[77]. Zn^{2+} is present in the prostate at ~1 mg/g dry weight[78], and about 150 μg/g wet tissue, the highest concentration of any tissue known[79]. In seminal plasma, Zn^{+2} is observed at concentrations ~2 mM[46]. PSA is inhibited by Zn^{+2} at concentrations as low as 10 – 100 μM[46]. The levels of Zn^{+2} in seminal fluid exceed that needed for PSA inhibition, suggesting possible inhibition of PSA activity while in the prostate.

3.2.3 Proteinase inhibitors of PSA

Various proteinase inhibitors are able to bind to active PSA and inhibit its enzymatic activity. These proteinase inhibitors only bind to active PSA. In the seminal plasma, protein C inhibitor (also known as PAI-1) is bound to 5% of active PSA where it is present at 3 – 4 μM[80]. In the bloodstream, α_1-antichymotrypsin (ACT) is a major binding serpin of PSA[66], where it acts by irreversibly binding to the active site of PSA through an acyl-bond[69]. Another strong inhibitor of PSA is α-Mac, which binds and completely encapsulates PSA[81]. This binding occurs through proteolytic cleavage of the bait region of α-Mac by active PSA, triggering a conformational change in α-Mac to enclose PSA[82]. Other minor proteinase inhibitors of PSA include inter-α-trypsin inhibitor, and α1-antitrypsin which bind to a small fraction of PSA in seminal plasma[8].

3.2.4 Proteolytic inactivation of PSA

Internal cleavage of the mature region of PSA results in an irreversible inactivation of this enzyme. The enzymes responsible for this are suspected to be the same enzymes that proteolytically activate PSA. hK2 has shown the ability to cleave PSA internally – although at a slower rate than removal of the pro-peptide – between Lys 145 - Lys 146, representing 10-25% of the PSA forms found in human seminal plasma[73]. PSA is also internally cleaved by hK5 between Arg 86 – Phe 86, and Lys 183 – Ser 183[75]. PSA isolated from human seminal plasma has been observed to be cleaved at these sites, suggesting that hK5 is active in seminal fluid where it is expressed along with PSA and hK2 and may be a physiological regulator of PSA activity[75].

3.3 Enzymatic substrates of PSA

PSA exerts its proteolytic activity using a catalytic triad characteristic of serine proteases, with the amino acids of the active site consisting of His-45, Asp-96 and Ser-192[83]. It has been shown to have a weak chymotrypsin-like activity, cleaving after hydrophobic or basic amino acid groups[83]. Semenogelins, the gel-forming proteins in semen, are thought to be the physiological substrate of PSA[9]. PSA assists in the liquefaction of semen by cleaving semenogelins I and II[84] and fibronectin[85].

PSA has also been shown to cleave proteins not involved in semen gel formation. PSA can cleave both IGFBP-3[86] and IGFBP-4[87], releasing bound IGFs. PSA can also cleave the regulatory pro-peptide of latent TGF-β2 to yield a biologically active mature TGF-β2[88,89]. As well, PSA is able to cleave and inactivate parathyroid hormone related protein (PTHrP), a protein involved in bone resorption and implicated in regulating prostate growth and calcium levels[90]. Another protein hydrolysable by PSA is human secretory leucocyte protease inhibitor (SLPI), a protease inhibitor of granulocytic elastase and cathepsin G[91]. SLPI is found in seminal plasma at a mean value of 22.8 mg/l and functions most likely to protect sperm cells and delicate proteins during an immune response[91]. Furthermore, PSA has been shown to cleave plasminogen to yield angiostatin-like fragments, peptides that are involved in angiogenesis[92]. Multiple components of the BM have also been found to be substrates for PSA, including fibronectin, laminin, gelatin and fibrinogen[45,88] as well Matrigel, a simulated BM[46].

3.4 Non-enzymatic activities of PSA

Recently, evidence has emerged showing that PSA may have effects independent of proteolytic activity. By treating prostate cancer cell lines with PSA isolated from seminal plasma, intracellular reactive oxygen species (ROS) are produced[93]. Abrogation of the ROS-inducing effects of PSA – using a monoclonal antibody that did not affect the enzymatic activity of PSA – shows that enzymatic activity of PSA is not necessary to induce ROS. Furthermore, exogenous recombinant PSA inhibits angiogenesis *in vitro* and *in vivo*[94]. Similar effects have been seen with enzymatically active PSA as well as an enzymatically inactive truncation mutant lacking the N-terminal isoleucine. The non-proteolytic activity of PSA may be due to ligand-receptor reactions not related to proteolytic activity. PSA has extensive homology with some growth factors on the amino acid level, notably γ-nerve growth factor (56%), α-nerve growth factor (51%) and EGF binding protein (53%)[83,93].

3.5 PSA testing used in prostate cancer diagnosis

The presence of PSA is measured in a patient's serum, with levels of PSA > 10 ng/ml being highly predictive of PCa, levels of PSA < 4 ng/ml predicting a low percentage of PCa occurrence and levels of PSA between 4 and 10 ng falling in the grey zone[22]. However, prostate cancer can even be detected in men with a serum PSA value below 4 ng/ml[22]. Other disease processes can lead to an increase in the level of PSA, such as

BPH, urinary tract infections, and prostatitis[95]. Increased serum PSA levels correlate to tumour volume and most probably result from leakage of PSA from the prostatic-ductal system – most likely due to prostate structure damage – into the prostatic stroma and subsequently into the blood stream[66].

PSA exists in several different molecular forms, and the standard serum PSA test measures total PSA. Total PSA consists of all immunodetectable PSA and is comprised of free PSA and PSA bound to the protein inhibitor ACT[69]. PSA can also be present bound to α-Mac, which accounts for a small fraction of bound PSA[69]. Because of its large size, α-Mac completely encapsulates PSA leaving no free epitope for detection in the PSA test[8,69]. In serum, PSA-ACT is the predominant form (60% - 95%), whereas 5% - 30% of the immunodetectable PSA is free PSA[96]. Free, uncomplexed PSA found in serum can exist in several more different forms, including two truncated forms of proPSA the inactive zymogen), and two minor forms of internally cleaved PSA (also called BPSA)[66].

To improve the use of PSA as a diagnostic tool, more specific clinical tests based on PSA have been developed. These include PSA density measurements, where the serum PSA level is divided by the prostate volume, the PSA velocity test which takes into account the rate of increase of PSA in the serum over time, and ratios of free PSA to protease complexed PSA[1]. As well, increasing levels of serum PSA have been used to predict PCa relapse after radical prostatectomy, radiation therapy and hormone ablation therapy[66].

3.6 The possible role of PSA in cancer invasion

PCa cells have been shown to consistently express PSA, although their levels of expression are lower on a per cell basis than the prostate epithelium[66]. Even in androgen-independent PCa, PSA is more often than not expressed, most likely due to an AR alteration which allows activity regardless of the presence of androgens[66]. Also, levels of Zn^{+2} – a major inhibitor of PSA activity – are decreased ~7 fold in PCa compared to normal prostatic tissue or BPH[78]. Two separate research groups have shown that decreasing the enzymatic activity of PSA using either monoclonal antibodies against active PSA[45] or Zn^{+2} at enzymatically inhibitory levels [46] decreases the *in vitro* invasive potential of the PSA-producing LNCaP cells. The following sections provide possible mechanisms of how PSA may be involved in PCa cell invasion.

3.6.1 Degradation of ECM and BM by PSA

Degradation of components of the ECM and BM are an essential step in PCa cell invasion. Since PSA has shown the *in vitro* ability to degrade fibronectin, laminin, gelatin and fibrinogen[45,88] and Matrigel (an assemblage of many BM components)[46], it is possible that some or all of these activities occur *in situ*. By degrading fibronectin and laminin, PSA is able to release integrin-mediated attachment of cells to the BM, as well as degrade a barrier for cells to enter into the stromal environment. In the stroma, degradation of gelatin (partially degraded collagens) can allow for further dissemination into the surrounding tissue. Furthermore, degradation of some matrix components can reveal cryptic sites that are used by tumour cells as a chemoattractant to induce migration, such as the MMP cleavage products of both laminin-5[97] and laminin-10[98].

3.6.2 Cleavage of IGFBPs by PSA

The release of IGF-I by PSA cleavage of IGFBP-3[86] and IGFBP-4[87] may be important in PCa invasion. By blocking the IGF-I receptor in PC-3 cells, both an upregulation of IGFBP-3 and a downregulation of MMP-2 has been found[99]. Similar effects are seen in human androgen-independent PtdCho-3 prostate carcinoma when transfected with antisense cRNA to downregulate the IGF-IR[61]. As well, it has been found in various PCa cell lines that IGF-I is able to induce uPAR expression, increasing motility and invasion[61]. As further evidence for the role of IGF-I in PCa, increases in serum levels of IGF-I have been found increased in PCa patients[100]. This evidence suggests that IGF-I – normally sequestered by IGFBPs – can increase invasive potential when released by PSA. The cleavage of IGFBP-3 itself also may have direct consequences for invasion independent of IGF-I, possibly by abolishing its intrinsic anti-proliferative and apoptotic effects as seen *in vitro* in PC-3 cells[44].

3.6.3 Activation of latent TGF-β by PSA

TGF-β is know for is dipolar role in cancer progression. Thus, the activation of TGF-β by PSA may be beneficial to PCa or detrimental, depending on the cancer stage. Prostate epithelial cells express TGF-β2 and PSA is able to activate this GF by proteolytic cleavage[89]. Although in early carcinogenesis this could lead to apoptosis and cell cycle arrest, PCa cells that have become resistant to these effects can take advantage of the numerous effects of TGF-β in enhancing invasion. These include EMT[54], activating tumour fibroblasts[25], and subverting androgen-suppressing effects through signalling pathway crosstalk[59].

4 Objectives

The purpose of this study was to further test the ability of PSA to change the *in vitro* invasive ability of PCa cell lines. The ability of PSA to affect invasion of PCa cell lines needs to be further studied. Others have shown that the invasion of LNCaP cells is decreased when the enzymatic activity of PSA is abolished[45,46], however, PC-3 cells transfected with PSA show an increase in migration, but not invasion[47]. To test the migration of cells, transwell membranes were used where the number of cells crossing a porous membrane represented cell migration. To test for cellular invasion, these transwell membranes were coated with a basement membrane extract (BME) to simulate a basement membrane as a barrier for cellular invasion. Two different methods were used to test the effect of PSA on invasion. Firstly, exogenous PSA – isolated from human seminal plasma – was added to PCa cells in invasion/migration chambers to test the effects of this enzyme on invasion and migration. Both the PSA-producing PCa cell line LNCaP and the non-PSA producing PCa cell line DU-145 were used. Secondly, we created separate expression vectors that encoded for preproPSA as well as a deletion mutant prePSA that consisted of an in-frame fusion between the pre secretory region and mature PSA. Two vector systems were used: one system controlled PSA under the high expression level CMV promoter, and the other controlled PSA expression using an ecdysone-inducible transcription initiator. These constructs were used to transfect DU-145 cells to allow for either preproPSA or prePSA expression. The effects of stable PSA expression in DU-145 clones were examined with regards to cell growth, invasion and migration.

5 Hypothesis

Exogenous PSA added to prostate cancer cells or prostate cancer cells that are genetically modified to secrete different forms of PSA will have a different invasive potential compared to cells that secrete mainly proPSA or no PSA at all.

Materials and Methods

Cell culture

DU-145 and LNCaP human prostate cancer cell lines were obtained from ATCC. DU-145 cells were maintained in MEM with Earle's salts (Sigma) – supplemented with 1 mM sodium pyruvate (HyClone), 0.1 mM MEM non-essential amino acids (HyClone), antibiotics (100 units/ml penicillin sodium, 100 μg/ml streptomycin sulphate and 0.25 μg/ml amphotericin B, obtained from Invitrogen), and 10% characterized FBS (HyClone). The LNCaP cell line was maintained in RPMI 1640 (Sigma) supplemented with 10 mM HEPES, antibiotics (100 units/ml penicillin sodium, 100 μg/ml streptomycin sulphate and 0.25 μg/ml amphotericin B, obtained from Invitrogen) and 10% characterized FBS (HyClone). The medium was changed three to four times per week and cells were passaged once or twice per week using 0.05% trypsin/5 mM EDTA (Invitrogen). Cell numbers and viability were determined using a Neubauer improved haemocytometer (La Fontaine) and 0.08% trypan blue (Gibco). Cells were alternatively counted using a Z1 Series Coulter Counter (Beckman). Cells were frozen at a concentration of 1 – 4 X 10^6 cells/ml in a mixture of 50% FBS (HyClone), 43% growth medium, and 7% DMSO (Sigma) in Cryogenic vials (Nalgene) at –80 °C overnight and transferred to liquid nitrogen the next day.

Standard molecular biology methods

Polymerase chain reaction (PCR)

PCR primers were designed using Gene Runner version 3.05 for Windows (Hastings Software) and were purchased from Invitrogen. All PCR reactions were run with a Deep

Vent Polymerase Kit (NEB Labs) or an Accutaq LA DNA polymerase kit (Sigma) using a Genius Thermal Cycler (Techne) and the conditions shown in Table 1 unless otherwise indicated. In a 50 μl volume, each PCR reaction mixture consisted of 0.2 μM of each forward and reverse primer, 0.5 mM dNTPs, 1 X PCR mix, and 2.5 U DNA polymerase. A list of all primers used is shown in Table 2. The PCR products were verified by electrophoresis in 1% agarose gel polymerized with 1 μg/ml ethidium bromide in 1 X TBE at 80 V for 30 minutes to 1 hour and visualized via DNA-bound ethidium bromide-induced UV fluorescence. DNA molecular weight markers used in gel electrophoresis at 10 μl/lane were obtained from Fermentas. DNA was isolated from gel excisions using a QIAquick gel extraction kit (Qiagen). DNA concentrations were measured by a BioPhotometer (Eppendorf) using Uvettes (Eppendorf) at 260 nm.

Table 1: Conditions for PCR amplification reactions

Cycle	Temperature (°C)	Time	Number of Cycles
Initial Denaturation	95	30 sec	1
Denaturing	95	30 sec	35
Annealing	variable	30 sec	
Extension	72	1 min	
Final Extension	72	10 min	1

Table 2: Primers used in PCR amplification reactions

Primer Name	Primer Sequence (5' – 3')
sense pcDNA3.PSA prepro primer A+C	GTTGAGCTAGCACCATGTGGGTCCCGGTTGT
as new A pcDNA3.PSA prepro primer	CATCACCTGGCCTGAGGAATC
sense b modpSTHMppPSA	GGCGTGGATAGCGGTTTGAC
anti-sense b modpSTHMppPSA	CGGAGCAGCATGAGGTCGTG
s mid modpSTHMppPSA	CCGTGACGTGGATTGGTGCTATTGTGGGAGGCTGGGAGTG
as mid modpSTHMppPSA	CACTCCCAGCCTCCCACAATAGCACCAATCCACGTCACGG
s BamHI pmodSTHM to pEGSH	GTTGAGGATCCGCCACCATGTGGGTCCCGGTTG
as BamHI pmodSTHM to pEGSH	GATGGTCGACGGCGCTATTCAG
PSA sense B 225-246	GGTCGGCACAGCCTGTTTCATC
PSA anti-sense B 582-603	GCGTCCAGCACACAGCATGAAC

Restriction enzyme digestion

Restriction digests were performed using enzymes acquired from Fermentas and using conditions and buffers as recommended by the manufacturer. In a 20 μl reaction mix, ~5 units of restriction enzyme were used to cleave 0.2 μg – 2 μg DNA overnight at 37 °C. The restriction enzymes were inactivated by heating at 65 °C or 80 °C (depending on the specific enzyme) for 10 minutes. Restriction digest products were run on a 1% agarose/TBE gel, gel-excised and purified using QIAquick gel extraction kit (Qiagen). Linearized plasmids were purified directly using the "DNA cleanup from enzymatic reactions" method in the QIAquick gel extraction kit. Extracted DNA was collected in ddH_2O or TE buffer (10 mM Tris-HCl pH 7.5, 1 mM EDTA).

DNA ligation reaction, transformation of bacteria, and DNA mini-prep

DNA ligations were performed using an overnight ligation in a low melting point agarose gel mixture. After restriction digestion of ~2 μg plasmid DNA and ~0.2 – 0.6 μg PCR product, digestion products were run on a 1.2 – 1.5% low melting point agarose gel in 1 X TBE with 1 μg/ml ethidium bromide. Appropriate restriction fragments were gel-excised and each excision fragment melted at 65 °C. For ligation reactions, melted gel fragments containing 0.01 μg – 0.1 μg digested plasmid (in ~2 μl) and 0.01 μg – 0.1 μg restriction enzyme digest PCR amplicons (in ~10 μl) were combined. Both were added to a mixture of 1 X T4 DNA ligase buffer and T4 DNA ligase (2U) (Promega) in a total of 40 μl and left at room temperature overnight. The next day, the ligation mixture was melted at 65 °C and added to 80 μl cold TCM buffer (10 mM Tris-HCl pH 7.5, 10 mM $CaCl_2$, 10 mM $MgCl_2$). 20 μl of this TCM/ligation mixture was added to 40 μl of competent JM109 *E.coli* (Promega) at $>10^7$ cfu/μg and put on ice for 10 minutes. To transform bacteria, the bacteria were heat-shocked for 45 seconds at 42 °C, then put on ice for 2 minutes. 400 μl S.O.C. medium was added to the bacteria and the mixture incubated at 37 °C for one hour at 225 RPM. Dependent on the resistance encoded by the plasmid, 100 – 200 μl bacteria were grown on selective agar plates containing either 50 μg/ml ampicillin or 50 μg/ml kanomycin overnight at 37 °C. Single colonies were isolated and grown in selective 5 ml LB media at 37 °C for one day at 225 RPM. Plasmid DNA from each culture was isolated using QIAprep spin miniprep kits (Qiagen) and tested for the correct DNA insert using restriction enzyme digestions.

Large scale isolation of plasmid DNA

To isolate large amounts of plasmids, 100 μl to 1 ml bacteria containing the correct plasmids (as determined by Miniprep and subsequent restriction enzyme digest) were grown in selective LB media specific for each plasmid (50 μg/ml ampicillin or 50 μg/ml kanomycin). The bacteria transformed with plasmid DNA were isolated by either midi-preps using a Flexiprep kit (Amersham) from a culture of 25 – 100 ml or by maxi-preps using QIAfilter plasmid maxi kit (Qiagen) from a culture of 100 – 400 ml grown overnight at 37 °C with 225 RPM shaking. Plasmid DNA isolated from the midi-preps or maxi-preps was further purified by ethanol precipitation using 1/10 of a volume of 3M sodium acetate and 2 times volume of ice-cold 100% ethanol and precipitated at –80 °C. DNA was redissolved in ddH_2O. To verify inserts, plasmids were sequenced at Paleo DNA Laboratories using specific primers for each plasmid.

Isolation of genomic DNA from mammalian cell lines

Cells were either trypsinized from a 10 cm cell culture plate or thawed from frozen cryogenic vials and centrifuged at 250 g for 5 minutes. Cells were washed with PBS and again centrifuged at 250 g. Genomic DNA was isolated using an Ultra Clean Tissue DNA Isolation Kit (Mo Bio) as per the manufacturer's instructions, and eluted in 50 μl TE buffer.

Vector systems used

modpSecTagPSA

The modpSecTagPSA plasmid contains a CMV promoter for high-level expression of cloned genes and is the template for all CMV plasmid systems used. This plasmid was created from a modified plasmid by ligating the 478 bp ClaI and XbaI restriction fragments from pcDNA3.PSA – a plasmid containing full length PSA cDNA (a kind gift from Dr. Hans Krause, Free University, Berlin) – into the 6.0 kb ClaI and XbaI restriction fragment from pSecTag2/Hygro/PSA (Invitrogen). The resulting plasmid modpSecTagPSA contains a 3' stop codon at the end of the PSA cDNA coding sequence before the His or Myc tags located on the pSecTag2/Hygro/PSA. The 5' end of the newly created modpSecTagPSA contained a truncated PSA sequence lacking the prepro sequence with a leading murine Igκ-chain V-J2-C signal peptide for secretion.

Ponasterone-inducible complete control® system

The Complete control® mammalian expression system (Stratagene) consists of a system of 2 plasmids for dual transfection into mammalian cells: pERV3 and pEGSH. The pERV3 plasmid contains the VgEcR gene, a transcriptional regulator that activates transcription in the presence of ponasterone A (PonA, Invitrogen) – an analogue of the insect hormone ecdysone – and represses basal transcription in the absence of PonA. This transcriptional regulation occurs at E/GRE recognition sequences, which are present in the pEGSH plasmid. The pEGSH plasmid also contains a multiple cloning site (MCS) downstream of the E/GRE sequences to allow inducible expression of the inserted gene. Using this system, DU-145 cells were first stably transfected with the pERV3. Several clones were selected using transient transfection with pEGSH-luc – a plasmid with the luciferase gene in the MCS of pEGSH – into clones stably expressing VgEcR, showing inducible expression of the luciferase gene by PonA. The pERV3 containing clone with the largest inducible expression and the least expression without PonA was subsequently transfected with a pEGSH plasmid containing the gene of interest.

Transient transfection of DU-145 cells

Transient expression of PSA was done using lipofection of DU-145 cells with plasmid DNA containing the DNA sequence coding for PSA. DU-145 cells were seeded at 5 X 10^4 cells/well in a 24-well plate (Corning) in 400 μl antibiotic-free media and allowed to adhere overnight. The next day, 50 μl Opti-MEM (Gibco) was mixed with 0.5 μg or 1.0 μg plasmid DNA, and in a separate tube 50 μl Opti-MEM (Gibco) was mixed with 6 μg (3 μl) Lipofectamine (Invitrogen). The contents of the two tubes were mixed and left at room temperature for 20 minutes. During this time, media was removed from the cells in the 24-well plates and replaced with 200 μl of Opti-MEM. After 20 minutes, the Opti-MEM was removed from the cells and 100 μl of the plasmid/lipofectamine mixture was added to the cells for ~20 hours. After this time, the lipofection/DNA mixture was removed and 400 μl DU-145 media was added. 100 μl conditioned media (CM) was removed after two days and then again after four days. Samples were subjected to Western blot analysis to determine the expression of PSA, as described in the "Western blot analysis" section.

Stable transfection of DU-145 cells using electroporation

Standard stable clone creation using electroporation

To prepare DU-145 cells for electroporation, the cells were trypsinized, centrifuged at 200 g for 5 minutes, and resuspended in ice-cold PBS at 1 X 10^7 cells/ml. Gene Pulser Cuvettes (Biorad) were filled with 400 μl cell suspension (4 X 10^6 cells) and between 1 μg to 10 μg plasmid DNA in ddH_2O. For some transfections, plasmid DNA was linearized by digesting with a restriction enzyme overnight before transfection, and the DNA purified using a QIAquick gel extraction kit (Qiagen) enzyme cleanup procedure. The cuvettes were put in a Gene Pulser II (Biorad) and subjected to voltages between 1000 V and 1500 V with either 1 or 2 pulses at 25 μF unless otherwise stated. Cells were resuspended in DU-145 growth media and seeded in 10-cm cell culture plates (Corning).

Stable clone selection

Twenty-four hours after electroporation, the medium was replaced with growth medium supplemented with selective agents appropriate for the transfected plasmid (G418 or Hygromycin, Invitrogen) at a concentration that leads to >95% cell death, as determined in "Cytotoxicity of antibiotics used in stable clone selection". The selective medium was replaced three times per week to remove unsuccessfully transfected cells killed by the selective agents. Once large single colonies were visible on the plate (~1 mm to 5 mm), they were isolated using cloning rings via trypsinization and grown in 6-well culture dishes. Once cells reached ~70% confluency, they were transferred to 10-cm cell culture plates. Upon reaching ~70% confluency in the 10 cm plates, a fraction of the cells in the plate were frozen in liquid nitrogen and the rest of the cells passaged for further study.

Luciferase assay for detection of a stable DU-pERV3 clone

A luciferase assay was used to determine the active presence of the ponasterone regulated transcription factor VgEcR of the pERV3 plasmid in transfected DU-145 cells. A modified version of the "Active Lysis Protocol..." from the Luciferase Assay Kit (Stratagene) was performed. Initially, DU-pERV3 clones were seeded at 3 X 10^5 cells/well in a 6-well plate with 2 ml of antibiotic-free DU-145 media and allowed to adhere overnight. The next day, 250 µl Opti-MEM (Gibco) was mixed with 0.1 µg to 7.5 µg of pEGSH-Luc plasmid DNA, and in a separate tube 250 µl Opti-MEM (Gibco) was mixed with 30 µg (15 µl) Lipofectamine (Invitrogen). The two tubes were mixed and left at room temperature for 20 minutes. During this time, media was removed from the cells in the 6-well plates and replaced with 2 ml of Opti-MEM. After 20 minutes, the Opti-MEM was removed from the cells and 500 µl of the plasmid/lipofectamine mixture was added to the cells for ~20 hours. After this time, the lipofection/DNA mixture was removed and each well was washed with PBS, and 2 ml antibiotic-free DU-145 media was added. To each well, various amounts of PonA – from 0 µM to 10 µM – were added 24 hours later, the medium was removed and the cells washed twice with PBS. To the washed cells was added from 75 µl – 100 µl cell lysis buffer (25 mM Tris-phosphate pH 7.8, 2 mM DTT, 2 mM 1,2-diaminocyclohexane-N,N,N′,N′-tetraacetic acid, 10% glycerol, and 1% Triton® X-100) and the cell/lysate buffer mixture was scraped into a microcentrifuge tube. The mixture was frozen at –80 °C for 20 minutes and then thawed briefly at 37 °C and vortexed for 20 seconds. 50 µl - 75 µl cell lysate (CL) was added to 100 µl luciferase substrate-assay buffer and after waiting ~8 seconds, the luminescence was measured over 30 seconds on a Fluorostar Optima (BMG Labs) plate reader. Relative luminescence units (RLU) were recorded as a measure of luciferase activity.

Western blot analysis for PSA detection

Cell conditioned media and/or cell lysates were collected from cells growing for 3-6 days and frozen at –20 °C in 6 X non-reducing sample buffer (350 mM Tris-HCl pH 6.8, 30% glycerol, 10% SDS, and 0.12% bromophenol blue). To prepare conditioned media, cells were grown to 50 – 90% confluency. Serum-containing media were removed, cells were washed with PBS and serum-free (SF) media was added to the cells. The cells were kept in the SF media for 3 – 6 days until the media was collected. For conditioned medium (CM) concentration, the collected CM was centrifuged for 10 minutes at 3,000 g to remove cells and large debris. The supernatant (CM) was added to 10 kDa cut-off YM-10 Centricon Centrifugal Filter Units (Millipore) and centrifuged at 4,000 g for 30 min – 4 hours. Concentrated CM was collected and the fold concentration was determined by the difference in fluid weight before and after centrifugation. To prepare cell lysates, cells were trypsinized and then centrifuged at 250 g for 5 minutes. Cells were washed with PBS, and then centrifuged again at 250 g. The pellet was resuspended in 100 μl NB buffer with PMSF (0.25M Sucrose, 0.2M NaCl, 10mM Tris-HCl pH 8.0, 2mM $MgCl_2$, 1mM $CaCl_2$, 1% TritonX-100, and 1mM PMSF) to lyse cells for 5 minutes on ice. The lysed cells were then centrifuged at 14,000 g in a microcentrifuge for 30 seconds. The supernatant was removed from the pellet of cell debris into a separate tube. For CL isolated from cells in 6-well and 24-well plates, 75 μl of the supernatant was removed from the solution and frozen at –20 °C with 15 μl of 6 X non-reducing sample buffer (total volume of 90 μl). For CL isolated from cells grown in 10 cm or larger plates, 150 μl NB buffer with PMSF was added as a diluent to 75 μl of the CL and the samples frozen at –20 °C with 45 μl of 6 X non-reducing sample buffer (total volume of 270 μl). As a positive control for the blots, commercially available PSA isolated from seminal plasma was used (Human prostate-specific antigen purified protein (AG650, Chemicon) or Prostate-Specific Antigen enzymatically active (ActPSA, Fitzgerald)). As a molecular weight marker, 10 μl to 15 μl Prestained SDS-PAGE standards (Bio-Rad) were loaded in at least one well of each gel. Proteins in the samples were separated on a 12% poly-acrylamide 0.1% SDS gel with a 4% stacking gel and a running buffer of 190 mM glycine, 25 mM Tris base, and 0.05% SDS at 100 V. The proteins were transferred to Hybond nitrocellulose (Amersham) in a carbonate transfer buffer (17 mM $NaHCO_3$, 5 mM Na_2CO_3 with 20% methanol) overnight at 20 V. The nitrocellulose blot was equilibrated for 10 minutes in TBST, and subsequently non-specific sites were blocked for 1 hour in TBST containing 8% powdered skim milk. The blot was transferred to a solution of mouse anti-PSA antibody A67-B/E3 (Santa Cruz) at 1:400 (0.5 μg/ml) in TBST with 5% powdered skim milk for 1.5 hours. After four 15-minute washes with TBST, the blot was incubated in a solution of goat anti-mouse IgG horseradish peroxidase-conjugated antibody (Santa Cruz) at a 1:2000 dilution (0.2 μg/ml) with 5% powdered milk in TBST. The blot was washed four times for 15 minutes in TBST. Detection of HRP was carried out using an enhanced chemiluminescence method as follows: the blot was transferred to a solution of 100 mM Tris-HCl pH 8.5, 9 X 10^{-3} % H_2O_2, 200 μM coumeric acid (Sigma) and 1.25 mM luminol (Sigma) for 1 minute. The blot was removed from the solution and exposed to Scientific imaging X-ray film (Kodak) for protein band detection. Densitometry of the bands was carried out using

Kodak 1D version 3.5 imaging software, and PSA concentrations were calculated using a standard curve determined by running three concentrations of ActPSA (1-20 ng/lane) on a Western blot.

Cell number determination using relative DNA content

Standard curve to determine cell numbers

To create standard curves, DU-145 cells were serially diluted from 6.0×10^4 to 4.7×10^2 cells in serum-supplemented medium, halving the cell number with each dilution. LNCaP cells were similarly serially diluted from 3.2×10^4 to 1.0×10^3 cells. Cells were seeded in four replicates of 200 μl medium/well in a 96-well plate and allowed to adhere overnight. The next day, media was removed from each well of the plate, replaced with 100 μl of ddH_2O, and frozen at –80 °C to lyse the cells and determine the DNA content as described in section "Measuring DNA to determine relative cell number". The DNA content determined in relative fluorescence units (RFU) was correlated with cell number to obtain a linear correlation between RFU and cell number.

Growth curve analysis

For growth assays, cells were plated at 1.0×10^3 (DU-145) or 5.0×10^3 (LNCaP) cells per well in clear 96-well cell culture plates (Corning) with 200 μl media specific to each cell type and experiment. In total, five identical plates were seeded, to be removed one per day. Cells were allowed to adhere overnight. In experiments using PonA, cells were plated in serum-containing media with 1 μM or 10 μM PonA along with the 100% ethanol (solvent) controls. In experiments using exogenous PSA, media was removed after the cells were allowed to adhere overnight and was replaced with serum-supplemented media containing 0.5 μg/ml, 1 μg/ml or 2 μg/ml PSA (AG650 or ActPSA), with the appropriate PBS buffer controls. Each day, over a period of 5 days, media was removed from each well of one plate, replaced with 100 μl of ddH_2O, and frozen at –80 °C to lyse the cells and determine the DNA content as described in section "Measuring DNA to determine relative cell number". A logarithmic growth curve was created from this data, and using the slope of the growth curve from days 3 – 5 the population-doubling time (PDT) was determined using Excel (Microsoft).

Cytotoxicity of antibiotics used in stable clone selection

To determine the concentration of antibiotic needed to decrease cell numbers by 95%, DU-145 cells (or selected transfected DU-145 subclones) were plated at 400 cells/well in 100 μl growth medium and allowed to adhere overnight. The next day, either (or both) of the antibiotics hygromycin B (Invitrogen) and G418 (Invitrogen) at concentrations ranging from 50 μg/ml to 900 μg/ml were added to the cells in 100 μl growth medium. Five days after the antibiotics were added to the wells, media was removed from each well, replaced with 100 μl of ddH_2O, and frozen at –80 °C to lyse the cells and determine the DNA content as described in the next section.

Measuring DNA to determine relative cell number using Hoechst 33258

Frozen plates containing the lysed cells were placed at room temperature to thaw. To each well containing the lysed cells in 100 μl ddH_2O, a 100 μl solution of 20 μg/ml Hoechst 33258 (Sigma) in TNE buffer (10 mM Tris-HCl pH 7.4, 2 M NaCl, 1 mM EDTA) was added and placed in the dark for 5 minutes. Hoechst 33258 binds to DNA from the lysed cells, resulting in a fluorescence shift to 460 nm, and a linear relationship between DNA and cell number is seen over a wide range of DNA. The DNA amount is directly proportional to cell number. The DNA-Hoechst fluorescence was measured using an excitation of 360 nm and emission of 460 nm on a FLx800 Multi-Detection Microplate Reader (Bio-Tek).

Activity assay to test for enzymatically active PSA

Enzymatic activity of PSA was measured using the cleavage of *p*-nitro-analine from the peptide substrate MeO-Suc-Arg-Pro-Tyr-*p*NA (S-2586, Chromogenix) in a 96-well plate. Each 240 μl reaction mix (per well) consisted of 200 μl activity buffer (200 mM Tris-HCl pH 8.0, 5 mM EDTA), 20 μl of either 5 mM or 10 mM S-2586, and 20 μl sample. This gave final concentrations of 167 mM Tris-HCl, 4 mM EDTA, and either 0.4 mM or 0.8 mM S-2586. The enzymatic activity was measured with or without 100 μg/ml of the irreversible chymotrypsin inhibitor TPCK (Sigma). Solutions were pipetted in a 96-well clear cell culture plate (Falcon) and incubated at 37 °C. Absorbance readings were taken hourly at 405 nm on a Powerwave XS microplate spectrophotometer (Biotek). Increasing absorbance at 405 nm corresponded to the release of *p*-nitro-analine from S-2586 due to enzymatic activity and results were calculated as ΔA_{405}/hour.

Cell invasion/migration assay

Standard curve to determine cell numbers using calcein AM

Cell number was correlated with calcein AM RFU to create a standard curve using the method as stated in the "96 Well BME Cell Invasion Assay" (Trevigen). To create a standard curve, cells were serially diluted and plated from 5.0 X 10^4 to 1.0 X 10^4 cells/well in 50 μl of proprietary "cell dissociation solution" (Trevigen) in an opaque 96-well plate. To this was added 50 μl of "cell dissociation solution" with 4 μg/ml calcein AM, for a final concentration of 2 μg/ml calcein AM/well. This cell solution was incubated for one hour at 37 °C and 5% CO_2. Viable cells take up calcein AM, which inside the cell, is then converted to the fluorescent calcein, accumulating inside the cell. The resulting fluorescence of the calcein within the cells was measured using an excitation of 485 nm and an emission of 520 nm using the top reader of a FLx800 Multi-Detection Microplate Reader (Bio-Tek).

Measuring cell invasion/migration

To determine the *in vitro* invasive or migratory ability of prostate cancer cell lines, "96 Well BME Cell Invasion Assay" (Trevigen) kits were used. 10-cm culture plates with cells at 50 – 90% confluency were washed three times with 5 ml of PBS and SF media was added overnight. For invasion assays, BME was plated on the membrane of the transmembrane chamber at concentrations ranging from 0.1 – 0.05 mg/well for DU-145 cells (as well as subclones made from this cell line) and 0.05 to 0.01 mg/well for LNCaP cells. To test cell migration, no BME was added. The following day, the SF medium was removed from the 10 cm plates and the cells were trypsinized, resuspended in SF medium, and centrifuged at 250 g for 5 minutes. Supernatant was carefully removed and the cells were resuspended in SF medium. To each insert was added 50 μl cells with either 1.0 X 10^5 or 5.0 X 10^4 cells/insert for LNCaP cells and 5.0 X 10^4 cells/insert for DU-145 cells. To the lower chamber of the transwell was added 150 μl of either 0.5 or 10% FBS growth medium as a chemoattractant. Invasion plates were incubated for 24 hours at 37 °C and 5% CO_2. The next day, the top chamber was washed once with PBS and the bottom chamber washed two times with PBS. The invaded/migrated cells were dissociated from the bottom of the insert by adding 100 μl of proprietary "cell dissociation solution" (Trevigen) containing 2 μg/ml calcein AM in the bottom well (while the insert sits in it) and incubating the plate 1 hour at 37 °C with 5% CO_2. The resulting fluorescence of calcein within the cells was measured by an excitation of 485 nm and an emission of 520 nm using the top reader of an FL X 800 Multi-detection microplate reader (Bio-Tek). Cell number was determined using calculations from cell type specific calcein AM standard cell curves as described previously.

Results

Western blot analysis of different PSA sources

To determine the expression of PSA by the human prostate cancer cell lines LNCaP and DU-145, Western blot analysis, using CM and CL, were carried out. These results were compared to commercially available PSA from different sources. AG650 and ActPSA are each isolated from human seminal plasma. AG650 PSA presented as a major band at 29 kDa by Western blot analysis (Figure 1A). This band most likely corresponds to mature PSA. When overexposed, additional bands were detected: one minor band visible slightly above (32 kDa) and one slightly below (26 kDa) the major band as well as a band at 56 kDa and another band above the 107 kDa molecular marker (Figure 1B). The bands at 26 kDa and 32 kDa most likely represent different molecular forms of PSA (i.e. either an internally cleaved form of PSA and zymogen form of PSA, respectively, or PSA with altered glycosylation patterns), and the band above 107 kDa may represent a complex formed between PSA and a protease inhibitor. Although the band at 56 kDa does not correspond to any known form of PSA, this may be due to protein dimerization in the stacking gel from excess ammonium persulphate.

Western blotting of ActPSA presented two separate bands: an upper band at 33 kDa and a lower band at 29 kDa (Figure 1A). This stands in contrast to the company's claim that ActPSA runs as a single band on SDS-PAGE. It is possible that these two forms both represent active PSA, yet differ in glycosylation patterns or some other post-translational modification and so run aberrantly in SDS-PAGE[101]. It is also possible that the 33 kDa band represents proPSA. Further bands were not detected, even upon overexposure.

Western blot analysis of conditioned media obtained from the androgen-sensitive LNCaP cells showed a single band at 29 kDa (Figure 1C). Both conditioned media and cell lysates obtained from the androgen-insensitive DU-145 cells were negative for PSA (Figure 1C), even when DU-145 CM was concentrated 26 times using a 10 kDa Centricon filtration unit (Figure 1D). Thus, LNCaP cells produced PSA, while DU-145 cells did not express PSA at any detectable level.

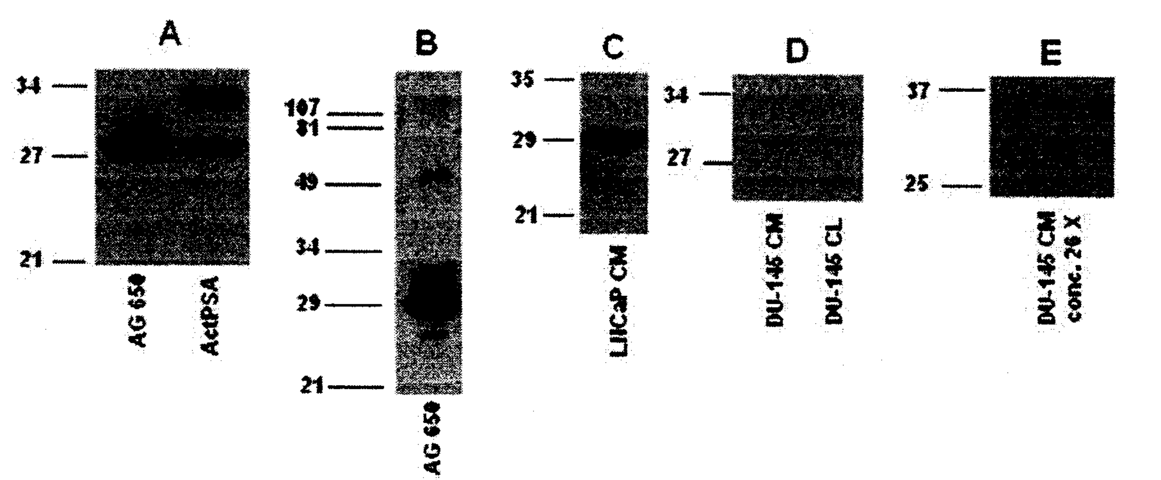

Figure 1: Western blotting for PSA of samples of cell-conditioned media and commercially isolated PSA

Western blotting for PSA of samples obtained from various sources. A) AG650: 20 ng; ActPSA: 20 ng. B) AG650: 20 ng. C) LNCaP CM: 30 μl from 6 ml media conditioned 5 days by 2 X 10^6 LNCaP cells. D) DU-145 CM: 10 μl from 6 ml media conditioned 3 days by 2 X 10^6 DU-145 cells; DU-145 CL: 41 μg cell lysate from the same DU-145 cells. E) ActPSA: 20 ng; DU-145 CM conc. 26X: 100 μl from 6 ml media conditioned 3 days by ~ 2 X 10^6 DU-145 cells. (Molecular weight markers in kDa).

Standard curves to relate cell number to DNA-Hoechst 33258 fluorescence

In order to directly associate cell number to Hoechst-DNA fluorescence, standard cell curves were created for each DU-145 and LNCaP cell lines. Cells were serially diluted and allowed to adhere overnight in order to find the linear range correlating cell number to fluorescence (RFU). The standard curves created using DU-145 and LNCaP cells are shown in Figure 2. For DU-145 cells, the linear range was found to be 4.7 X 10^2 – 6.0 X 10^4 cells/well and, using a standard curve created from a linear regression function, 0.461 RFU was found to represent one cell (R^2 of 0.9877). For LNCaP cells, the linear range was found to be 1 X 10^3 – 3 X 10^4 cells/well and, using a standard curve created from a linear regression function, 0.425 RFU was found to represent one cell (R^2 of 0.9841). These values were used to determine cell number from RFU in future experiments using the Hoechst assay.

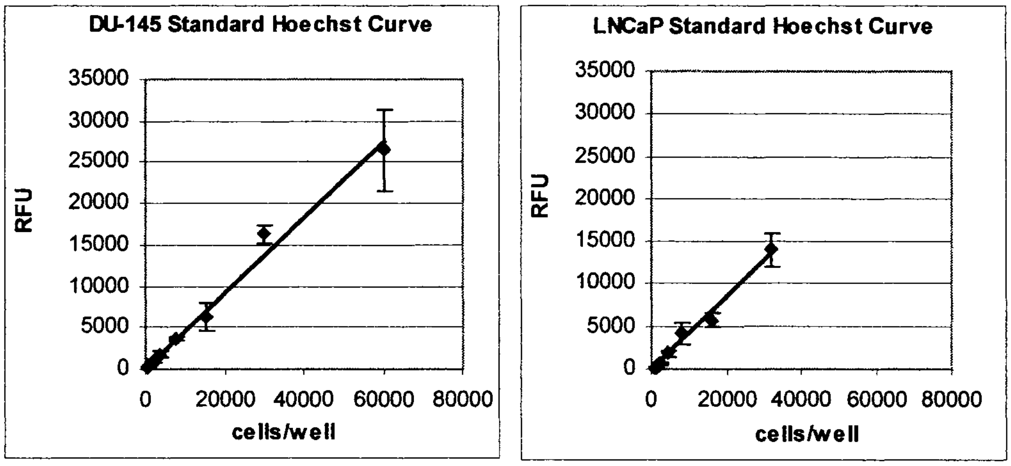

Figure 2: Standard curves relating cell number to DNA-Hoechst fluorescence

DU-145 and LNCaP cells were serially diluted, seeded in 96-well plates and allowed to adhere overnight. To relate cell numbers to Hoechst-DNA fluorescence, standard curve plates were subjected to the Hoechst-DNA fluorescence assay. Linear regression was used to create a standard curve relating RFU and cell number. DU-145 cells yielded 0.461 RFU/cell (R^2 = 0.9877) while LNCaP cells gave 0.425 RFU/cell (R^2 = 0.9841). Error bars represent standard deviation from 4 duplicates.

Enzymatic activity of PSA on the synthetic peptide substrate S-2586

In order to test the enzymatic activity of PSA, proteolytic cleavage of the chromogenic substrate S-2586 was used as an indicator for the enzyme's chymotrypsin-like activity. This synthetic peptide contains para-nitro analine on the C-terminus and, upon enzymatic release from the peptide, absorbs light at 405 nm. The change in absorbance at 405 nm over time is therefore an indicator of specific enzymatic activity for chymotrypsin-like enzymes, including PSA. S-2586 is not activated by other kallikreins with trypsin-like activity, such as hK2[72]. Both AG650 and ActPSA showed similarly low activity towards this substrate (Table 3). TPCK – an irreversible proteinase inhibitor of chymotrypsin – was added to determine if there was an inhibitory effect on the enzymatic activity of AG650 in PBS. As shown in Table 3, TPCK did not change the enzymatic activity.

Table 3: Enzymatic Activity of PSA on S-2586

PSA Source*	Activity (ΔA_{405}/hour/µgPSA/ml)	
	Control	100 µg/ml TPCK
AG650	0.0028 ± 0.0013	0.0028 ± 0.0002
ActPSA	0.0032 ± 0.0010	-

Enzymatic activity of PSA on the peptide substrate S-2586 was followed hourly over six hours to determine ΔA_{405}/hour/µgPSA/ml. Error is represented at ± standard deviation in duplicate reactions within 1-2 separate experiments.

Effect of exogenous PSA on cell growth

Since it has been shown that PSA has an effect on cell proliferation in osteoblasts[88], as well as prostate stromal cells[102], the effect of exogenous PSA on the proliferation of the prostate cancer cell lines DU-145 and LNCaP was investigated. Knowledge of any changes in cell proliferation due to PSA was also important in order to account for variation in cell number in future migration/invasion experiments. Cells were seeded and allowed to adhere overnight and the next day, AG650 PSA and ActPSA were added to cells at concentrations of 0.5, 1 and 2 μg/ml in five separate cell culture plates along with controls. At 0, 24, 48, 72 and 96 hours, cell numbers were determined for each PSA concentration using Hoechst-DNA standard curves relating RFU to cell number. Using these data, the PDTs were calculated over the logarithmic growth time period from 48 to 96 hours.

The PDT of DU-145 cells amounted to 23.1 ± 1.3 hours (Figure 3A,B), whereas the LNCaP cells grew more slowly, with a PDT of 31.0 ± 5.0 hours (Figure 3C,D). There was little change in the PDTs of either DU-145 or LNCaP cells when using concentrations of 0.5, 1 or 2 μg/ml of AG650 or ActPSA. Although there was a 27.4% increase in the PDT of DU-145 cells using 2 μg/ml AG650, the difference was not significant most likely due to the large SEM (Figure 3A). Oppositely, there was a 13, 12 and 17% decrease in PDT using 0.5, 1, and 2 μg/ml ActPSA, respectively (Figure 3B). For the LNCaP cells, we observed an increase in PDT when using 1 μg/ml of either AG650 or ActPSA, where the PDT was increased by 16 and 57%, respectively. However, the error was considerable on each of these measurements (Figure 3C,D).

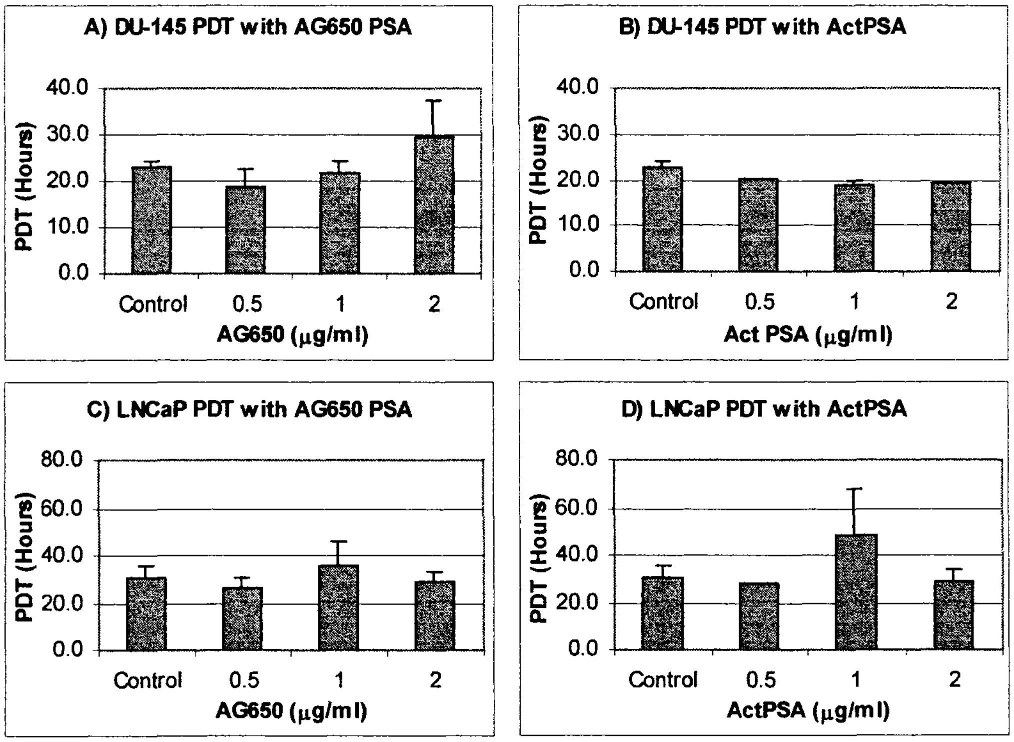

Figure 3: Effects of PSA on population-doubling time of DU-145 and LNCaP cells

DU-145 cells (A,B) were seeded at 1,000 cells/well and LNCaP cells (C,D) were seeded at 5,000 cells/well. After overnight adherence, AG650 PSA or ActPSA were added to the cells in fresh medium at concentrations of 0.5, 1 and 2 μg/ml. Cells were plated in triplicate per 96-well plate and were grown for 4 days in the presence of PSA. The cell number was determined using Hoechst-DNA RFU standard curves. PDTs were determined using the slope of the cell number determined over days 2-4 of the growth curve. Error bars represent SEM of PDTs determined from 2 duplicate experiments, with 4 duplicate wells/day (n = 8).

Standard curves to relate DU-145 and LNCaP cell number to calcein-related fluorescence

The invasion and migration assays each used the hydrolysis of calcein AM and the resulting accumulation of cytoplasmic calcein fluorescence to determine the number of invaded or migrated cells. In order to correlate cell number to cytoplasmic calcein RFU in these experiments, standard curves were created for each the DU-145 and LNCaP cell lines. Cells were serially diluted and incubated with calcein AM to find the linear range correlating cell number with RFU. The standard curves for DU-145 and LNCaP cells are shown in Figure 4. For DU-145 cells, the linear range was found to be 98 – 12,500 cells/well and for LNCaP cells, the linear range was found to be 198 – 12,500 cells/well, each using a linear regression standard curve ($R^2 > 0.99$ for both cell types). It was found that one DU-145 cell produced 0.133 RFU while each LNCaP cell produced 0.299 RFU after a one-hour incubation.

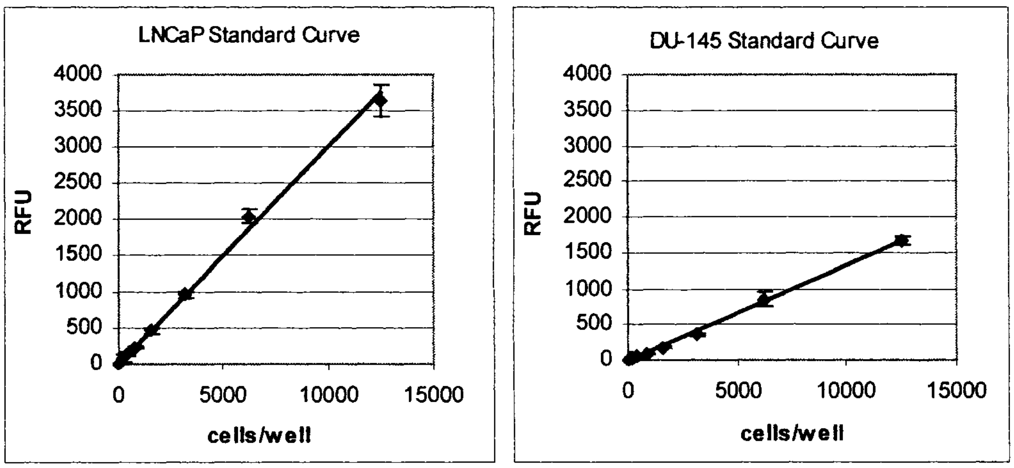

Figure 4: Standard curves relating cell number to calcein fluorescence of LNCaP and DU-145 cells

DU-145 and LNCaP cells were serially diluted, plated in 96-well plates and incubated in "cell dissociation solution" with 2 µg/ml calcein AM for one hour. Calcein levels within the cells were measured by fluorescence at 520 nm using an excitation of 485 nm. Linear regression was used to create a standard curve relating RFU to cell number. DU-145 cells yielded 0.113 RFU/cell (R^2 = 0. 9981) while LNCaP cells gave 0.299 RFU/cell (R^2 = 0.9967). Error bars represent standard deviation from 2-8 duplicates.

Effects of exogenous PSA on DU-145 cell invasion and migration

To test the effects of exogenous PSA on invasion and migration, DU-145 and LNCaP cells were seeded in transmembrane chambers and were allowed to traverse the membrane over 24 hours. Various conditions were used to test for invasive and migratory differences. Medium supplemented with either 0.5 or 10% FBS was used as a chemoattractant in the lower chamber of the invasion well. To test cell invasiveness, BME – used as an *in vitro* simulated BM – was employed at different concentrations to coat the transmembranes in the chambers and act as a barrier to all but invasive cells. For the more invasive DU-145 cells, BME concentrations ranging from 0.1 – 0.05 mg BME/well were used and for the less invasive LNCaP cells, 0.05 – 0.01 mg BME/well were used.

Using 10% FBS-supplemented medium as a chemoattractant for DU-145 cells, an average of 693 ± 65 cells were able to invade through 0.1 mg BME/well and an average of 2343 ± 336 cells were able to invade through 0.05 mg BME/well (Figure 5). This corresponds to 1.4 and 4.7% of the 50,000 cells seeded, respectively. No significant changes were seen in the invasion of DU-145 cells using concentrations of AG650 or ActPSA between 0.5 – 2 μg/ml. Although there appeared to be a dose-dependent decrease in invasion of DU-145 cells using ActPSA and invasion through 0.05 mg BME/well, these results were not statistically significant (p values using Student's t-test > 0.05). Cell migration of DU-145 cells using 10% FBS as a chemoattractant gave RFU readings beyond the linear range of the standard cell curve relating calcein RFU to cell number, therefore were not interpretable (i.e. cell number > 12,500/well). Unfortunately, RFUs determined for the invasion of LNCaP cells using this method were below the linear range of the standard cell curve, therefore cell numbers were not quantifiable (i.e. cell number < 198/well).

Since no significant changes were seen in the invasion or migration of DU-145 cells, the assays conditions were changed. In order to lower possible enzymatic inhibitory effects on PSA by protease inhibitors potentially present in FBS, its concentration was decreased from 10% (v/v) in medium to 0.5% when used as a chemoattractant for the cells. Also, only the lower concentrations of 0.05 mg BME/well for DU-145 cells and 0.01 mg BME/well for LNCaP cells were used in the invasion assays with 0.5% FBS supplemented medium as a chemoattractant. As well, the maximum concentration of PSA used was increased to 5 μg/ml ActPSA, in order to increase the possibility of PSA having an effect on invasion or migration. AG650 was not used in these assays due to potential aberrant results from impurities. DU-145 cells showed an average of 1292 ± 85 cells/well invaded and 953 ± 139 cells/well migrated when growth media supplemented with 0.5% was used as a chemoattractant (Figure 6). This corresponds to 2.6% of cells invaded and 1.9% of cells migrated from the 50,000 cells plated. There was no significant difference in invasion or migration of DU-145 cells using 2 or 5 μg/ml ActPSA. Although there appears to be a dose-dependent decrease in invasion of DU-145 cells using 2 – 5 μg/ml ActPSA, these results were not statistically significant ($p > 0.05$). Similar to the assays using 10% FBS as a chemoattractant, the RFU values determined for the invasion as well as the migration of LNCaP cells was below that seen for the linear range of the calcein RFU standard cell curve, and therefore cell number was not quantifiable.

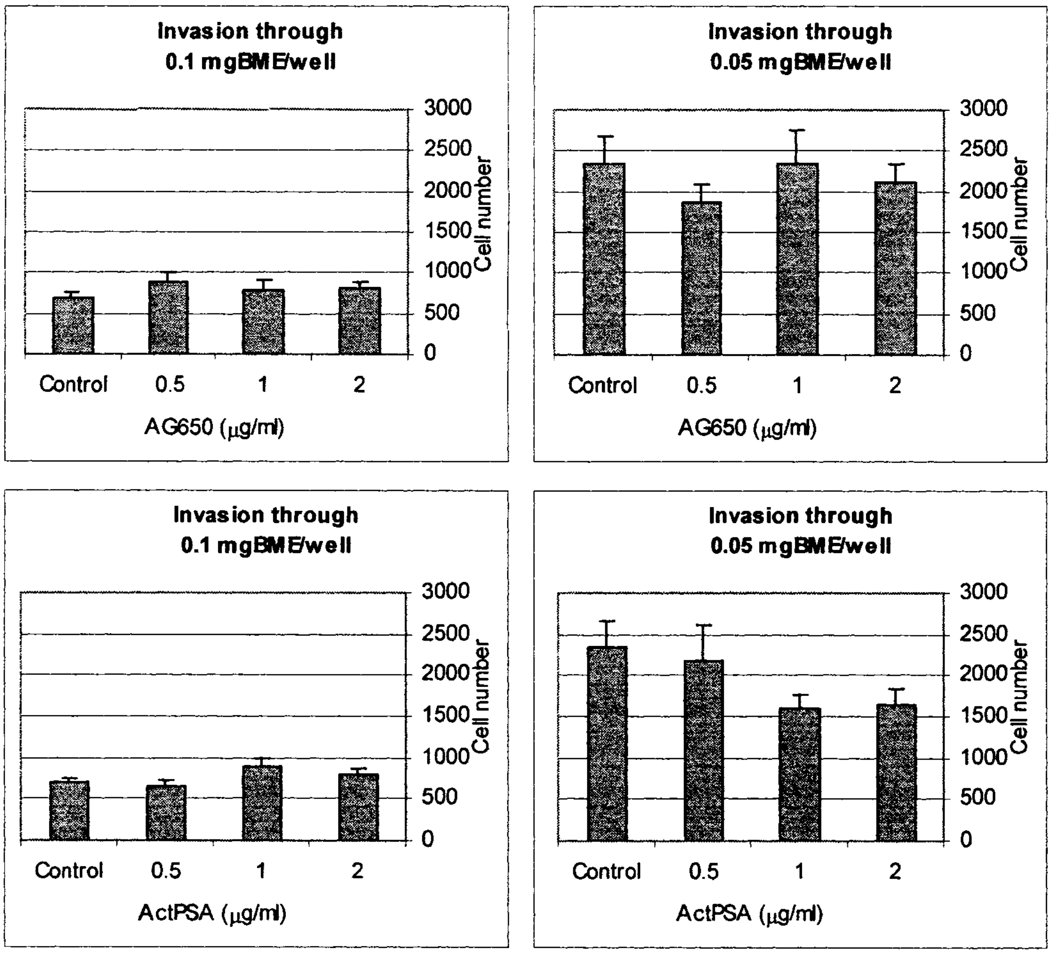

Figure 5: Effect of exogenous PSA on the invasion of DU-145 cells using 10% FBS as a chemoattractant

DU-145 cells were seeded at $5X10^4$ cells/well in SF medium and incubated for 24 hours in invasion chambers with either 0.1 or 0.05 mg BME/well. Varying concentrations of AG650 or ActPSA were added to each well. The bottom wells of the invasion chambers contained DU-145 growth medium supplemented with 10% FBS. After 24 hours, the relative amount of cells on the underside of the membrane (i.e. invaded cells) were determined using the relative fluorescence units (RFU) from hydrolysed calcein AM, representing cell number. Error bars represent SEM from 2 separate experiments, with cells seeded in triplicate.

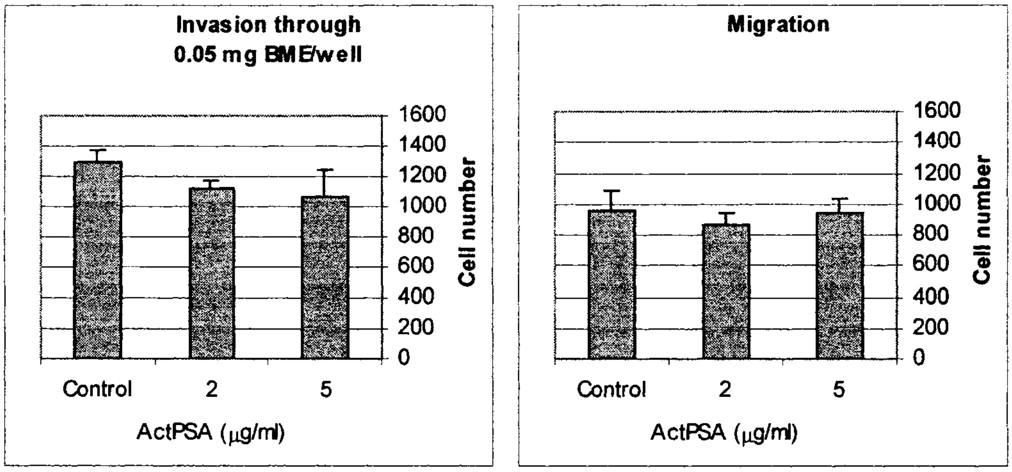

Figure 6: Effect of exogenous ActPSA on the invasion and migration of DU-145 cells using 0.5% FBS as a chemoattractant

DU-145 cells were seeded at 5X10^4 cells/well and incubated for 24 hours in invasion chambers with either 0.05 mgBME/well or lacking BME. Varying concentrations of ActPSA were added to each well. The bottom wells of the invasion chambers contained DU-145 growth medium supplemented with 0.5% FBS. After 24 hours, the relative amount of invaded cells were determined using the relative fluorescence units (RFU) from hydrolysed calcein AM, representing cell number. Error bars represent SEM from 2-3 separate experiments, with cells seeded in duplicate or triplicate.

Creation of the modpSTHMppPSA plasmid

Since the exogenous sources of PSA may not have been purely enzymatically active forms of PSA – as suggested by the multiple bands show in Western blot analysis (Figure 1) – we decided to transfect DU-145 cells with cDNA for the PSA gene. A plasmid vector system using the CMV promoter for high-level constitutive gene expression was chosen for the insertion of PSA cDNA.

In order to create a plasmid with the full length PSA gene, PCR primers were used that amplified a region of the pcDNA3.PSA corresponding to the first 350 bp of the PSA gene. The 31 bp forward primer "Sense pcDNA3.PSA prepro primer A+C" 5'GTTGA<u>GCTAGC</u>ACC*ATG*TGGGTCCCGGTTGT3' contained an NheI restriction site (underlined), and a transcription initiation site (italicized). The 21 bp reverse primer "as new A pcDNA3.PSA prepro primer" 5'CATCACCTGGCCTGAGGAATC3' was a reverse compliment of the PSA coding sequence from 325 – 346 bp downstream of the initiation site. A PCR reaction with these two primers was run using the conditions in Table 1 with an annealing temperature of 59 °C. The product was run on an agarose gel, the ~360 bp fragment (Figure 7A) was excised from the gel and the DNA was isolated. The ends of the isolated PCR product were then cleaved using a double digest with NheI and ClaI restriction enzymes, leaving 4 bp overhangs on the 5' and 3' ends, respectively. The initial coding sequence for Igκ and a portion of the PSA coding region in the plasmid modpSecTagPSA was removed using the restriction enzymes NheI and ClaI. Each digestion product was run on an agarose gel, excised and gel-extracted; the correct PCR product digest was ~333 bp and the modpSecTagPSA digest product was ~6 kb in size (Figure 7B). These digest products were ligated overnight and the ligation product was used to transform competent JM109 *E. coli*. A double restriction digest with NdeI and HindIII was performed on the isolated plasmid DNA to confirm the presence of the "preproPSA" (Figure 7C). The insert was verified by forward DNA sequencing using the primer "Sense pcDNA3.PSA prepro primer A+C" and reverse DNA sequenced using the "as new A pcDNA3.PSA prepro primer", each for ~1kb. A diagram explaining the components of this plasmid is shown in Figure 10.

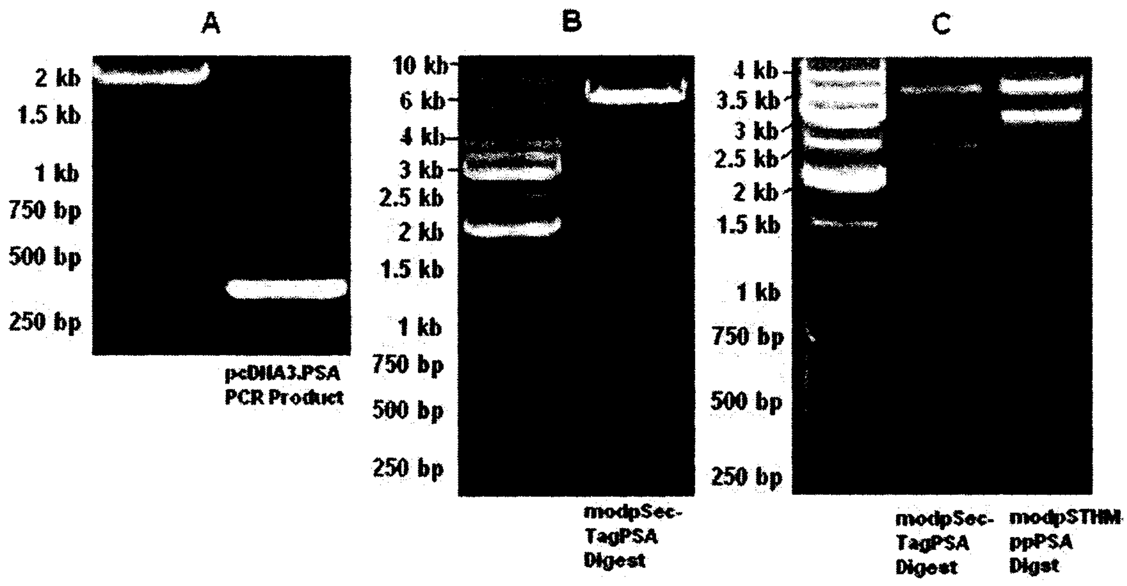

Figure 7: Creation of the modpSTHMppPSA vector

A) PCR reaction using pcDNA3.PSA as a template and the primers "Sense pcDNA3.PSA prepro primer A+C" and "as new A pcDNA3.PSA prepro primer". The amplified region of ~360 bp is shown.

B) ClaI and NheI double digestion of the modpSecTagPSA plasmid. The digestion product bands were observed at ~6.1 kb and 400bp (faintly).

C) NdeI and HindIII double digest to verify a positive JM109 clone with the modpSTHMppPSA plasmid. The digest product bands of modpSecTagPSA observed at ~3.5 kb, 2.4 kb and 513 bp were compared to the digestion product bands of modpSTHMppPSA at ~3.5 kb and 2.7 kb.

Creation of the modpSTHMprePSA plasmid

Not only did we want to express full-length PSA cDNA, we also wanted to create a vector system that would allow expression of enzymatically active PSA without the need for extracellular activation by other proteases. To do this, we created a deletion mutation of the "pro" region to allow mature PSA to be secreted outside of the cell instead of as the zymogen proPSA. The deletion of the "pro" sequence was accomplished such that the secretory "pre" sequence would be in coding sequence with the mature PSA sequence. Proper cleavage of the "pre" region from the prePSA deletion mutant would theoretically yield the secretion of enzymatically active PSA.

To create a plasmid lacking the "pro" region of the PSA gene, a deletion mutation was made from modpSTHMppPSA (a flow diagram of this process is shown in Figure 8). First, two separate PCR reactions were used that flanked the 21 bp "pro" region. The reaction "PCR 1" amplified the 322 bp region from the middle of the CMV promoter to the end of the "pre" region of the modpSTHMppPSA plasmid. This was accomplished by a PCR reaction with an annealing temperature of 58 °C using the sense primer "sense b modpSTHMppPSA" 5'GGCGTGGATAGCGGTTTGAC3' and the anti-sense primer "as mid modpSTHMppPSA" 5'CACTCCCAGCCTCCCACAAT*AGCACCAATCCACGTCACGG3'*. The underlined region compliments the first 20 bp of the mature PSA sequence, and the italicised region compliments the last 20 bp of the "pre" region. The second PCR reaction, "PCR 2", amplified the 332 bp region of modpSTHMppPSA from the beginning to the middle of the mature PSA coding sequence. The "PCR 2" reaction was carried out using the conditions in Table 1, with an annealing temperature of 59 °C, using the anti-sense primer "anti-sense b modpSTHMppPSA" 5'CGGAGCAGCATGAGGTCGTG3' and the sense primer "s mid modpSTHMppPSA" 5'*CCGTGACGTGGATTGGTGCT*ATTGTGGGAGGCTGGGAGTG3'. Again, the italicised region compliments the last 20 bp of the "pre" region and the underlined region compliments the first 20 bp of the mature PSA sequence. The products of the "PCR 1" and "PCR 2" reactions were run on an agarose gel and the 322 bp and 332 bp bands, respectively, (Figure 9A) were extracted from the gel.

The next step was to attach the products of "PCR 1" and "PCR 2" into a linear DNA sequence. To attach the two fragments (360 ng "PCR 1" and 420 ng "PCR 2") both were added together in a PCR reaction using an annealing temperature of 59 °C together with primers "sense b modpSTHMppPSA" and "anti-sense b modpSTHMppPSA". This "PCR 3" reaction takes advantage of the overlapping regions created from "as mid modpSTHMppPSA" and "s mid modpSTHMppPSA", allowing the "PCR 1" and "PCR 2" products to combine. The "PCR 3" product was run on an agarose gel and the ~614 bp-sized band (Figure 9B) gel isolated and 0.58 mg of the isolated fragment was subjected to a double restriction digestion with NheI and ClaI. This product was run on an agarose gel and the ~310 bp-sized band was gel extracted. The plasmid modpSTHMppPSA was also subjected to a double restriction digest with NheI and ClaI and the digestion product run on an agarose gel and the 6.0 kb sized band (Figure 9C) was extracted from the gel. The 310 bp fragment from the "PCR 3" product digestion and the 6.0 kb fragment from the modpSTHMppPSA were ligated together. This ligation product was used to transform competent JM109 *E. coli*, and a double digest with NdeI and ClaI was performed on the isolated DNA to confirm the presence of the "prePSA" insert in the modpSTHMprePSA (Figure 9D). The insert was verified by forward DNA sequencing using the primer "Sense pcDNA3.PSA prepro primer A+C" and reverse DNA sequenced using the "as new A pcDNA3.PSA prepro primer", each for ~1kb. A diagram explaining the components of this plasmid is shown in Figure 10.

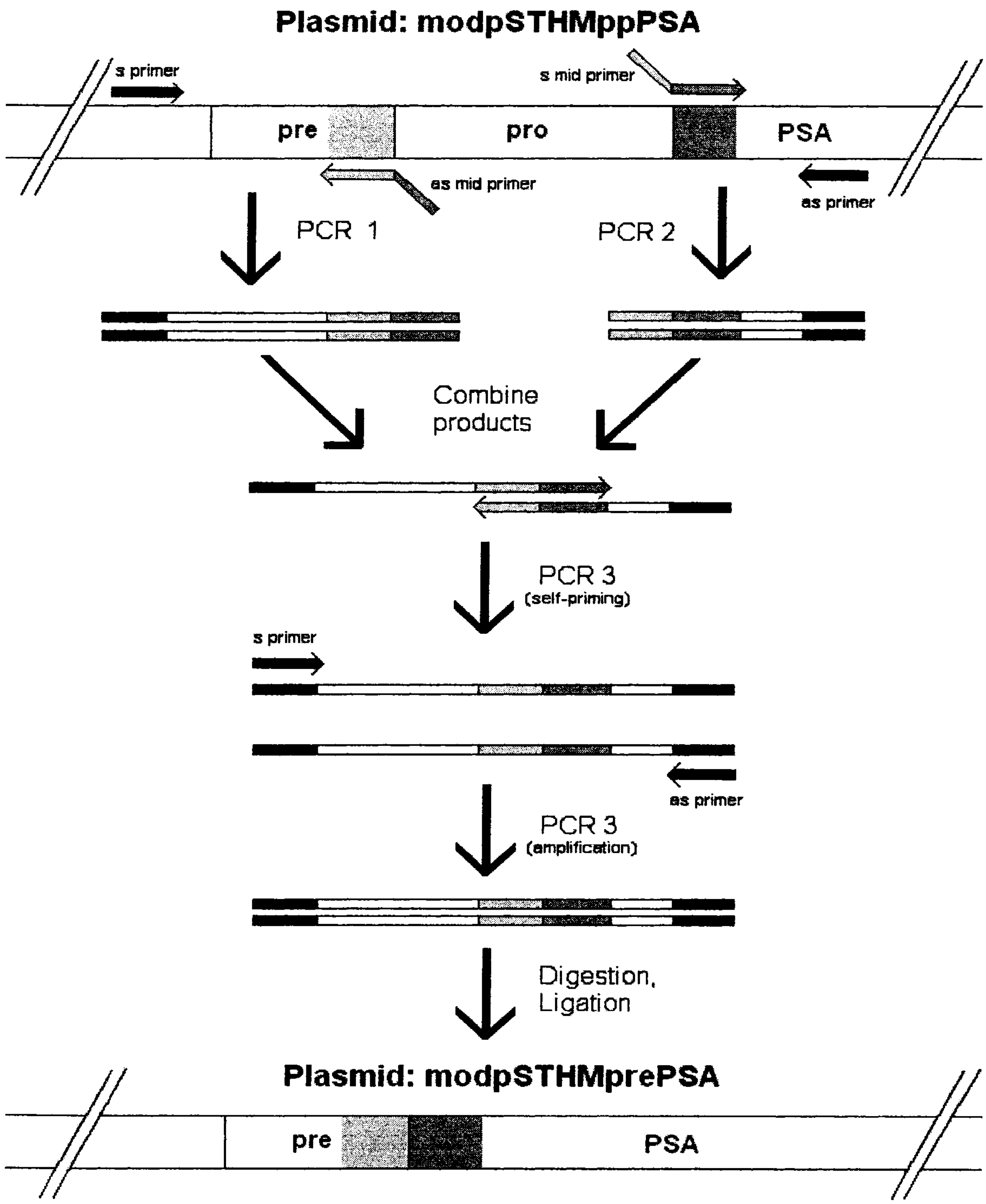

Figure 8: Schematic representation of the PCR based deletion of "pro" region of PSA gene

See the section "<u>Creation of the modpSTHMprePSA plasmid</u>" for details.

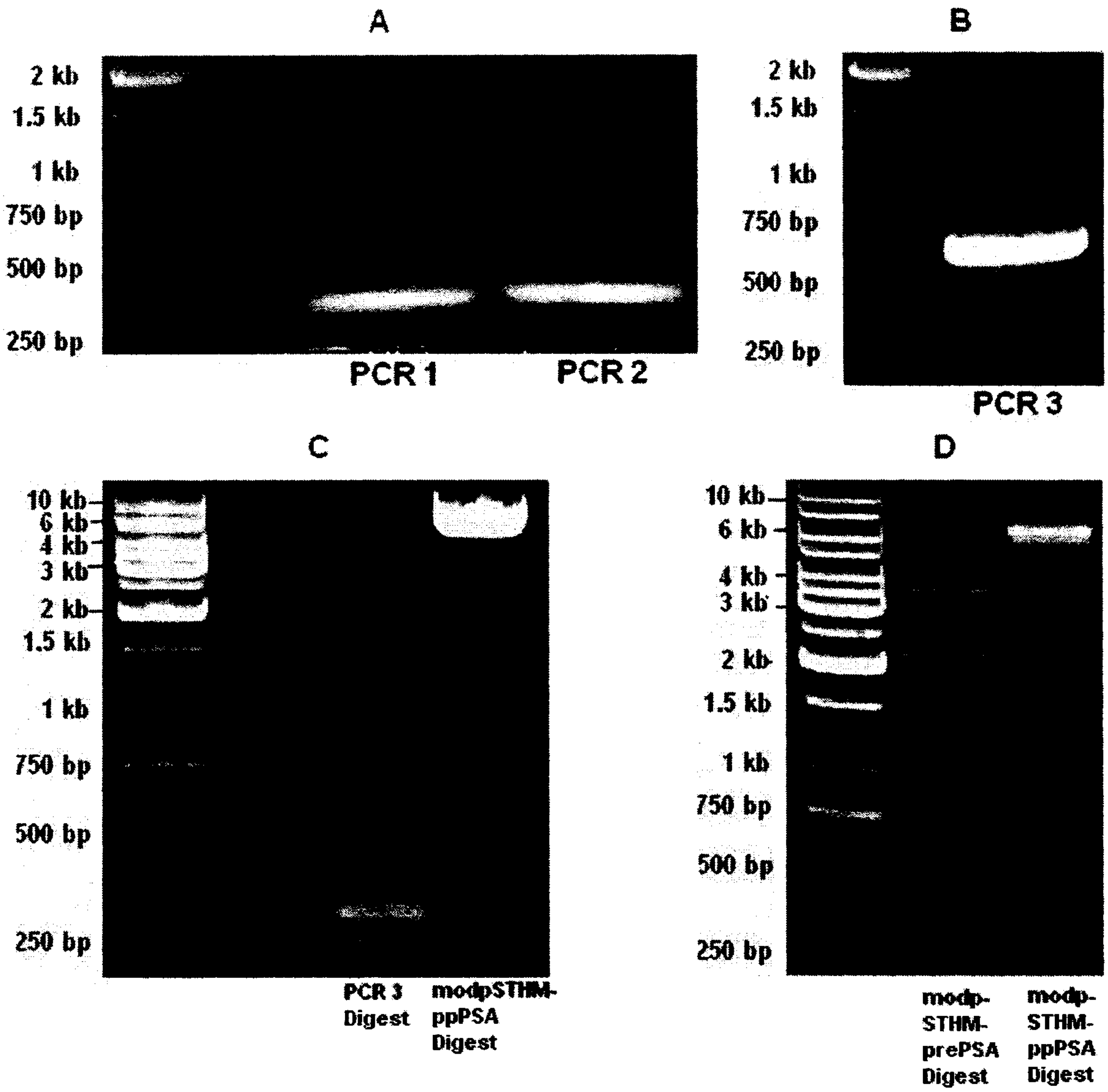

Figure 9: Creation of the modpSTHMprePSA vector

A) Two PCR reactions that surround the "pro" region of the PSA gene. PCR 1: The primers "sense b modpSTHMppPSA" and "as mid modpSTHMppPSA" were used to amplify the band at ~322 bp; PCR 2: The primers "s mid modpSTHMppPSA" and "anti-sense b modpSTHMppPSA" were used to amplify the ~332 bp band.

B) The PCR 3 product was amplified using PCR products of PCR 1 and PCR 2 as well as the primers "sense b modpSTHMppPSA" and "anti-sense b modpSTHMppPSA" to obtain a ~614 bp band.

C) NheI and ClaI double restriction enzyme digestions. PCR 3: digest produced bands at ~310 bp and 253 bp (50 bp fragment not seen). ModpSTHMppPSA: produced bands at ~ 6 kb and 380 bp.

D) NdeI and ClaI double restriction enzyme digestions to verify a positive JM109 clone with the modpSTHMprePSA plasmid. The modpSTHMprePSA digest produced bands at ~3.5 kb, 2.1 kb and 722 bp. As a control, modpSTHMppPSA digest gave bands at ~3.5 kb, 2.1 kb and 743 bp.

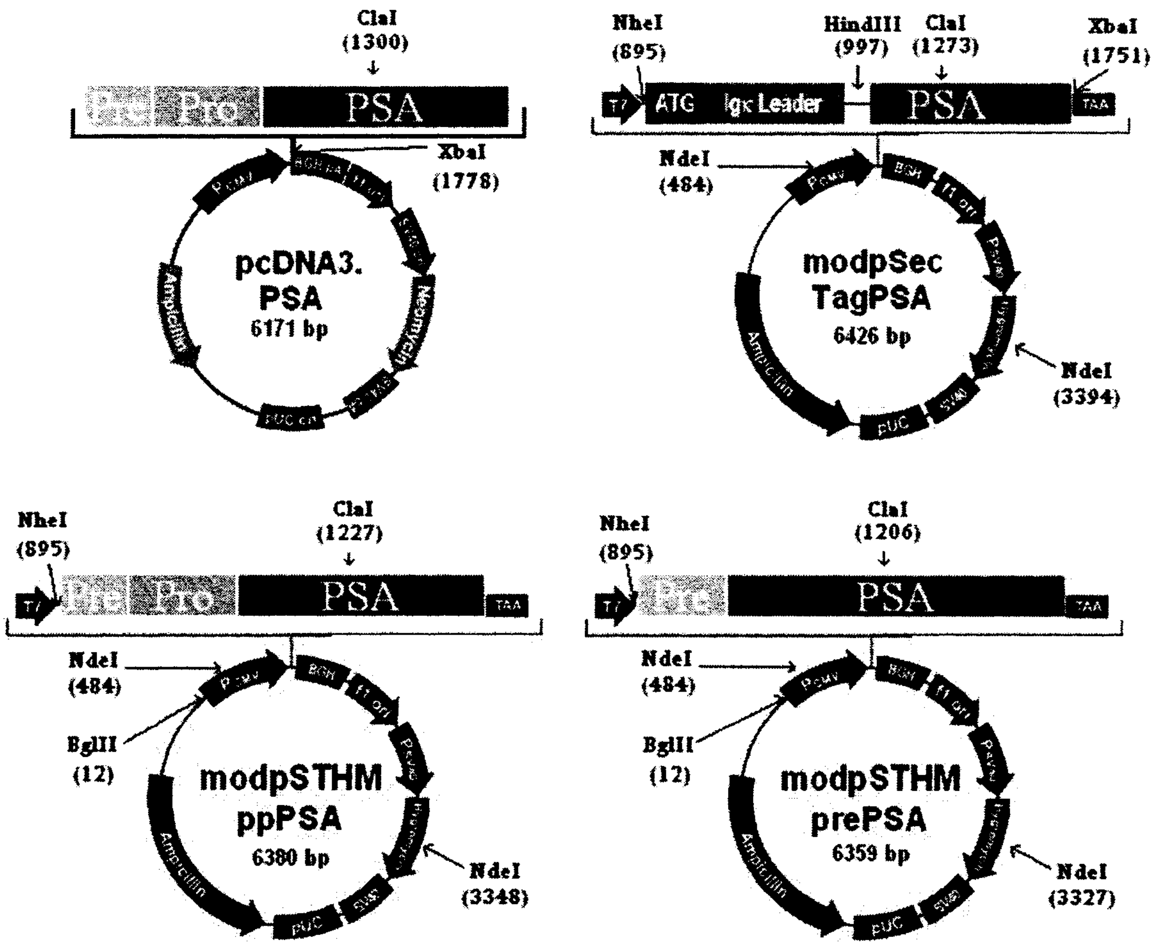

Figure 10: Schematic diagrams of CMV promoter vector systems used*

These pictures represent each respective plasmid in their circularized forms. Extensions above plasmid circle represent the multiple cloning site of the vector with the different versions of the PSA gene inserted. Arrows represent enzymatic digestion sites for the designated restriction enzymes. Vector components:

P_{CMV}	Human cytomegalovirus immediate-early promoter/enhancer for high-level gene expression
T7	T7 promoter/priming site for *in vitro* transcription
Igκ leader	Murine Igκ-chain leader sequence for secretion of fusion protein
TAA	Bovine growth hormone polyadenylation signal for efficient transcription termination and polyadenylation of mRNA
fl ori	fl origin allows rescue of single stranded DNA in bacteria
P_{SV40}	PSV40 early promoter and origin allows efficient, high-level expression of the hygromycin resistance gene and episomal replication in cells expressing the SV40 large T antigen
Hygromycin	Hygromycin resistance gene (Hygromycin B-phosphotransferase) that allows for selection of stable transfectants
SV40	SV40 polyadenylation signal that allows for efficient transcription termination and polyadenylation of mRNA
pUC	pUC origin that allows for high-copy number replication and growth in *E. coli*
Ampicillin	Ampicillin resistance gene (β-lactamase) that allows for selection in *E. coli*

*(all vector diagrams were modified from Invitrogen)

Stable transfection of DU-145 cells with modpSTHMppPSA and modpSTHMprePSA

DU-145 cells were transfected separately with either modpSTHMppPSA or modpSTHMprePSA plasmid DNA, using the methods described in "Standard stable clone creation using electroporation". Electroporation parameters used (with a capacitance of 50 μF) are shown in Table 4. Some cells were transfected with linearized plasmid DNA to increase the chance of a stable transfectants by controlling the site of plasmid cleavage before integration into the DU-145 genome. modpSTHMppPSA and modpSTHMprePSA plasmids were linearized using the restriction enzyme BglII and the linearized plasmids were purified. This digestion results in a single cut in each plasmid within a non-coding region upstream of the CMV promoter. As a vector control, modpSecTagPSA was digested with both NheI and XbaI restriction enzymes to remove the entire PSA gene. The resulting linearized truncated plasmid was run on an agarose gel and the extracted band at ~5.5 kb was used in electroporation for the DU-noPSA clones. Transfected cells were selected using growth media supplemented with 200 μg/ml hygromycin B as a selective agent, a concentration that resulted in ~5% cell survival after 5 days, as determined by previous studies in our lab. Nomenclature of each subclone and the number of colonies isolated is shown in Table 4.

Table 4: Electroporation Parameters for Transfection of DU-145 Cells with modpSTHMppPSA and modpSTHMprePSA Plasmids

Transfected Plasmid	Amount of Plasmid	Cell Number Transfected	Linearization	Voltage	Clone Names	Colonies Isolated
modpSTHMppPSA	3 μg	4 X 10^6	No	1000V then 2000V	D-ppPSA	6
modpSTHMppPSA	3 μg	4 X 10^6	No	1500 V	D-ppPSA	
modpSTHMppPSA	~1-5 μg	4 X 10^6	BglII	1500 V	DU-ppPSA	5
modpSTHMprePSA	3 μg	4 X 10^6	No	1000V X2	D-prePSA	1
modpSTHMprePSA	3 μg	4 X 10^6	No	1500 V	D-prePSA	
modpSTHMprePSA	~1-5 μg	4 X 10^6	BglII	1500 V	DU-prePSA	7
modpSecTagPSA	~1-5 μg	4 X 10^6	NheI and XbaI	1500 V	DU-noPSA	7

Expression of PSA from stable and transient DU-145 transfects

To screen the stable D(U)-ppPSA and D(U)-prePSA clones for secretion of PSA, CM was analyzed using Western blotting. A band corresponding to PSA was only visible from two of the ppPSA clones: D-ppPSA-1 (Figure 11A) and DU-ppPSA-2 (Figure 11B). However, PSA in the CM of each of these clones was only detected from cells growing the second passage after transfection. All subsequent passages of each clone were negative for PSA as determined by Western blot analyses, even after concentration of SF CM as much as 25 times using a 10 kDa cut-off filter. PSA was not detectable in the CM of any of the D(U)-prePSA clones, regardless if the CM was concentrated.

Since the presence of PSA was not observed in the D(U)-prePSA CM, transient transfections were performed to assess whether the modpSTHMprePSA was able to produce PSA within DU-145 cells. DU-145 cells were transiently transfected with 1 and 2 μg of modpSTHMprePSA using lipofectamine. Western blot analyses were performed on 2 and 3 day CM (Figure 11C). PSA was detectable using both amounts of plasmid on days 2 and 3 in a plasmid dose-dependent manner. This proved that the prePSA deletion mutant encoded in the modpSTHMprePSA plasmid could be expressed by DU-145 cells and that this form of PSA was detectable using Western blotting.

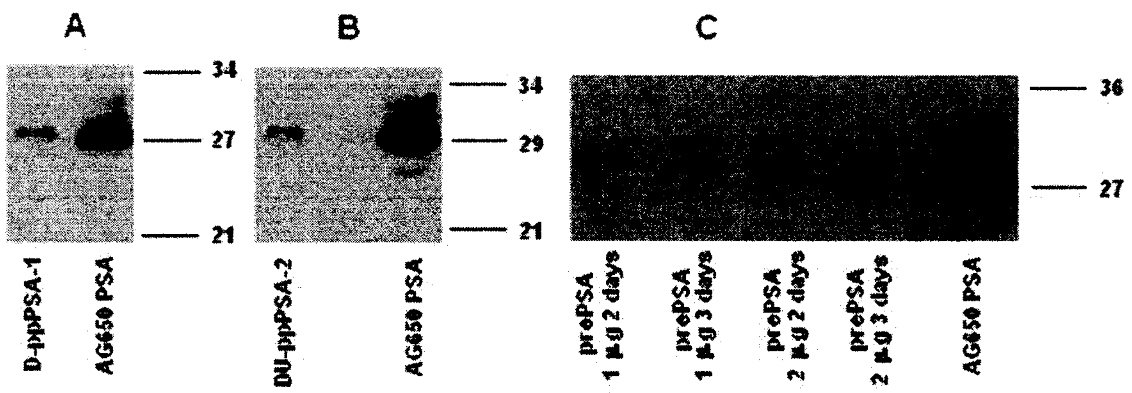

Figure 11: Expression of PSA using the CMV promoter system

Western blots showing PSA from stably transfected clones (A,B) and transient transfections (C,D). AG650 PSA: 20 ng of protein was added per well. A+B) 33 µl of 3 day serum-supplemented CM from D-ppPSA-1 (A) or DU-ppPSA-2 (B) the 2nd passage after transfection. C) CM of DU-145 cells transfected with 1-2 µg modpSTHMprePSA, which was conditioned for 2 or 3 days post transfection. 33 µl of CM was loaded per lane.

Stable Transfection of DU-145 cells with pERV3

Since stable clones of DU-145 cells transfected with modpSTHMppPSA and modpSTHMprePSA did not show stable expression of PSA, we decided to create clones of DU-145 cells that could express ppPSA and prePSA in an inducible manner. A double transfection system was chosen that used a combination of a plasmid encoding a PonA inducible transcriptional activator (pERV3) and a cloning vector with a binding site for the transcription activator (pEGSH). Diagrams for these plasmids are shown in Figure 15. Stable transfection with pERV3 is this first step in this system, in order to obtain a cell line that expresses VgEcR, a transcriptional activator that is turned on by PonA.

DU-145 cells were electroporated with pERV3 using the electroporation parameters shown in Table 5. For some transfections, the restriction enzyme PstI was used to linearize the plasmid pERV3. This results in a single cut in the region upstream of the CMV promoter; the linearized plasmid was purified and used in electroporation to maximize the chances of obtaining a stable clone. Transfectants were grown in medium containing 400 μg/ml G418 as a selective agent. This concentration was selected because it was the lowest concentration that resulted in 5% of cells surviving in 5 days (Figure 12). Nomenclature and number of clones isolated of each subclone are shown in Table 5.

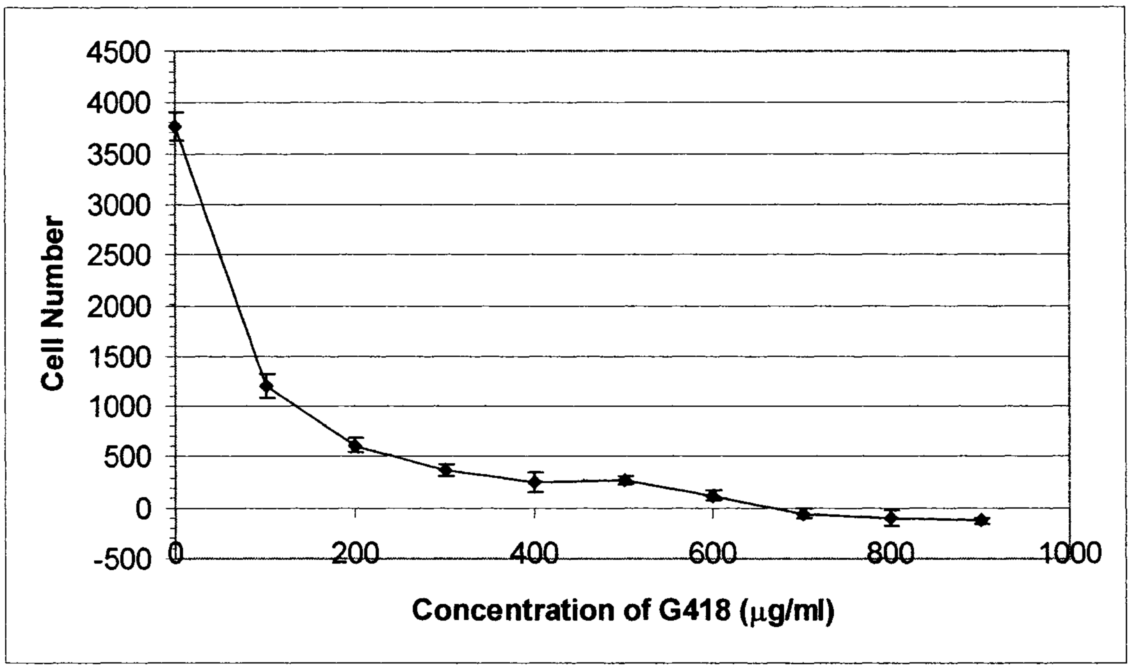

Figure 12: Cytotoxicity of G418 in DU-145 cells

DU-145 cells seeded at 400 cells/well were treated with varying concentrations of G418. After a period of 5 days, DNA content/well was determined using the Hoechst-DNA assay and compared to control cells. Error bars represent SEM of 8 replicates per experiment from 2 identical experiments.

Table 5: Electroporation parameters for transfecting pERV3 into DU-145 cells

Transfected Plasmid	Amount of Plasmid	Cell Number Transfected	Linearization	Voltage	Clone Names	Colonies Isolated
pERV3	3 μg	4 X 10^6	No	1500 V	DU-pERV3 A	9
pERV3	6 μg	4 X 10^6	No	1500 V	DU-pERV3 B	9
pERV3	7.6 μg	4 X 10^6	PstI	1500 V	DU-pERV3 C	9

Selection of a stable DU-pERV3 clone using the luciferase assay

In order to select a stable DU-pERV3 clone, each clone was subjected to the luciferase assay. To accomplish this, cells were transiently transfected with the pEGSH-luc plasmid – a pEGSH construct encoding the luciferase gene – and cell lysates were assayed for luciferase activity. A clone positive for VgEcR expression from the pERV3 plasmid should show an increasing amount of luciferase activity with an increasing amount of PonA. This was observed for the clone DU-pERV3 C3, a subline transfected with linearized pERV3. The DU-pERV3 C3 clone showed a useful level of induction (Figure 13), while all other DU-pERV3 clones tested showed similar induction patterns to the parent DU-145 cells (data not shown). There was also an increasing level of induction in the DU-pERV3 C3 cells as the amount of transiently transfected pEGSH-luc decreased. The percent increase of RLU over control when induced by 10 μM PonA was 255 ± 108, 674 ± 321, and 1875 ± 836% when transiently transfected with 7.5, 1.0 and 0.1 μg pEGSH-luc respectively. This is strong evidence for stable expression of the VgEcR transcription activator, because when less pEGSH-luc is used in the transient transfection, there will be a lower copy number of plasmids per cell. Since there are fewer plasmids per cell, there is a greater ratio of VgEcR proteins to pEGSH-luc plasmids within each cell to be able to regulate the luciferase gene. Therefore, as plasmid copy number goes down, the percent induction goes up. The DU-pERV3 C3 clone was chosen for secondary transfection with the pEGSH constructs containing ppPSA and prePSA.

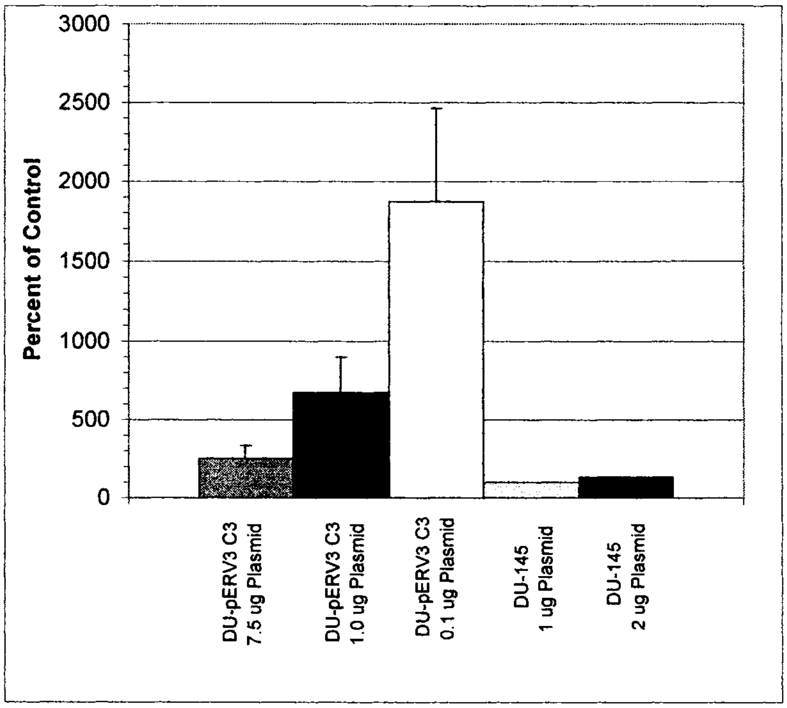

Figure 13: Luciferase assay of pEGSH-luc transfected DU-pERV3 C3 and DU-145 cells

DU-pERV3 C3 and DU-145 cells (5 X 10^5 each) were transiently transfected with the amount of pEGSH-luc shown. Cell lines were incubated overnight post transfection in 0 μM or 10 μM PonA. Cell lysates were harvested and a luciferase assay done to determine the level of luciferase activity in the cells. RLU values of the cells treated with 10 μM PonA were compared as a percentage of the RLU from the solvent control treated cells. Error bars represent SEM of 2-3 identical experiments.

Creation of the pEGSHppPSA plasmid

To insert the full-length preproPSA cDNA sequence into the pEGSH plasmid, primers were used that amplified an 879 bp segment containing the preproPSA gene from the modpSTHMppPSA. The 33 bp forward primer "s BamHI pmodSTHM to pEGSH" 5'GTTGAGGATCC*GCCACCATG*TGGGTCCCGGTTG3' contained a BamHI site (underlined) and a modified Kozak sequence (italicized). The 22 bp reverse primer "as BamHI pmodSTHM to pEGSH" 5'GATGGTCGACGGCGCTATTCAG3' was reverse complimentary to a region outside of the XhoI restriction site on the modpSTHMppPSA plasmid, downstream of the preproPSA gene stop codon. The PCR reaction was run using the conditions in Table 1 with an annealing temperature of 60.5 °C. The product was run on an agarose gel, the ~879 bp fragment (Figure 14A) was excised from the gel and the DNA was isolated. The ends of the isolated PCR product were then removed using a double digest with BamHI and XhoI restriction enzymes. Similarly, pEGSH was also digested using BamHI and XhoI (both in the MCS) to allow insertion of the PCR product. Each digestion product was run on an agarose gel, excised and gel-extracted; the correct PCR product digest was ~802 bp and the pEGSH digest product was ~4.8 kb in size (Figure 14B). These digestion products were ligated overnight and the ligation product was used to transform competent JM109 *E.coli*. A restriction digest with PstI was performed on the plasmid DNA to confirm the presence of the "preproPSA" insert in the pEGSH plasmid (Figure 14C). The insert was verified by forward DNA sequencing using the primer "s BamHI pmodSTHM to pEGSH" and reverse sequencing using the primer "as new C pcDNA3.PSA prepro primer" each for ~1kb. A diagram explaining the components of this plasmid is shown in Figure 15.

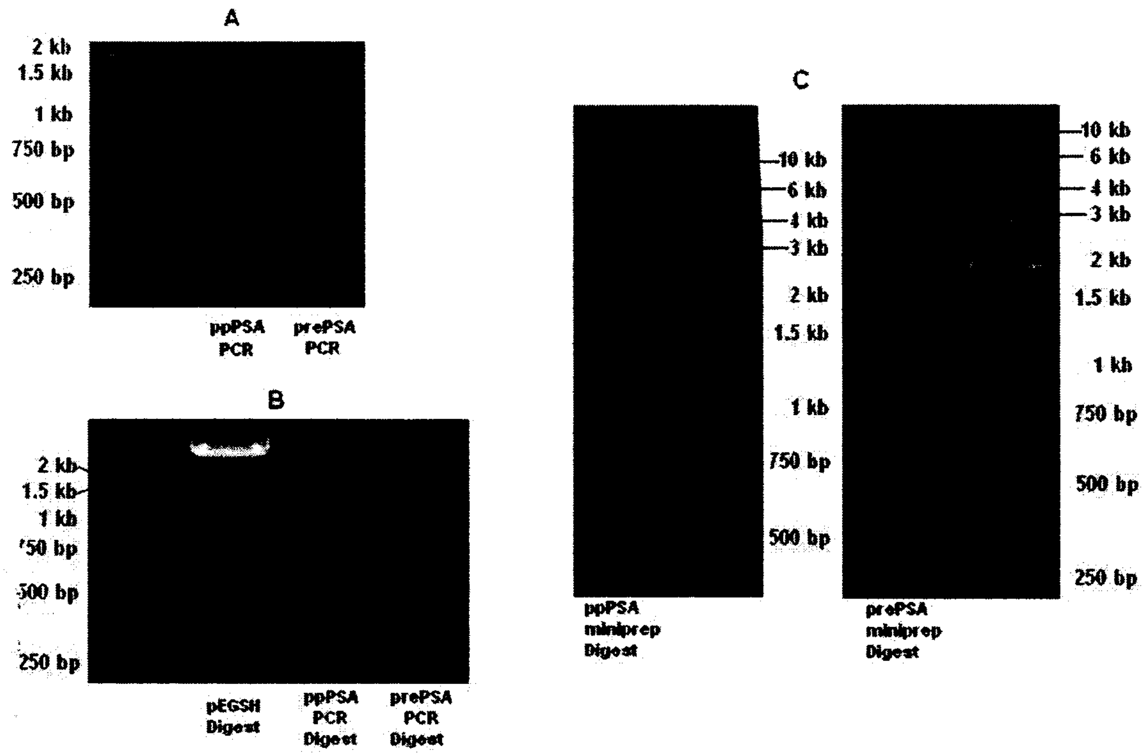

Figure 14: Creation of the pEGSHppPSA and pEGSHprePSA Vectors

A) PCR products of amplified PSA genes from the different modpSTMH plasmids. ppPSA PCR: amplified preproPSA from modpSTHMppPSA using the primers "s BamHI pmodSTHM to pEGSH" and "as BamHI pmodSTHM to pEGSH" to create an ~879 bp band; prePSA PCR: amplified prePSA from modpSTHM using the primers "s BamHI pmodSTHM to pEGSH" and "as BamHI pmodSTHM to pEGSH" to create an ~858 bp fragment.

B) BamHI and XhoI double restriction enzyme digestion of pEGSH and PCR products for ligation. pEGSH digest: gave a band at ~4.8 kb; ppPSA PCR digest: gave a band at 801 bp; prePSA digest: gave a band at 780 bp.

C) PstI restriction enzyme digestion to verify positive JM109 clones. ppPSA miniprep digest: gave bands at ~3.7 kb, 1.5 kb and 393 bp; prePSA digest: gave bands at ~3.7 kb, 1.5 kb, and 393 bp.

Creation of the pEGSHprePSA plasmid

To insert the prePSA gene into the pEGSH plasmid, primers were used to amplify an 858 bp segment containing the prePSA gene in modpSTHMprePSA. The 33 bp forward primer "s BamHI pmodSTHM to pEGSH" 5'GTTGAGGATCC*GCCACCATG*TGGGTCCCGGTTG3' contained a BamHI site (underlined) and a modified Kozak sequence (italicized). The 22 bp reverse primer "as BamHI pmodSTHM to pEGSH" 5'GATGGTCGACGGCGCTATTCAG3' was reverse complimentary to a region outside of the XhoI restriction site on the modpSTHMprePSA plasmid, downstream of the prePSA gene stop codon. The PCR reaction was run using the conditions in Table 1 with an annealing temperature of 60.5 °C, and the product was run on an agarose gel. The ~858 bp fragment (Figure 14A) was excised from the gel and the DNA was isolated. The ends of the isolated PCR product were then removed using a double restriction enzyme digest with BamHI and XhoI. Similarly, pEGSH was also cleaved in the MCS with BamHI and XhoI restriction enzymes to allow insertion of the PCR product. Each digestion product was run on an agarose gel, excised and gel-extracted; the correct PCR product digest was ~776 bp and the pEGSH digest product was ~4.8 kb in size (Figure 14B). These digest products were ligated overnight and the ligation product was used to transform competent JM109 *E.coli*. A restriction digest with PstI was performed on the plasmid DNA to confirm the presence of the "prePSA" insert in the pEGSH plasmid (Figure 14C). The insert was verified by forward DNA sequencing using the primer "s BamHI pmodSTHM to pEGSH" and reverse sequencing using the primer "as new C pcDNA3.PSA prepro primer", each for ~1kb. A diagram explaining the components of this plasmid is shown in Figure 15.

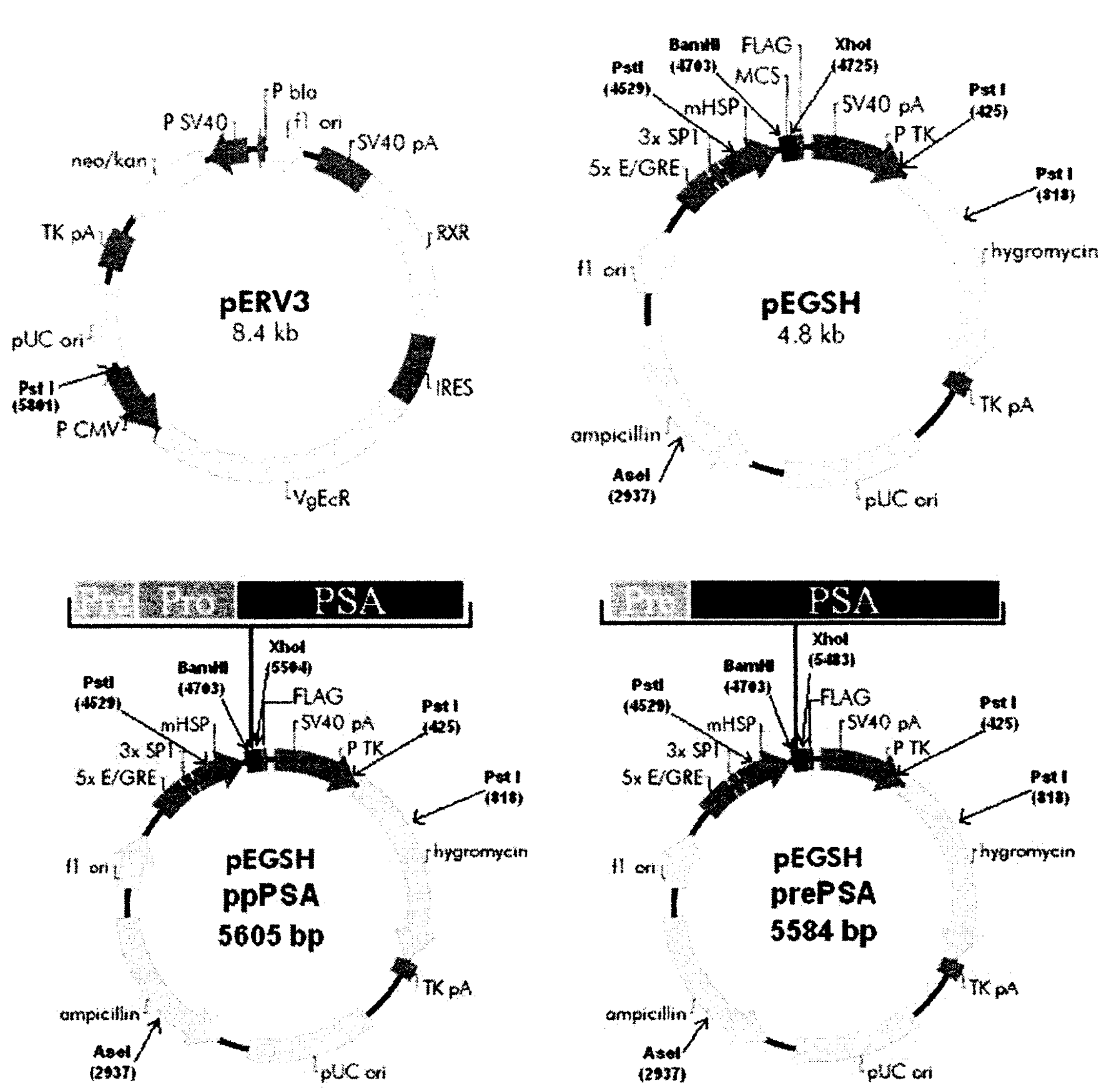

Figure 15: Schematic diagrams of Complete Control® vectors used*

These pictures represent each respective plasmid in their circularized forms. Extensions above plasmid circle represent the multiple cloning site of the vector with the different versions of the PSA gene inserted. Arrows represent enzymatic digestion sites for the designated restriction enzymes. Vector components**:

RXR	retinoid-X-receptor ORF
IRES	internal ribosome entry site
VgEcR	synthetic VP16-glucocorticoid/ecdysone receptor ORF
TK pA	HSV-thymidine kinase polyA signal
neo/kan	neomycin/kanamycin resistance ORF
P bla	*bla* promoter
P TK	HSV-thymidine kinase promoter
5 X E/GRE	5 X ecdysone/glococorticoid responsive elements
3 X SP1	3 X Sp1 binding sites
mHSP	minimal heat shock promoter
FLAG	FLAG tag

* (all vector diagrams were modified from Stratagene)

** (for explanation of the functions of the following components, see Figure 10: f1 ori, SV40 pA, P CMV, pUC ori, hygromycin, P SV40)

Stable transfection of DU-pERV3 C3 Cells with pEGSHppPSA, pEGSHprePSA and pEGSH

DU-pERV3 C3 cells were electroporated with pEGSH, pEGSHppPSA, and pEGSHprePSA using the parameters shown in Table 6. Some cells were transfected with linearized plasmid DNA to increase the chance of a stable transfectants by controlling the site of plasmid cleavage before integration into the DU-145 genome. The restriction enzyme AseI was used to linearize pEGSHppPSA and pEGSHprePSA prior to transfection. This enzyme cleaves the plasmid only once in the middle of the ampicillin resistance portion of the gene. As a vector control, DU-pEVR3 C3 cells were transfected with an empty pEGSH vector.

To select for plasmid positive clones, transfectants were grown in medium containing 400 μg/ml G418 and 100 μg/ml hygromycin B as selective agents. The concentration of G418 was chosen as this was the concentration used to select for DU-pERV3 clones. The concentration of hygromycin B was selected as it was the lowest concentration that resulted in ~5% cell survival in 5 days when 400 μg/ml G418 was already present (Figure 16). After 2 weeks growth of the transfected DU-pERV3 C3 cells, the hygromycin B concentration was increased to 150 μg/ml to increase selective pressure for the pEGSH plasmid constructs. Nomenclature of each subclone and the number of clones isolated is shown in Table 6.

Table 6: Electroporation Parameters for Transfecting pEGSH, pEGSHppPSA and pEGSHprePSA plasmids into DU-pERV3 C3 Cells

Transfected Plasmid	Amount of Plasmid	Cell Number Transfected	Linearization	Voltage	Clone Names	Colonies Isolated
pEGSHppPSA	3 μg	2×10^6	AseI	1500 V, then 1000 V	DU-pERV3 C3 ppPSA	18
pEGSHprePSA	3 μg	2×10^6	AseI	1500 V, then 1000 V	DU-pERV3 C3 prePSA	18
pEGSH	3 μg	2×10^6	No	1500 V	DU-pERV3 C3 EGSH	3

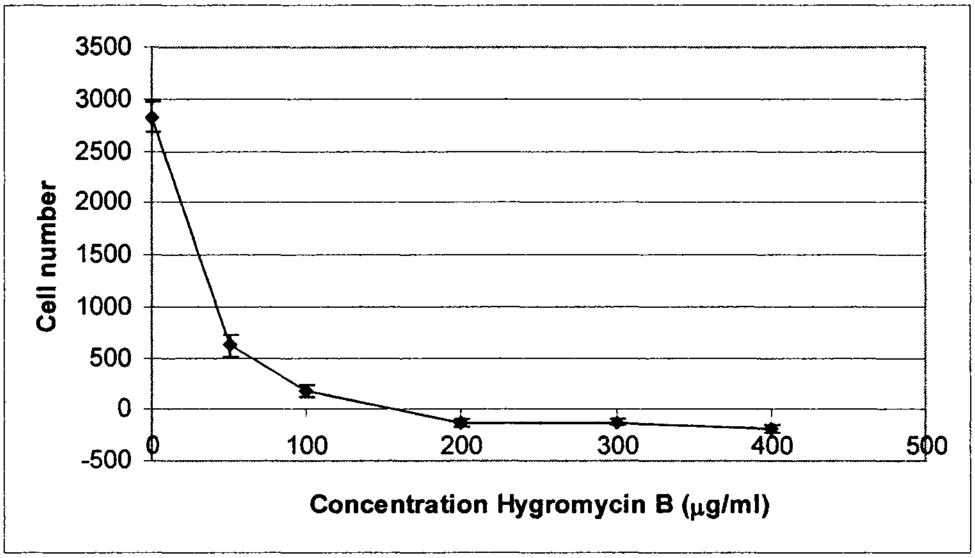

Figure 16: Cytotoxicity of hygromycin B with 400 μg/ml G418 in DU-pERV3 C3 cells

DU-pERV3 C3 cells seeded at 400 cells/well were treated with varying concentrations of hygromycin B with a constant concentration of 400 μg/ml G418. After a period of 5 days, DNA content/well was determined using the Hoechst-DNA assay and compared to control. Error bars represent SEM of 8 replicates per experiment from 2-4 identical experiments.

Detection of recombinant PSA cDNA in genomic DNA of DU-pERV3 C3 ppPSA/prePSA subclones

In order to detect the presence of an integrated portion of the recombinant PSA cDNA gene in the genome of the DU-pERV3 C3 ppPSA and prePSA subclones, a PCR reaction was used to differentiate the introduced PSA cDNA from genomic *klk3* DNA. Genomic DNA was isolated from each ppPSA/prePSA subclone, as well as the control EGSH subclones, the parent DU-145 line and the LNCaP cell line. A 379 bp region of the PSA cDNA was amplified from the location 225 – 603 bp downstream of the start codon. To differentiate between integrated PSA cDNA and the naturally occurring *klk3* gene, primers were designed that surrounded the fourth intron of the genomic PSA encoding gene that spans 171 bp. The amplification of the *klk3* gene segment extends across 550 bp compared to an amplification of integrated PSA cDNA which spans 379 bp. The forward primer "PSA sense B 225-246" 5'GGTCGGCACAGCCTGTTTCATC3' corresponds to bases 225 – 246 downstream of the start codon of PSA cDNA, and the reverse primer "PSA anti-sense B 582-603" 5'GCGTCCAGCACACAGCATGAAC3' corresponds to the reverse compliment of bases 582 – 603 downstream of the start codon in PSA cDNA. A PCR reaction was run for each clone using the conditions in Table 1 with an annealing temperature of 60 °C and an extension time of 30 seconds. The results of the PCR amplification of genomic DNA from DU-145, LNCaP and DU-pERV3 C3 subclones transfected with pEGSH constructs are shown in Figure 17. As expected, PCR amplification of all of the DU-pERV3 C3 ppPSA (with the possible exception of ppPSA2) and DU-pERV3 C3 prePSA genomic DNA showed the presence of the *klk3* gene with a band at ~550 bp (upper band) as well as the presence of the PSA cDNA with a band at ~379 bp (lower band). Amplification using the DU-145, LNCaP or DU-pERV3 C3 pEGSH genomic DNA produced only the single band at ~550 bp and did not show a band at 379 bp, indicating the absence of PSA cDNA. These results verify that the portion of the PSA cDNA from 225 – 603 bp downstream of the start codon was integrated into the genome of the DU-pERV3 C3 ppPSA and prePSA subclones.

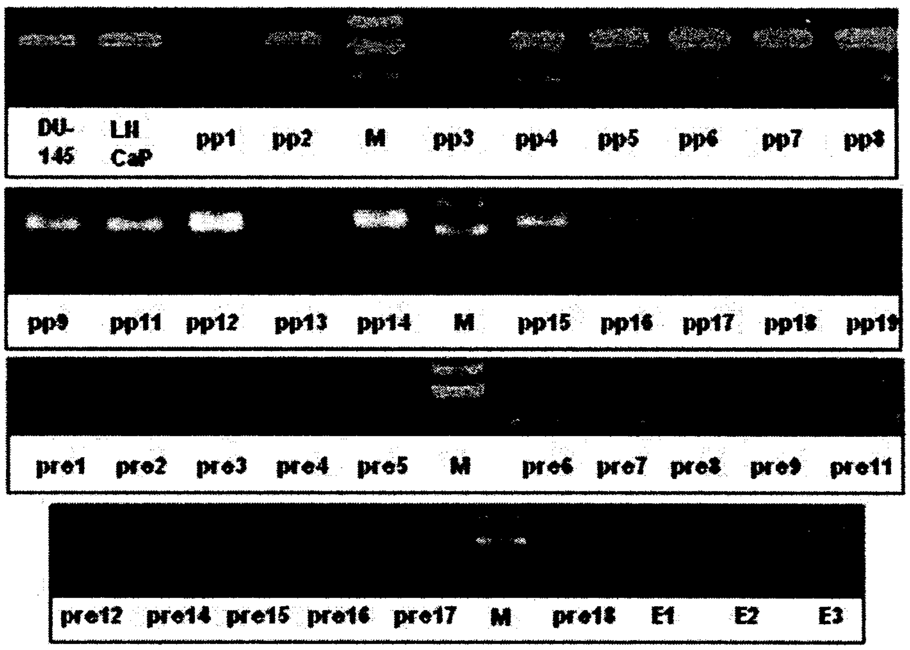

Figure 17: Detection of PSA cDNA inserted into genomic DNA

Genomic DNA from DU-145, LNCaP and DU-pERV3 C3 subclones transfected with pEGSH constructs were subjected to PCR amplification. Primers used spanned a 379 bp region of PSA cDNA (lower band), and 550 bp region in the wild type hK3 gene (upper band). pp#: refers to DU-pERV3 C3 ppPSA sublcones; pre#: refers to DU-pERV3 C3 prePSA subclones; E#: refers to DU-pERV3 C3 pEGSH subclones; M: molecular weight markers of 600 bp (upper), 500 bp (middle), 400 bp (lower).

Induction of PSA secretion from DU-pERV3 C3 ppPSA/prePSA subclones using ponasterone A

After determining that all of the DU-pERV3 C3 ppPSA/prePSA subclones contained PSA cDNA in their genome, clones were tested for their ability to secrete PSA when induced with PonA. A total of three DU-pERV3 C3 ppPSA subclones (pp6, pp9 and pp13), two DU-pERV3 C3 prePSA subclones (pre2 and pre7) were chosen for further study. These subclones were chosen as, upon initial screening, they showed high expression of recombinant PSA when induced with 10 μM PonA. As well, two DU-pERV3 C3 pEGSH subclones (E2 and E3) were chosen randomly for use as vector control cells. To induce PSA expression, each subclone was seeded in selective growth medium, and the next day the medium was changed to SF medium, containing either 10 μM PonA or a solvent control. Cells were allowed to condition the SF medium for 4 – 5 days, then the CM was concentrated using 10 kDa cut-off filters and assayed for PSA levels using Western blot analysis. Each of the pp6, pp9, pp13, pre2 and pre7 subclones tested showed PSA secretion into the medium regardless of the presence of PonA (Figure 18). The pp-subclones produced a PSA band at 29 kDa while the pre-subclones produced a band for PSA at 28 kDa. No PSA was detected in CM obtained from the vector control E2 or E3 cells.

Although the DU-pERV3 C3 ppPSA and DU-pERV3 C3 prePSA subclones did secrete PSA in the absence of PonA, there were marked increases in the level of PSA secretion ranging from 132.5 – 280.2% when induced by 10 μM PonA (Table 7). The levels of PSA secreted from the DU-pERV3 C3 ppPSA cells ranged from 0.119 – 0.461 ng/ml/10^5cells/day and the levels of PSA secreted from the DU-pERV3 C3 ppPSA cells ranged from 0.034 – 0.218 ng/ml/10^5cells/day. These values ranged from ~18 – 250 fold lower than secreted by LNCaP cells, which produce 8.6 ± 3.5 ng/ml/10^5cells/day.

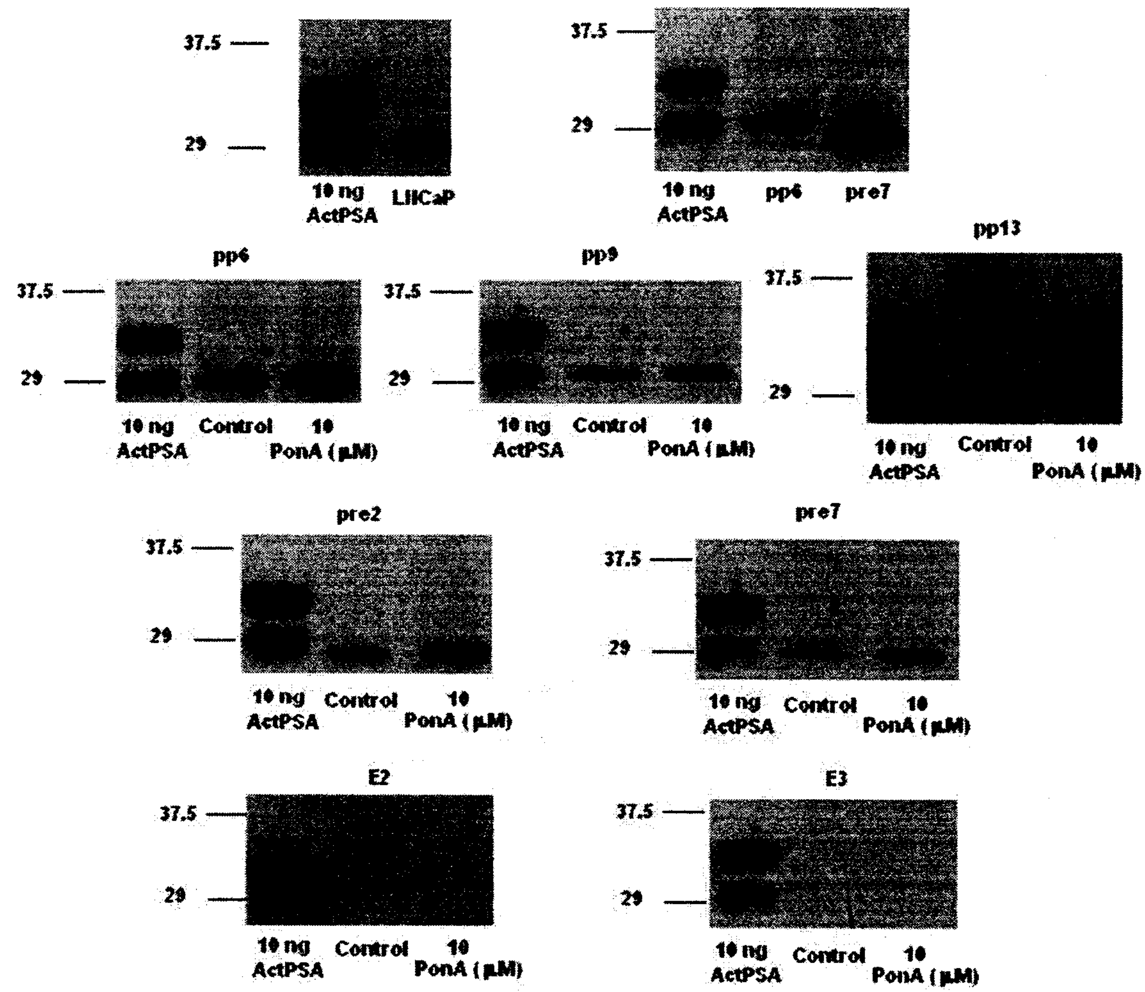

Figure 18: Western blot showing PSA expression from DU-pERV3 C3 ppPSA and DU-pERV3 C3 prePSA subclones

Western blotting was used to determine relative levels of PSA secretion between PonA-induced and solvent control cells. SF conditioned media was collected from DU-pERV3 C3 ppPSA/prePSA/EGSH subclones after a period of 4 – 5 days in the presence of 10 μM PonA or a solvent control. CM was concentrated with a 10 kDa cut-off filter and media loaded in each individual gel was standardized to cell number. Each individual blot represents the difference between control and 10 μM PonA induced, but do not relate relative PSA levels between the clones.

Table 7: PSA secretion level and percent PonA-induction using densitometry of Western blotting of DU-pERV3 C3 ppPSA/prePSA conditioned media

10 μM PonA Induced Subclone	Secreted PSA Level ($ng/ml/10^5 cells/day$)*	% Secreted PSA (untreated control)
DU-pERV3 C3 ppPSA6	0.461 ± 0.072	236.7 ± 9.3
DU-pERV3 C3 ppPSA9	0.119 ± 0.041	273.8 ± 104.0
DU-pERV3 C3 ppPSA13	0.145 ± 0.055	132.5 ± 29.4
DU-pERV3 C3 prePSA2	0.034 ± 0.010	280.2 ± 39.5
DU-pERV3 C3 prePSA7	0.218 ± 0.184	207.6 ± 38.3
LNCaP	8.6 ± 3.5	-

*PSA levels were calculated using a linear regression standard curve created from densitometry of three ActPSA standards per Western blot (1 – 20 ng/lane). Cell number was determined on the day CM was collected. Error is represented as ± SEM from 2-3 measurements.

Enzymatic activity of conditioned media from DU-pERV3 C3 ppPSA/prePSA/EGSH subclones on S-2586

In order to test for enzymatic activity of PSA secreted by each the DU-pERV3 C3 ppPSA and DU-pERV3 C3 prePSA subclones, conditioned medium was collected and concentrated. Cells were allowed to condition the medium for 5 days, and media was concentrated using a 10 kDa cut-off filter. As a control used to simulate the conditions for enzymatic activity of PSA in CM, ActPSA was diluted in SF DU-145 medium as a sample buffer and used as an enzymatic activity control. As well, to increase the chances of seeing small amounts of PSA activity, the concentration of S-2586 was increased from 0.4 mM to 0.8 mM.

Activity of ActPSA on the substrate S-2586 was detectable at a concentration of 10 μg/ml but not at 0.8 μg/ml. The levels of PSA in the concentrated CM were below the level detectable by this assay (Table 8). Furthermore, the concentrated CM from all of the DU-pERV3 C3 subclones showed activity on S-2586, regardless of TPCK concentration. Due to the low levels of PSA produced and the activity of concentrated

DU-pERV3 C3 ppPSA/prePSA/EGSH media on the substrate, no correlation was seen between enzymatic cleavage of S-2586 and clones that secreted PSA.

Table 8: Enzymatic activity of DU-pERV3 C3 ppPSA/prePSA/EGSH conditioned medium on the chromogenic substrate S-2586

Sample Source	Control	10 μM PonA	Control with 100 μg/ml TPCK	10 μM PonA with 100 μg/ml TPCK	[PSA] in Reaction (ng/ml)**	Medium Concentration Level
ActPSA*	0.0020	-	0.0018	-	10,000	-
pp6	0.0062	0.0052	0.0089	0.0097	37 (54)	40.2 X
pp9	0.0036	0.0035	0.0083	0.0090	10 (21)	30.8 X
pp13	0.0245	0.0184	0.0225	0.0172	197 (378)	220 X
pre2	0.0049	0.0057	0.0051	0.0069	5 (12)	51.7 X
pre7	0.0365	0.0482	0.0379	0.0490	32 (50)	220 X
E2	0.0330	0.0333	0.0332	0.0411	0	230 X
E3	0.0026	0.0027	0.0059	0.0042	0	35.5 X

Medium was conditioned by the various subclones and concentrated using a 10 kDa cut-off filter. ΔA_{405}/hr was calculated over 0 – 6 hours of activity. *ActPSA values are in ΔA_{405}/hr/ngPSA/ml. All other values are in ΔA_{405}/hr. ** PSA concentration is reported as control and (10 μM PonA).

Population-doubling time analysis of DU-pERV3 C3 ppPSA/prePSA/EGSH subclones

The PDTs of each the DU-pERV3 C3 ppPSA, DU-pERV3 C3 prePSA and DU-pERV3 C3 pEGSH subclones were analyzed to determine if any growth changes were apparent between the different PSA-expressing subclones. As well, since the DU-pERV3 C3 ppPSA and DU-pERV3 C3 prePSA showed an increase in PSA expression levels with an increase of PonA, the growth differences were determined between PonA induced and control cells. Each subclone was seeded in DU-145 medium containing solvent control, 1 or 10 μM PonA for 5 days. Each day, the cell numbers were determined, and using the numbers from hours 72, 96 and 120, population-doubling times were calculated (Figure 19). PDTs did not vary significantly for any of the cell lines using different concentrations of PonA, nor was there any significant variance in the PDT between the

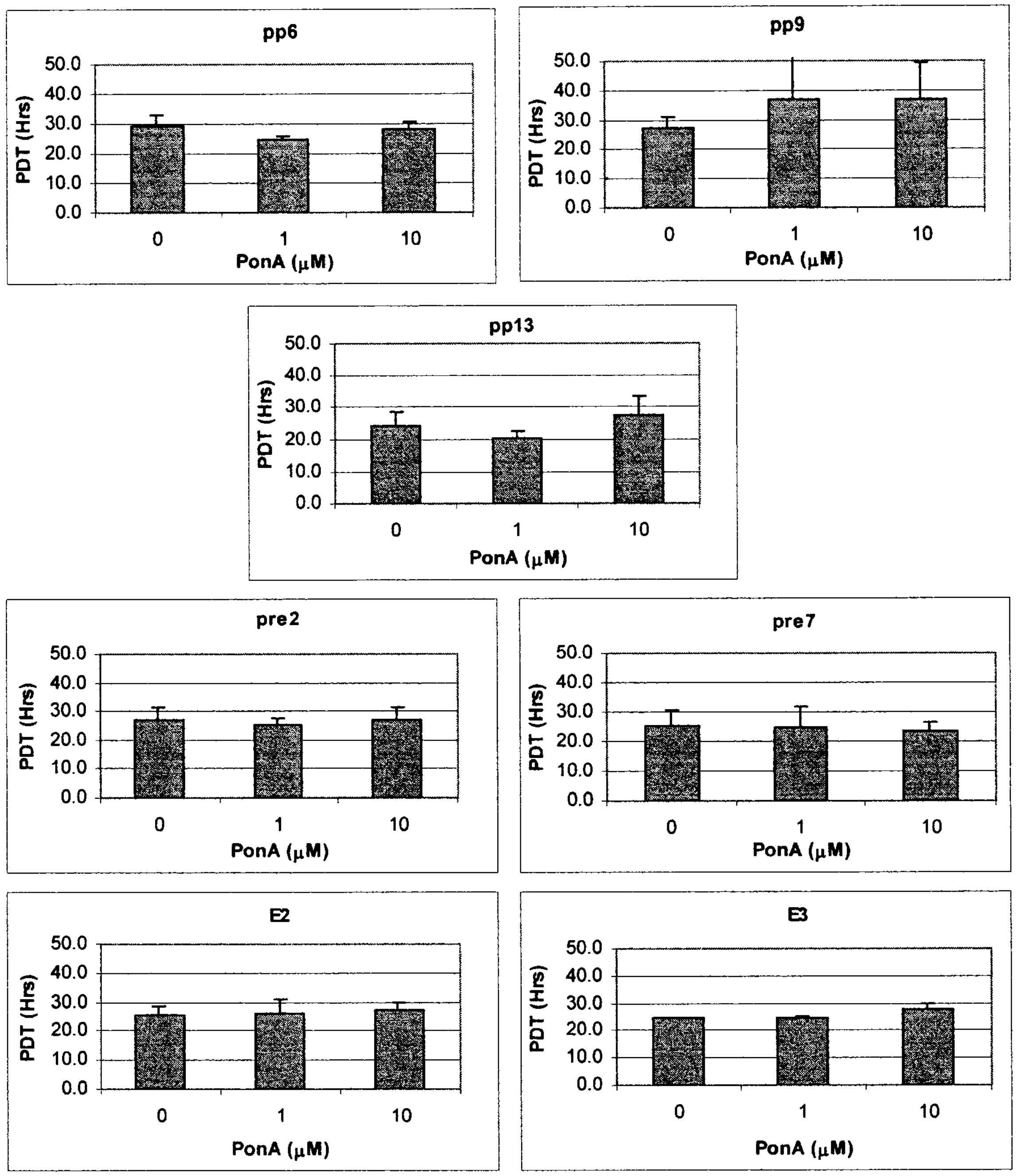

Figure 19: Population-doubling times of DU-pERV3C3ppPSA, DU-pERV3C3prePSA and DU-pERV3C3pEGSH subclones with varying amounts of PonA

Population-doubling times for DU-pERV3C3ppPSA, DU-pERV3C3prePSA and DU-pERV3C3pEGSH subclones were determined using linear regression of the growth curve over 72 – 120 hours. Error bars represent SEM from PDTs determined from 2 identical experiments.

clones ($p > 0.05$). Although the PDTs for pp9 using 1 and 10 μM PonA were 133.4% and 134.3% higher than that of the 0 μM PonA control respectively, this difference is not significant probably due to the relatively large variance.

Standard curves to relate pp6, pre2 and E3 cell number to calcein related fluorescence

In order to accurately measure the number of invaded or migrated cells, standard curves relating calcein RFU to cell number were created for the pp6, pre2, and E3 clones. Each subclone was serially diluted and incubated with calcein AM to find the linear range correlating cell number with RFU. The standard curves for pp6, pre2 and E3 are shown in Figure 20. The three subclones tested showed a near identical correlation of cell number to RFU. For all cells, the linear range was found to be 98 – 12,500 cells/well, the same as for DU-145 cells. It was found that one pp6 cell produced 0.157 RFU, one pre2 cell produced 0.150 RFU, and one E3 cell produced 0.150 RFU ($R^2 > 0.99$ for all three subclones). These standard curves were used to calculate the number of cells in migration/invasion assays. To calculate the cell number of a subclone for which there was no standard curve, a standard curve from another subclone of the same type was used (i.e. to calculate pp9 or pp13 cell number, the standard curve created for pp6 was used).

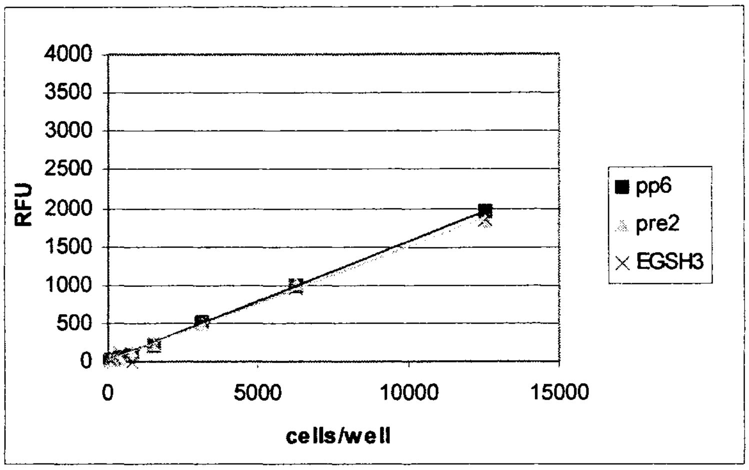

Figure 20: Standard curves relating cell number to calcein fluorescence of pp6, pre2 and E3 cells

pp6, pre2 and E3 cells were serially diluted, seeded in a 96-well plates and incubated in "cell dissociation solution" with 2 μg/ml calcein AM for one hour. Calcein levels within the cells were measured by fluorescence at 520 nm using an excitation of 485 nm. Linear regression was used to create standard curves relating RFU and cell number. pp6 cells yielded 0.157 RFU/cell (R^2 = 0.9987), pre2 cells yielded 0.150 RFU/cell (R^2 = 0.9970), and E3 cells yielded 0.150 RFU/cell (R^2 = 0.9938). Data points represent 2 duplicates.

Differences in the invasion and migration between DU-pERV3 C3 ppPSA/prePSA/EGSH subclones

Migration and invasion assays of DU-pERVC3ppPSA/prePSA/EGSH subclones were used to determine any changes induced by the different forms of PSA. The effects of PonA induction of PSA were also tested by comparing the difference between invasion and migration of 10 μM PonA induced cells with untreated control cells. DU-145 medium containing 0.5% FBS was used as a chemoattractant through transwell membranes over a 24 hour period, with a coating of 0.05 mg BME/well for invasion assays.

Significant differences were seen in the invasive and migratory abilities of the different subclone types, however no significant difference was seen within each subclone when the cells were induced with PonA. The percentage of invasion and migration of pp and pre subclones compared to empty vector control (E subclone) cells can be seen in Table 9 and Table 10, respectively.

Each of the pp6, pp9 and pp13 subclones showed increased invasion (Figure 21) compared to the E2 and E3 cells, and a smaller increase in migration (Figure 22), regardless of the concentration of PonA. However, this increase was not statistically significant for any of the subclones, with the exception of the invasiveness of pp13 compared to E2 without PonA induction. Interestingly, there was variability between the pp subclones: pp6 showed nearly equal invasion and migration, pp9 showed a higher migration than invasion, and, oppositely, pp13 showed a higher invasion than migration. Furthermore, the migration level of pp13 cells was lower than E2 cells when comparing non-induced controls, which was in stark contrast to the significant increase in pp13 invasion compared to E2 invasion. This variability did not reflect the amount of PSA produced by each subclone, as pp6 produced ~ 4 times as much PSA as the pp9 subclone and ~ 3 times as much PSA as the pp13 subclone, whereas the pp13 subclone showed the highest invasion levels and the pp9 subclone showed the highest levels of migrations. In general, the invasion and migration of pp subclones was higher than those of the EGSH vector control.

Conversely, there was a large decrease in both the invasiveness (Figure 21) and migration (Figure 22) of the pre2 and pre7 subclones as compared to the E2 and E3 empty vector controls. These results were found to be statistically significant (p values < 0.05), with the exception of the pre2 and pre7 when compared to the migration of E2 in the presence of 10 μM PonA. The invasion of the pre2 subclone was as low as 28.6% of the E3 control and the invasion of the pre7 subclone was as low as 32.2% of the E3 control. The difference in migration was similar, with the migration of the pre2 subclone being as low as 62.9% compared to E2 and the pre7 subclone being as much as 67.6% lower that E2. Although the pre7 subclone produced ~ 6.5 times more PSA than the pre2 subclone, the migration and invasion rates of each subclone were very similar. Interestingly, although the pre2 and pre7 subclones showed the lowest invasion of all of the subclones, there was an increase in their invasiveness with 10 μM PonA as compared to the solvent control. However, a similar increase was seen in the E2 and E3 subclones.

When comparing the DU-pERV3 C3 ppPSA and prePSA subclones in both invasion and migration, there was an obvious and statistically significant increase of the pp subclones over the pre subclones ($p < 0.05$). These data show that ppPSA-expressing subclones markedly increased invasion and migration as compared to the prePSA-expressing subclones.

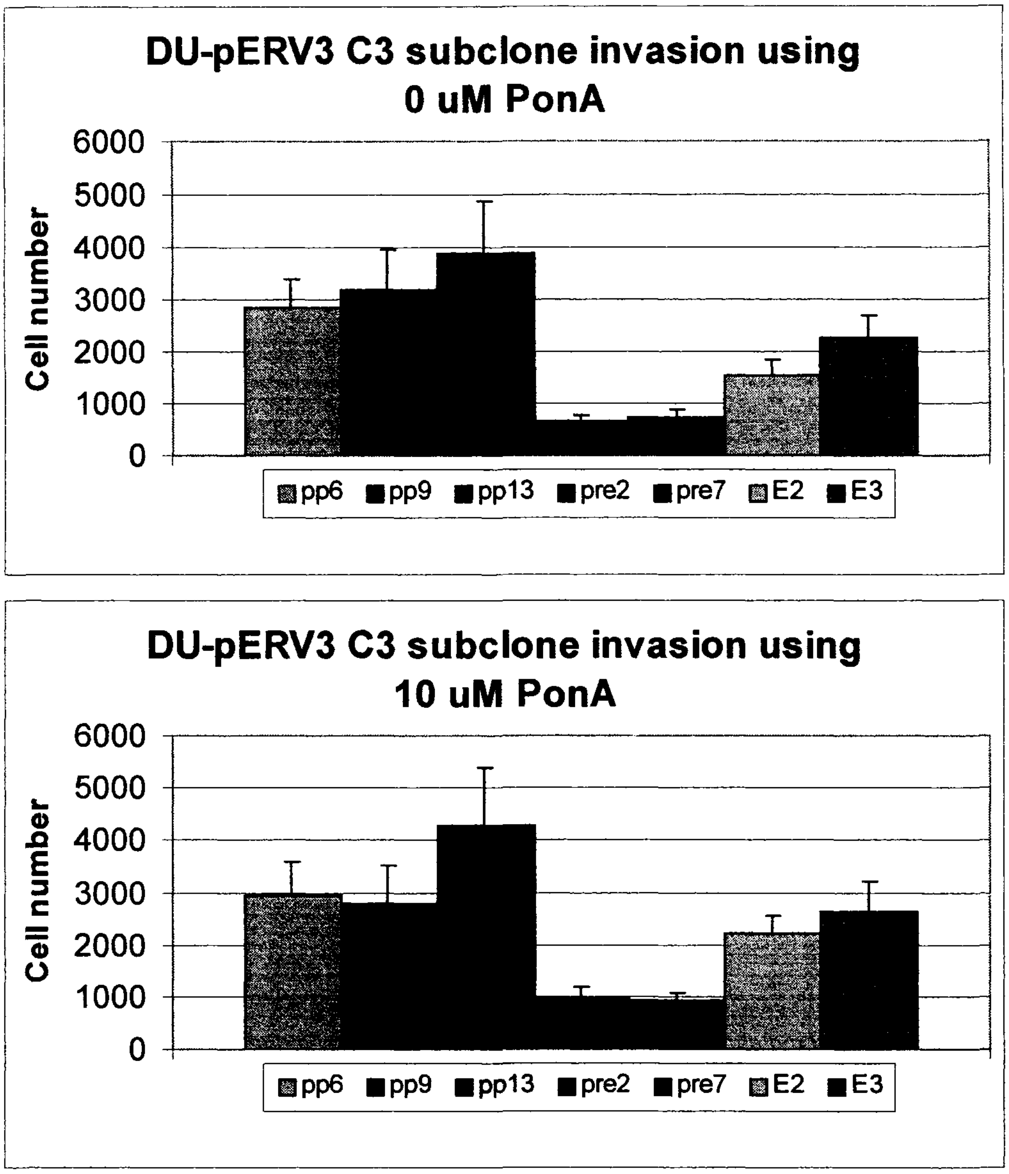

Figure 21: Invasion of DU-pERV3 C3 ppPSA/prePSA/EGSH cells through 0.05 mg BME/well

DU-pERV3C3ppPSA/prePSA/EGSH cells were seeded at $5X10^4$ cells/well in SF medium and incubated for 24 hours in invasion chambers with 0.05 mg BME/well. Cells were seeded along with either 10 μM PonA or a solvent control. The bottom wells of the invasion chambers contained DU-145 medium supplemented with 0.5% FBS as a chemoattractant. After 24 hours, the number of invaded cells was determined using the relative fluorescence units (RFU) from hydrolysed calcein AM, and cell number determined using the appropriate standard curve. Error bars represent SEM from 3 separate experiments, with cells seeded in duplicate.

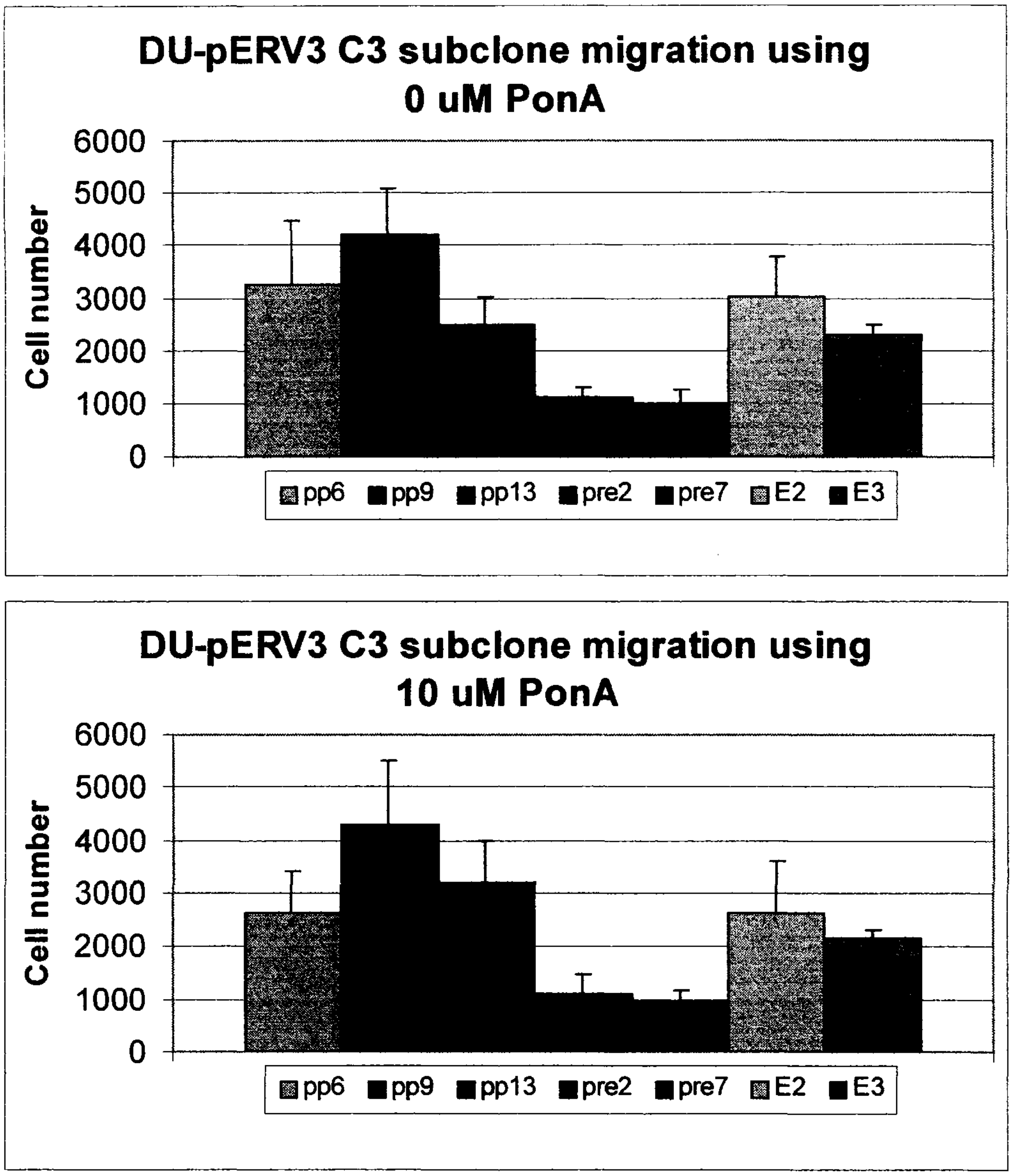

Figure 22: Migration of DU-pERV3 C3 ppPSA/prePSA/EGSH cells

DU-pERV3C3ppPSA/prePSA/EGSH cells were seeded at $5X10^4$ cells/well in SF medium and incubated for 24 hours in migration chambers. Cells were seeded along with either 10 μM PonA or a solvent control. The bottom wells of the migration chambers contained DU-145 medium supplemented with 0.5% FBS as a chemoattractant. After 24 hours, the number of migrated cells was determined using the relative fluorescence units (RFU) from hydrolysed calcein AM, and cell number determined using the appropriate standard curve. Error bars represent SEM from 3 separate experiments, with cells seeded in duplicate.

Table 9: Comparison of invasive capabilities of DU-pERV3 C3 ppPSA and prePSA subclones compared to DU-pERV3 C3 EGSH controls

Subclone	Percent invasion of control E2	Percent invasion of 10 μM PonA E2	Percent invasion of control E3	Percent invasion of 10 μM PonA E3
pp6	184.8 ± 34.7	132.4 ± 27.7	124.3 ± 23.4	112.5 ± 23.5
pp9	208.9 ± 48.4	124.5 ± 33.8	140.5 ± 32.5	105.8 ± 28.7
pp13	254.2 ± 63.1*	191.8 ± 49.2	170.9 ± 42.5	162.9 ± 41.8
pre2	42.6 ± 7.3*	42.5 ± 11.1*	28.6 ± 4.9*	36.1 ± 9.5*
pre7	47.8 ± 10.7*	40.3 ± 8.0*	32.2 ± 7.2*	34.2 ± 6.8*
E2	100.0 ± 20.0	100.0 ± 14.7	67.2 ± 13.4	84.9 ± 12.5
E3	148.7 ± 27.8	117.7 ± 25.3	100.0 ± 18.7	100.0 ± 21.5

Conditions for invasion assay are described in Figure 21. Subclones were compared as a percentage of total E2 or E3 invaded cells. Error represents percent SEM from 3 separate experiments with cells plated in duplicate. * Indicates p value < 0.05 using Student's t-test.

Table 10: Comparison of invasive capabilities of DU-pERV3 C3 ppPSA and prePSA subclones compared to DU-pERV3 C3 EGSH controls

Subclone	Percent migration of control E2	Percent migration of 10 μM PonA E2	Percent migration of control E3	Percent migration of 10 μM PonA E3
pp6	107.4 ± 41.3	99.5 ± 29.7	140.5 ± 54.0	121.1 ± 36.1
pp9	139.7 ± 29.0	162.8 ± 46.7	182.8 ± 37.9	198.0 ± 56.9
pp13	81.9 ± 17.9	120.5 ± 30.7	107.1 ± 23.4	146.6 ± 37.3
pre2	37.1 ± 6.2*	42.4 ± 14.3	48.5 ± 8.1*	51.6 ± 17.3*
pre7	32.4 ± 6.9*	36.6 ± 10.6	42.4 ± 9.0*	44.5 ± 12.9*
E2	100.0 ± 25.2	100.0 ± 36.9	130.8 ± 32.9	121.7 ± 44.9
E3	76.4 ± 6.1	82.2 ± 5.7	100.0 ± 8.0	100.0 ± 6.9

Conditions for migration assay are described in Figure 22. Subclones were compared as a percentage of total E2 or E3 invaded cells. Error represents percent SEM from 3 separate experiments with cells plated in duplicate. * Indicates p value < 0.05 using Student's t-test.

Discussion

Synthesis and secretion of PSA from DU-145 cells

The DU-145 cell line was used as a model to show the direct effects of PSA expression in a PCa derived cell void of natural PSA production. It is known that the androgen-independent DU-145 cell line does not produce PSA or its encoding mRNA[103]. A goal of this study was to produce two distinct DU-145 subclones: one that produced full length ppPSA to be secreted as a zymogen, and one clone that produced prePSA to be secreted as active PSA. DU-145 cells were transfected with plasmids containing either the full-length ppPSA cDNA or a truncation mutant lacking the 7 amino acid regulatory "pro" region, prePSA.

The first attempt at stable clone formation was done using plasmids encoding PSA under the control of the CMV promoter, which induces high expression of the gene under its control. Upon electroporating DU-145 cells with modpSTHMppPSA, two clones (D-ppPSA-1 and DU-ppPSA-2) were established that expressed PSA, although this expression turned out to be transient. No stable clones were established using modpSTHMprePSA, yet transient expression from modpSTHMprePSA was seen using a lipofection method of transfection. This showed that the modpSTHMprePSA plasmid was indeed able to express PSA in DU-145 cells. It is possible that stable clones were not able to be isolated because the high levels of PSA expressed by these plasmids were unhealthy for the cells. Colonies initially growing from stable transfections with these plasmids often had numerous dead cells within the colony as compared to the vector control. Therefore, a selection for an inactivation of the CMV-promoted PSA may have been occurring in tandem with selection for the hygromycin resistance gene. This could be the reason why the D-ppPSA-1 and DU-ppPSA-2 clones soon lost expression of PSA. On the other hand, gene silencing after transfection is common, and the lack of stable PSA expression may also be due to a more generic mechanism, such as promoter methylation or inactivation of the region in which the PSA gene was inserted into. Denmeade et al. have transfected DU-145 cells with a vector able to produce full length PSA using a CMV promoter[104], so it would seem probable that stable transfectants using modpSTHMppPSA would be feasible under optimal conditions. However, the number of passages that DU-145 cells were able to express PSA for was not published, so it is possible that the clones used in those experiments also lost PSA expression over time. Although production of ppPSA at higher levels was most likely not toxic to the DU-145 cells, prePSA may have been, as even short term stable clones were not observed.

To circumvent the possible toxicity of PSA production in DU-145 cells, an inducible expression system was used to create DU-145 subclones with PSA expression under the control of the insect hormone analogue PonA. DU-pERV3 C3 cells were selected since their stable expression of the PonA inducible transcription initiator VgEcR encoded by the pERV3 plasmid showed the highest levels of induction. The DU-pERV3 C3 clone was subsequently transfected with each of the pEGSHppPSA and pEGSHprePSA plasmids to obtain subclones with the ability to produce ppPSA and prePSA, respectively. This resulted in DU-pERV3C3ppPSA cells that secreted 0.119 – 0.461 ng PSA/ml/10^5cells/day and DU-pERV3C3prePSA cells that secreted 0.034 – 0.218 ng PSA/ml/10^5cells/day when induced with 10 μM PonA. The PSA secreted from the DU-pERV3C3ppPSA subclones was in the range of 1.4 – 5.4% of LNCaP cell PSA production and the PSA secreted from the DU-pERV3C3prePSA subclones was in the range of 0.4 – 2.5% of LNCaP cell PSA production.

The level of PSA induction using 10 μM PonA ranged from 132.5 – 273.8% for DU-pERV3C3ppPSA subclones and from 207.6 – 280.2% for DU-pERV3C3prePSA subclones above those of controls. Of interest is the fact that the level of PSA production was relatively high in the absence of PonA. Ecdysone inducible systems are known for their lack of "leakiness" as compared to other inducible systems[105], so the control levels of PSA were expected to be much lower. As well, induction of the transiently transfected pEGSH-Luc plasmid in DU-pERV3 C3 cells showed high levels of relative induction by 10 μM PonA compared to control. This is similar to what others see using this same plasmid system in other mammalian cells[106]. Furthermore, upon transient transfection of DU-pERV3 C3 ppPSA6 cells – which showed 237% secretion of PSA when induced with 10 μM PonA – with pEGSH-Luc, an induction level in luciferase activity of 2849% was seen (data not shown). This suggests that the VgEcR transcriptional initiator is operational in the ppPSA6 cells, but that the level of induction from the pEGSHppPSA promoter was not as high as from the pEGSH-Luc promoter. This lack of strong induction of PSA could be due to a number of factors. For one, the pEGSH-Luc plasmid was transiently transfected for the luciferase assay, whereas the pEGSHppPSA and pEGSHprePSA plasmids were stably transfected. There may be a difference in the ability of VgEcR to activate the free pEGSH-Luc plasmid in the cytoplasm as compared to the PSA genes that were integrated into the genome. Furthermore, the induction with PonA of the pEGSH-luc plasmid in the luciferase assay was done in serum-supplemented medium for 24 hours post transfection, whereas the induction of PSA was done over 4 –

5 days in SF medium. The longer time was used to accumulate enough PSA in the CM for Western blot analysis, and SF medium was used because serum-supplemented medium contains too high a concentration of proteins that would "obstruct" the 10 kDa filter. As well, possible inhibitors from the FBS could bind and sequester PSA. Also, VgEcR requires natively expressed co-repressors to stop basal level transcription of the VgEcR controlled genes in the absence of the inducer, PonA. It is possible that the co-repressors needed for VgEcR assisted repression of the PSA gene constructs were not produced in DU-145 cells in the absence of serum. Therefore, over 4 – 5 days, the expression may have become "leaky" and the level of induction reduced. Similarly, it is also possible that co-activators needed for VgEcR promoted activation in the presence of PonA were not produced in DU-145 cells in the absence of serum, leading to a decrease in transcriptional activation. Finally, 10 μM PonA was added only once at the beginning of the 4 – 5 day induction period, and it is unknown if components of the DU-145 medium or factors secreted by DU-145 cells have the ability to degrade PonA over time. Thus, a higher level of PSA induction and expression using PonA may be feasible by varying experimental conditions, such as induction time, medium used, and the number of times PonA is added to the medium.

Molecular forms and enzymatic activity of PSA from different sources

In order to accurately understand the effects of PSA on PCa cell lines, the molecular forms of PSA in question should be understood. Two commercial preparations of PSA isolated from human seminal plasma, AG650 and ActPSA, were used to determine the effects of exogenous PSA on PCa cell lines. Each preparation presented a major band at

29 kDa when subjected to Western blot analysis, however neither preparation appeared as a single band. This 29 kDa band most likely represents the enzymatically active form of PSA, as ~80% of PSA isolated from human seminal plasma is found in the enzymatically active form[71]. The prostate cancer cell line LNCaP is an androgen-dependant cell line that endogenously produces PSA. Western blot analysis of CM from this cell line revealed a single band for PSA at 29 kDa. This most likely represents a variety of PSA forms with very similar molecular weight, including active PSA and inactive forms due to improper N-terminal processing[107]. These include the under-processed PSA forms with 2 and 4 N-terminal amino acids from the pro-region remaining attached to the mature PSA chain, yielding an inactive enzyme[107]. Active PSA often runs on an SDS-PAGE at 33 kDa under reducing conditions, whereas under the non-reducing conditions – as used in these experiments – mature PSA runs at a lower molecular weight closer to 29 kDa[72]. The extra bands present for each AG650 and ActPSA most likely represented different forms of PSA, including internally cleaved, zymogen, complexed with inhibitors, and/or altered glycosylation. In this study, each band was recognized by the PSA specific monoclonal antibody A67-B/E3. This antibody has been shown to be highly specific for PSA, and does not cross react with hk2[108], the most common co-purification contaminant with PSA[109]. AG650 included a high molecular weight band (> 107 kDa) as well, which most likely represented an inhibitor-bound PSA, such as a complex with ACT. We assume that although each AG650 and ActPSA contained enzymatically active PSA, they also contained PSA in other forms as well as possibly other unidentified contaminants, such as hK2.

Western blotting of CM from the DU-pERV3 C3 ppPSA subclones presented a band at 29 kDa and PSA bands from DU-pERV3 C3 prePSA subclones presented a band at 28 kDa. This difference corresponds well with the deletion of the 0.8 kDa "pro" APLILSR sequence in the prePSA gene. Although this would suggest that the major form of PSA found in AG650 and ActPSA was proPSA, this is not the case, as total protein level can affect the migration of proteins in an SDS-PAGE. Upon addition of ActPSA to a lane containing DU-pERV3 C3 ppPSA CM, the PSA band from the ppPSA subclone was present slightly higher than the 29 kDa ActPSA band, but below the 33 kDa ActPSA band (data not shown). Furthermore, upon addition of ActPSA to a lane containing DU-pERV3 C3 prePSA CM, the PSA band from the prePSA subclone was present at nearly the exact same weight as the 29 kDa ActPSA band (data not shown).

Each the AG650 and ActPSA isolates showed chymotrypsin-like enzymatic activity indicative of PSA by hydrolysis of the substrate S-2586. The activity of each form was also not affected to an appreciable degree by the chymotrypsin inhibitor TPCK. Enzymatic activity of concentrated CM from the DU-pERV3 C3 ppPSA, DU-pERV3 C3 prePSA and DU-pERV3 C3 EGSH subclones on the substrate S-2586 was measured to test for the presence of PSA activity. Unfortunately, the CM from each subclone showed activity on the S-2586 substrate that was not abrogated by the chymotrypsin inhibitor TPCK, regardless of the presence of PSA. As well, the concentrations of PSA secreted by each subclone were below the limit of detection in this assay. Thus, the activity of PSA secreted from these DU-145 subclones could not be determined.

For enzymatic activity of PSA, it is critical that the cleavage site be exactly at the initial isoleucine of mature PSA, as cleavage on either side of this amino acid results in an inactive enzyme[110]. This is most likely due to stabilization of the substrate binding pocket by the N-terminal isoleucine by interaction with an internal aspartic acid[111]. This inhibitory "pro" region likely blocks this interaction. The objective of using pEGSHppPSA was to obtain an enzymatically inactive form of PSA, whereas pEGSHprePSA was created to allow cells to secrete active PSA. It was found by Denmeade et al. that PSA produced from DU-145 cells using full-length PSA cDNA under a CMV promoter does not show enzymatic activity[104]. This was thought to be due to the lack of co-secretion of an activating enzyme such as hK2[73]. It is therefore likely that the PSA produced from DU-pERV3 C3 ppPSA subclones was also in an inactive form, as the same coding sequence for PSA was used in the same cell line. Although the "pro" region was deleted in prePSA, it is possible that this form of PSA was not properly processed into mature PSA. Studies have shown that deletion of a "pro" regulatory region after a "pre" secretory sequence can lead to improper cleavage[112]. However, since the N-terminus of the mature PSA sequence is an aliphatic amino acid (isoleucine) similar to the beginning of the "pro" sequence (alanine), it is plausible that correct cleavage takes place.

Future experiments to test each form of PSA for enzymatic activity could include zymography with a more specific substrate to PSA, such as semenogelin I or II. Also, reducing SDS-PAGE would show if the PSA forms produced by the cells are whole or if they are fragmented and being held together by disulphide bridges, which is not always apparent under non-reducing conditions[113]. Finally, N-terminal sequencing would show the percentage of PSA molecules with the N-terminal isoleucine needed for activity.

The effect of different forms of PSA on prostate cancer cell growth

The effects of PSA on PCa cell growth were tested over a period of five days. Firstly, two commercially obtained sources of PSA isolated from human seminal plasma (AG650 and ActPSA) were added to the serum-supplemented medium of DU-145 and LNCaP cells to test the effects of PSA on PCa cell growth. No statistically significant effect of either exogenous AG650 or ActPSA – used at concentrations from 0.5 – 2 μg/ml – was seen on the growth of the DU-145 or LNCaP cell lines. This concentration range was chosen because it was calculated that 5×10^5 LNCaP cells secrete 2.2 ± 0.9 μg/ml over a period of 5 days into SF medium. Although ActPSA decreased the PDT of DU-145 cells slightly, these results were not statistically significant. In this study, the PDT of DU-145 cells seems to be on the decline with increasing concentrations of ActPSA, as the results approach significance at 2 μg/ml ($p = 0.07$).

Secondly, differences in the growth properties of cells secreting different forms of PSA were examined. Similar to the experiments using exogenous PSA sources, there was no statistically significant difference in cell growth between the DU-pERV3 C3 ppPSA, DU-pERV3 C3 prePSA, or vector control cells. Although the PDT of the pp6 and pp9 subclones was higher than that of the vector controls, the PDT of the pp13 subclone was not. As well, the differences in the PDT between the p6/pp9 subclones and vector controls were not significant, due to relatively large variance. This lack of PSA effect on PCa cell growth corresponds with the results of Denmeade et al., who show that full length ppPSA expressed in DU-145 cells does not change their growth properties[104]. Full length ppPSA expression through genetic modification also gave no difference in the growth properties of another androgen-independent PCa cell line, PC-3, as shown by two separate groups[47,104]. The PSA from the CM of each the DU-145 and PC-3 cells has been shown to be inactive[104]. It is notable that prePSA produced from the DU-pERV3 C3 prePSA cells also did not change the PDT, indicating a lack of toxicity of prePSA at the levels secreted.

It is possible that the lack of effects on PCa cell growth may be due to PSA inhibitors in the growth medium or secreted by the cells. The growth medium used for each cell type was supplemented with 10% FBS, which contains inhibitors for PSA, notably ~300 μg/ml α–Mac and ~40 μg/ml ACT[114]. However, Western blot analysis of medium conditioned for 5 days – with various concentrations of AG650 or ActPSA – by either DU-145 or LNCaP medium showed a band representing PSA at 29 kDa at intensity similar to the same amount of pure PSA sample (data not shown). This indicates that PSA was not completely complexed with either of these major inhibitors in the serum-supplemented medium, as PSA forms SDS-PAGE stable complexes with both α–Mac and ACT[82]. As well, Corey et al. show that LNCaP cells secrete PSA in the free form into 10% FBS-supplemented medium, including the third of the PSA that is secreted in the active form[103]. Furthermore, Denmeade et al. show a similar lack of growth changes upon addition of exogenous human seminal purified PSA at concentrations from 0.1 – 1 μg/ml to both DU-145 and PC-3 cells[104], using a growth supplemented SF medium.

Looking at the results from this study as well as those done by others, it seems that PSA has no effect on the growth of PCa cells. However, it has been shown that PSA has the ability to indirectly enhance the growth of osteoblasts[88], as well as increase prostate stromal cell growth[102]. PSA from seminal plasma added to osteoblasts in culture, at concentrations as low as 25 ng/ml, is able to stimulate cell growth, presumably through activation of TGF-β[88]. Similarly, enzymatically active exogenous PSA increases the growth of prostate stromal cells at concentration of 100 μg/ml[102], which is 50 times greater than the highest concentrations used in this study. It has also been shown that the enzymatic activity of PSA is responsible for the increase in growth, as the addition of inhibitory levels of Zn^{+2} abrogate the effects[102]. As well, they show that a further increase in growth of these cells can be caused by an enzymatic release of IGF-I from IGFBP-3, mediated by PSA[102]. In a separate study, Wilding et al. show that the growth of DU-145 cells is reduced by 25% using TGF-β at concentrations of 200 pM, and that this growth-reducing effect is lost after a period of 5 days[115]. It would then reason that mature PSA activating latent TGF-β in the growth medium could decrease DU-145 cell growth. However, the DU-pERV3 C3 prePSA cells examined in this study may not have been affected by TGF-β growth reducing effects caused by this mechanism. Therefore, the cells would have been producing active PSA for a period of much longer than a week, presumably increasing the amount of active TGF-β, which the cells would become acclimatized to over time. LNCaP cells do not express either TGF-β RI or RII – due to promoter methylation[116] – and would not be affected adversely by an increase in TGF-β concentration[117]. As well, it is plausible that active PSA may have a positive effect on PCa cell growth, as it has been shown that active PSA can degrade both IGFBP-3 and IGFBP-4[87] so that IGF-I is freed to interact with surface receptors. It has been shown that LNCaP cell growth is unaffected by IGF-I, even though these cells secrete this growth factor[117]. DU-145 cells do not produce IGF-I, however they do produce IGFBP-2/-3/-4/-6[118]. Also, DU-145 cells have also been shown to increase their DNA synthesis upon addition of IGF-I to the growth medium[15]. Therefore, it is reasonable to assume that if active PSA were to cleave both IGFBP-3 and IGFBP-4, releasing IGF-I from the FBS, the growth of DU-145 cells could increase. It is possible that PSA can have a positive or negative effect on DU-145 cell growth through IGF-I and TGF-β respectively. The concentrations of exogenous PSA possibly need to be higher.

The effect of different forms of PSA on *in vitro* prostate cancer cell migration and invasion

To test the migratory changes induced by PSA, DU-145 and LNCaP cells were allowed to traverse a transwell membrane. Invasive changes induced by PSA were studied using the same transwell membrane coated with a simulated basement membrane. No statistically significant change in migration or invasion was seen for the DU-145 cells upon addition of AG650 or ActPSA at concentrations from 0.5 – 5 μg/ml. Notably, there was a consistent (if not statistically significant) decrease in the invasion of DU-145 cells through 0.05 mg/ml BME using both 0.5 or 10% FBS as a chemoattractant, with concentrations of ActPSA ranging from 0.5 – 5 μg/ml. A decrease in invasion was not seen when using AG650 PSA, however this preparation of PSA was only stated to be 90% pure by the manufacturer, so it is possible that any effects caused by PSA may have been counteracted by unknown contaminants. Unfortunately, the invasion and migration of LNCaP cells occurred at levels too low to be accurately quantified using the experimental parameters employed in this study. PSA-producing subclones derived from DU-145 cells were also assayed for migration and invasion. The DU-pERV3 C3 ppPSA subclones showed a moderate increase in invasion and a slight increase in migration over the vector control DU-pERV3 C3 pEGSH cells. Conversely, the DU-pERV3 C3 prePSA cells showed a statistically significant decrease in both migration and invasion compared to the vector control cells. Interestingly, DU-pERV3 C3 ppPSA subclones expressing higher levels of ppPSA (i.e. pp6) did not show consistently increased invasion or migration over subclones with lower ppPSA expression (i.e. pp9). Similarly, DU-pERV3 C3 prePSA subclones expressing higher levels of prePSA (i.e. pre7) did not show consistently increased invasion or migration over prePSA subclones with lower ppPSA expression (i.e. pre2). As well, no trend in invasion or migration was seen through increasing the level of PSA produced by PonA induction. Therefore, what seems to be changing the invasion of the cells appears to be a phenotype change, since differences in cellular invasion and migration do not correspond directly with the amount of PSA produced, only the form.

The results found in this study are similar to those found by Veveris-Lowe et al.[47]. They genetically modified the androgen-independent PC-3 cell line with the ability to produce ppPSA and these cells show an increase in migration but not invasion[47]. This increase in migration was reasoned to be caused by an EMT, as the cells expressed lower E-cadherin levels and higher vimentin levels than the vector controls[119]. Although the activity of PSA has not been determined in those experiments, Denmeade et al. found that PSA secreted by PC-3 cells (genetically modified to produce ppPSA) is inactive[104]. Thus, it is likely that the form of PSA produced in the Veveris-Lowe experiments is also inactive. Since inactive PSA is produced by PC-3 cells, and the cells undergo an EMT, there seems to be an effect of PSA in the PC-3 cells that is not due to its proteolytic activity. This is interesting, as these results are similar to what was seen for the DUpERV3 C3 ppPSA cells in this study, which were also transfected with a ppPSA-producing vector. However, an increase in invasion was also seen for the DU-pERV3 C3 ppPSA cells as compared to controls, and a less pronounced increase in migration. Both native DU-145 and PC-3 cells express vimentin[120], however, vimentin expression is upregulated in PC-3 cells transfected with ppPSA[47]. As well, E-cadherin is expressed in both cell types, and expression of this cell-cell adhesion protein is almost completely lost in PC-3 cells transfected with ppPSA[47]. To assess if there was an EMT in the DU-pERV3 C3 ppPSA subclones, it would be useful to determine the levels of vimentin and E-cadherin. The increase in cellular migration and invasion by the ppPSA expressing cells in this study further supports the theory that PSA causes cellular effects independent of proteolytic activity.

The data obtained in this study also suggest that enzymatically active PSA decreased cellular invasion, both from an exogenous source, and – more prominently – when prePSA was produced by the cells. This is the opposite to what was found by others in previous experiments testing invasion of LNCaP cells. Although the invasion and migration of LNCaP cells was not quantifiable in this study, it has been found by Webber et al. that if the activity of PSA is blocked using monoclonal antibodies against the active site, LNCaP cells show a decreased invasion[45]. Similar results have been seen by Ishii et al., who used antibodies against active PSA or the addition of inhibitory levels of Zn^{+2}, and show decreased *in vitro* invasiveness of LNCaP cells[46]. Yet under the same conditions, PC-3 cells – which do not produce PSA – do not show a change in invasion[46]. Each of these examples points to active PSA contributing to the invasive potential of LNCaP cells.

It is possible that some of the increasing effects on LNCaP cell invasion thought to be due to PSA are actually due to hK2. hK2 has the ability to activate the zymogen forms of both PSA, uPA and can inactivate PAI-1[121]. As well, hK2 can degrade fibronectin and IGFBP-2/-3/-4/-5[44]. At first, some of the enzymatic activities of hK2 were actually thought to be contributed by PSA, however, Frenette et al. show that it is actually hK2 which is responsible for the activation of uPA[109]. This is due to the fact that hK2 and PSA (hK3) are about 80% homologous to each other on the amino acid level[121], and hK2 is easily (and accidentally) co-purified with PSA[109]. Ishii et al. admit in their paper that the decrease in LNCaP invasion might actually be due to hK2 and not PSA, as Zn^{+2} inhibits both PSA and hK2, and the antibody they used against PSA might also cross react with hK2[46]. However, it is unlikely that the same is true for the LNCaP invasion experiments done by Webber et al., as they used the anti-PSA antibody ER-PR8 (M 0750) to block invasion[45]. When studied in an international panel analyzing numerous anti-PSA antibodies for epitope localization, enzymatic activity inhibition, and cross-reactivity, ER-PR8 did not show cross reactivity with hK2, and inhibited PSA enzymatic activity by ~50%[108]. Nevertheless, this does not necessarily mean that it is the enzymatic activity of PSA that is responsible for the increase in invasion, as this antibody may also block protein-receptor interactions of PSA through steric hindrance. This is a plausible explanation, as LNCaP cells have been shown to mainly secrete enzymatically inactive forms of PSA, constituting at least 2/3 of the total PSA in LNCaP CM[103,107,122]. The effects of PSA upregulation or the addition of exogenous PSA on LNCaP invasion and migration has not been studied. Since decreasing the activity of PSA lowers the invasive potential of LNCaP calls, it would be interesting to see if exogenous active PSA would increase LNCaP cell invasion. This would help prove that enzymatically active PSA does assist in the invasion of LNCaP cells.

Unexpectedly, when using 0.5% FBS, the migration of all cells tested was often similar to or only slightly less than the invasion. This difference may have been due to the low adherence of the cells to the cell-transwell membrane under the low FBS conditions. When seeding DU-145 cells in cell culture plates using 0.5% FBS-supplemented medium, they take longer to adhere than when using 10% FBS-supplemented medium (data not shown). It is likely that DU-145 cells (and subclones) more readily adhere to the BME coating than to the transwell membrane, as BME simulates a natural substrate for epithelial cells. Although the cells must first degrade the BME before migrating through the transwell membrane in the invasion assay, this may happen at a more rapid pace than cells adhering to the transwell membranes in the absence of BME in the migration assays. Furthermore, as the cells degrade the BME, chemotactic fragments may be revealed from cryptic sites on BME molecules, further increasing the invasive potential of the invasive cells over that of those migrating through the membrane alone.

The reasons why prePSA produced by the DU-pERV3 C3 prePSA cells would decrease both invasion and migration to such a striking degree is less clear, and there are numerous possible rationales. Firstly, PSA has been shown to increase the invasion of LNCaP cells, not DU-145 cells. LNCaP cells are androgen-sensitive, whereas DU-145 cells are androgen-independent, so it is likely that if there are any cellular effects due to PSA activity on invasion or migration that they may have different effects on each cell type. Furthermore, the experiments in this study used FBS-supplemented medium as a chemoattractant, yet the previous studies testing LNCaP invasion used NIH-3T3 CM[45] and SF medium (with the BM itself presumably acting as the chemoattractant)[46]. This could lead to different factors being activated or degraded by active PSA. Since both the invasion and migration of DU-pERV3 C3 prePSA cells was decreased compared to controls, it is unlikely that the degradation of BM components mediated by active PSA had much effect on decreasing cellular invasion of this cell type. It seems probable from these results that there is a competing effect between the actions of proPSA and mature PSA on cancer invasion, with proPSA having receptor-mediated effects and mature PSA having enzymatic effects. As opposite effects were seen from the ppPSA and prePSA producing cells, it seems likely that there is some proteolytic activity that causes the large differences in invasion and migration. Such activity could include the cleavage or proteinase-activated receptors (PARs) being responsible for the effects mediated by prePSA[44], however this is just speculation. Finally, on the other hand, there is the possibility that the PSA secreted by DU-pERV3 C3 prePSA cells was not proteolytically active, and that the decrease in migration and invasion was due to protein-protein interactions. In contrast, the PSA produced by DU-pERV3 C3 ppPSA cells may become activated in the invasion assays by some factor within the BME. It has been shown that reconstitution of Matrigel (a similar *in vitro* BM simulate to BME) can activate plasminogen to plasmin[123], so it is reasonable to assume there may be an activated protease in the BME that could proteolytically activate ppPSA.

There are multiple steps that can be taken to further clarify the effects of the different forms of PSA through the use of the DU-pERV3 C3 ppPSA and DU-pERV3 C3 prePSA subclones. For one, the invasion and migration time could be increased to 48 hours to allow the possibility of more significant differences between the clones, as well as allow for quantifiable levels of invasion/migration for the LNCaP cell line. The original 24 hours was chosen because the number of DU-145 cells migrating towards 10% FBS was above the range of accurate quantification at 24 hours, and it was expected that a longer time period of invasion would show the same results. With the concentration of FBS decreased to 0.5%, the migration was significantly reduced, approximately to the level of invasion. Furthermore, since PSA is able to affect the growth of prostate stromal cells[102], this might have an affect on *in vivo* invasion of cancer cells, as PSA might stimulate the release of chemotactic factors from prostate stromal cells. It would be interesting to plate DU-pERV3 C3 ppPSA and DU-pERV3 C3 prePSA cells in the top of invasion chamber, with prostate stromal cells in the bottom to determine effects more similar to *in vivo* conditions. Finally, the secreted forms of PSA in the medium of DU-pERV3 C3 ppPSA and DU-pERV3 C3 prePSA cells still need to be determined. CM from each of these cell types could also be used in invasion and migration assays with the native DU-145 cells to further prove the effects of each PSA type. There was an obvious difference in invasion seen between prePSA and ppPSA subclones as well as empty vector control cells, showing that prePSA had some effect on the cancer cells different than seen from the expression of full length ppPSA.

Conclusion

The main goal of this study was to determine the effect that different forms of PSA had on prostate cancer cellular invasion. To a point, this was accomplished. The experiments in this study show that exogenous active PSA was able to decrease the invasion of DU-145 cells. It was also found that DU-145 subclones genetically modified to produce ppPSA had increased invasive potential, while DU-145 subclones genetically modified to produce prePSA had greatly decreased invasive potential. Although the form of PSA secreted from the prePSA producing cells was not fully characterized, it is likely that this was an active form of PSA. The cells producing prePSA also showed a large decrease in migration, and this most likely contributed heavily to their lack of invasiveness.

We conclude here that active PSA decreased the invasive potential of DU-145 prostate cancer cells, while the production of inactive PSA increases their invasive potential. This conclusion seems to conflict with the idea that active PSA increases invasion of prostate cancer cells, as found by others. However, most of the work done previously concerning PSA and invasion was on other prostate cancer cell lines, so it appears that the actions of PSA on prostate cancer cell invasion *in vitro* are not straightforward. The effect of PSA may be different for androgen-dependent prostate cancer cell lines than for androgen-independent cells.

To truly understand the effects that each form of PSA had on invasion, each form will have to be full characterized. If the ppPSA producing cells produce mainly or entirely inactive PSA and the prePSA producing cells produce mainly inactive PSA, these DU-145 subclones could prove important in differentiating any number of effects caused by zymogen PSA or the enzymatically active form. As well, *in vivo* studies introducing the ppPSA and prePSA-producing DU-145 subclones into mice would provide valuable insight into the effect of each PSA form on tumour invasion. Since PSA is used prevalently as a diagnostic tool, it would be useful to determine if active PSA benefits, hinders, or is not involved at all in tumour invasion.

References

1. Routh,J.C. & Leibovich,B.C. Adenocarcinoma of the prostate: epidemiological trends, screening, diagnosis, and surgical management of localized disease. *Mayo Clin. Proc.* **80**, 899-907 (2005).

2. Jemal,A. *et al.* Cancer statistics, 2006. *CA Cancer J. Clin.* **56**, 106-130 (2006).

3. Crawford,E.D. Epidemiology of prostate cancer. *Urology* **62**, 3-12 (2003).

4. Foster,C.S., Cornford,P., Forsyth,L., Djamgoz,M.B. & Ke,Y. The cellular and molecular basis of prostate cancer. *BJU. Int.* **83**, 171-194 (1999).

5. Arya,M. *et al.* The metastatic cascade in prostate cancer. *Surg. Oncol.* (2006).

6. Marandola,P. *et al.* Molecular biology and the staging of prostate cancer. *Ann. N. Y. Acad. Sci.* **1028**, 294-312 (2004).

7. Frick,J. & Aulitzky,W. Physiology of the prostate. *Infection* **19 Suppl 3**, S115-S118 (1991).

8. Ward,A.M., Catto,J.W. & Hamdy,F.C. Prostate specific antigen: biology, biochemistry and available commercial assays. *Ann. Clin. Biochem.* **38**, 633-651 (2001).

9. Lilja,H. Cell biology of semenogelin. *Andrologia* **22 Suppl 1**, 132-141 (1990).

10. Russell,P.J., Bennett,S. & Stricker,P. Growth factor involvement in progression of prostate cancer. *Clin. Chem.* **44**, 705-723 (1998).

11. Edwards,J. & Bartlett,J.M. The androgen receptor and signal-transduction pathways in hormone-refractory prostate cancer. Part 1: Modifications to the androgen receptor. *BJU. Int.* **95**, 1320-1326 (2005).

12. Pienta,K.J. & Smith,D.C. Advances in prostate cancer chemotherapy: a new era begins. *CA Cancer J. Clin.* **55**, 300-318 (2005).

13. Culig,Z., Klocker,H., Bartsch,G. & Hobisch,A. Androgen receptors in prostate cancer. *Endocr. Relat Cancer* **9**, 155-170 (2002).

14. Gioeli,D. Signal transduction in prostate cancer progression. *Clin. Sci. (Lond)* **108**, 293-308 (2005).

15. Culig,Z. *et al.* Regulation of prostatic growth and function by peptide growth factors. *Prostate* **28**, 392-405 (1996).

16. Erbersdobler,A., Augustin,H., Schlomm,T. & Henke,R.P. Prostate cancers in the transition zone: Part 1; pathological aspects. *BJU. Int.* **94**, 1221-1225 (2004).

17. McNeal,J.E. & Bostwick,D.G. Intraductal dysplasia: a premalignant lesion of the prostate. *Hum. Pathol.* **17**, 64-71 (1986).

18. Bostwick,D.G. Prostatic intraepithelial neoplasia (PIN): current concepts. *J. Cell Biochem. Suppl* **16H**, 10-19 (1992).

19. Dong,J.T. Prevalent mutations in prostate cancer. *J. Cell Biochem.* **97**, 433-447 (2006).

20. Bonaccorsi,L. *et al.* Signaling mechanisms that mediate invasion in prostate cancer cells. *Ann. N. Y. Acad. Sci.* **1028**, 283-288 (2004).

21. Edwards,J. & Bartlett,J.M. The androgen receptor and signal-transduction pathways in hormone-refractory prostate cancer. Part 2: Androgen-receptor cofactors and bypass pathways. *BJU. Int.* **95**, 1327-1335 (2005).

22. Thompson,I.M. *et al.* Prevalence of prostate cancer among men with a prostate-specific antigen level < or =4.0 ng per milliliter. *N. Engl. J. Med.* **350**, 2239-2246 (2004).

23. Wilt,T. Prostate cancer (non-metastatic). *Clin. Evid.* 1023-1038 (2003).

24. Pisansky,T.M. External-beam radiotherapy for localized prostate cancer. *N. Engl. J. Med.* **355**, 1583-1591 (2006).

25. Zigrino,P., Loffek,S. & Mauch,C. Tumor-stroma interactions: their role in the control of tumor cell invasion. *Biochimie* **87**, 321-328 (2005).

26. Sahai,E. Mechanisms of cancer cell invasion. *Curr. Opin. Genet. Dev.* **15**, 87-96 (2005).

27. Geho,D.H., Bandle,R.W., Clair,T. & Liotta,L.A. Physiological mechanisms of tumor-cell invasion and migration. *Physiology. (Bethesda.)* **20**, 194-200 (2005).

28. Mueller,M.M. & Fusenig,N.E. Friends or foes - bipolar effects of the tumour stroma in cancer. *Nat. Rev. Cancer* **4**, 839-849 (2004).

29. Tuxhorn,J.A., Ayala,G.E. & Rowley,D.R. Reactive stroma in prostate cancer progression. *J. Urol.* **166**, 2472-2483 (2001).

30. Stewart,D.A., Cooper,C.R. & Sikes,R.A. Changes in extracellular matrix (ECM) and ECM-associated proteins in the metastatic progression of prostate cancer. *Reprod. Biol. Endocrinol.* **2**, 2 (2004).

31. Lipponen,P. *et al.* High stromal hyaluronan level is associated with poor differentiation and metastasis in prostate cancer. *Eur. J. Cancer* **37**, 849-856 (2001).

32. Nagle,R.B. Role of the extracellular matrix in prostate carcinogenesis. *J. Cell Biochem.* **91**, 36-40 (2004).

33. Knox,J.D. *et al.* Differential expression of extracellular matrix molecules and the alpha 6-integrins in the normal and neoplastic prostate. *Am. J. Pathol.* **145**, 167-174 (1994).

34. Duffy,M.J. The urokinase plasminogen activator system: role in malignancy. *Curr. Pharm. Des* **10**, 39-49 (2004).

35. Duffy,M.J. & Duggan,C. The urokinase plasminogen activator system: a rich source of tumour markers for the individualised management of patients with cancer. *Clin. Biochem.* **37**, 541-548 (2004).

36. Festuccia,C. *et al.* Plasminogen activator system modulates invasive capacity and proliferation in prostatic tumor cells. *Clin. Exp. Metastasis* **16**, 513-528 (1998).

37. Hojilla,C.V., Mohammed,F.F. & Khokha,R. Matrix metalloproteinases and their tissue inhibitors direct cell fate during cancer development. *Br. J. Cancer* **89**, 1817-1821 (2003).

38. Vihinen,P. & Kahari,V.M. Matrix metalloproteinases in cancer: prognostic markers and therapeutic targets. *Int. J. Cancer* **99**, 157-166 (2002).

39. Westermarck,J. & Kahari,V.M. Regulation of matrix metalloproteinase expression in tumor invasion. *FASEB J.* **13**, 781-792 (1999).

40. Nagase,H. & Woessner,J.F., Jr. Matrix metalloproteinases. *J. Biol. Chem.* **274**, 21491-21494 (1999).

41. Egeblad,M. & Werb,Z. New functions for the matrix metalloproteinases in cancer progression. *Nat. Rev. Cancer* **2**, 161-174 (2002).

42. Morgia,G. *et al.* Matrix metalloproteinases as diagnostic (MMP-13) and prognostic (MMP-2, MMP-9) markers of prostate cancer. *Urol. Res.* **33**, 44-50 (2005).

43. Sheng,S. The urokinase-type plasminogen activator system in prostate cancer metastasis. *Cancer Metastasis Rev.* **20**, 287-296 (2001).

44. Borgono,C.A. & Diamandis,E.P. The emerging roles of human tissue kallikreins in cancer. *Nat. Rev. Cancer* **4**, 876-890 (2004).

45. Webber,M.M., Waghray,A. & Bello,D. Prostate-specific antigen, a serine protease, facilitates human prostate cancer cell invasion. *Clin. Cancer Res.* **1**, 1089-1094 (1995).

46. Ishii,K. *et al.* Evidence that the prostate-specific antigen (PSA)/Zn2+ axis may play a role in human prostate cancer cell invasion. *Cancer Lett.* **207**, 79-87 (2004).

47. Veveris-Lowe,T.L. *et al.* Kallikrein 4 (hK4) and prostate-specific antigen (PSA) are associated with the loss of E-cadherin and an epithelial-mesenchymal transition (EMT)-like effect in prostate cancer cells. *Endocr. Relat Cancer* **12**, 631-643 (2005).

48. Yamazaki,D., Kurisu,S. & Takenawa,T. Regulation of cancer cell motility through actin reorganization. *Cancer Sci.* **96**, 379-386 (2005).

49. Slack-Davis,J.K. & Parsons,J.T. Emerging views of integrin signaling: implications for prostate cancer. *J. Cell Biochem.* **91**, 41-46 (2004).

50. Engbring,J.A. & Kleinman,H.K. The basement membrane matrix in malignancy. *J. Pathol.* **200**, 465-470 (2003).

51. Banyard,J. & Zetter,B.R. The role of cell motility in prostate cancer. *Cancer Metastasis Rev.* **17**, 449-458 (1998).

52. Somlyo,A.V. *et al.* Rho-kinase inhibitor retards migration and in vivo dissemination of human prostate cancer cells. *Biochem. Biophys. Res. Commun.* **269**, 652-659 (2000).

53. Guo,W. & Giancotti,F.G. Integrin signalling during tumour progression. *Nat. Rev. Mol. Cell Biol.* **5**, 816-826 (2004).

54. Chung,L.W., Baseman,A., Assikis,V. & Zhau,H.E. Molecular insights into prostate cancer progression: the missing link of tumor microenvironment. *J. Urol.* **173**, 10-20 (2005).

55. Rosso,F., Giordano,A., Barbarisi,M. & Barbarisi,A. From cell-ECM interactions to tissue engineering. *J. Cell Physiol* **199**, 174-180 (2004).

56. Bissell,M.J. & Radisky,D. Putting tumours in context. *Nat. Rev. Cancer* **1**, 46-54 (2001).

57. Hagedorn,H.G., Bachmeier,B.E. & Nerlich,A.G. Synthesis and degradation of basement membranes and extracellular matrix and their regulation by TGF-beta in invasive carcinomas (Review). *Int. J. Oncol.* **18**, 669-681 (2001).

58. Micke,P. & Ostman,A. Tumour-stroma interaction: cancer-associated fibroblasts as novel targets in anti-cancer therapy? *Lung Cancer* **45 Suppl 2**, S163-S175 (2004).

59. Bello-DeOcampo,D. & Tindall,D.J. TGF-betal/Smad signaling in prostate cancer. *Curr. Drug Targets.* **4**, 197-207 (2003).

60. Wang,G.K. & Zhang,W. The signaling network of tumor invasion. *Histol. Histopathol.* **20**, 593-602 (2005).

61. Papatsoris,A.G., Karamouzis,M.V. & Papavassiliou,A.G. Novel insights into the implication of the IGF-1 network in prostate cancer. *Trends Mol. Med.* **11**, 52-55 (2005).

62. Weber,M.J. & Gioeli,D. Ras signaling in prostate cancer progression. *J. Cell Biochem.* **91**, 13-25 (2004).

63. Sensabaugh,G.F. Isolation and characterization of a semen-specific protein from human seminal plasma: a potential new marker for semen identification. *J. Forensic Sci.* **23**, 106-115 (1978).

64. Catalona,W.J. *et al.* Measurement of prostate-specific antigen in serum as a screening test for prostate cancer. *N. Engl. J. Med.* **324**, 1156-1161 (1991).

65. Belanger,A. *et al.* Molecular mass and carbohydrate structure of prostate specific antigen: studies for establishment of an international PSA standard. *Prostate* **27**, 187-197 (1995).

66. Balk,S.P., Ko,Y.J. & Bubley,G.J. Biology of prostate-specific antigen. *J. Clin. Oncol.* **21**, 383-391 (2003).

67. Lundwall,A. & Lilja,H. Molecular cloning of human prostate specific antigen cDNA. *FEBS Lett.* **214**, 317-322 (1987).

68. Lovgren,J., Valtonen-Andre,C., Marsal,K., Lilja,H. & Lundwall,A. Measurement of prostate-specific antigen and human glandular kallikrein 2 in different body fluids. *J. Androl* **20**, 348-355 (1999).

69. Lilja,H. Biology of prostate-specific antigen. *Urology* **62**, 27-33 (2003).

70. Wang,M.C. *et al.* Prostate antigen: a new potential marker for prostatic cancer. *Prostate* **2**, 89-96 (1981).

71. Zhang,W.M., Leinonen,J., Kalkkinen,N., Dowell,B. & Stenman,U.H. Purification and characterization of different molecular forms of prostate-specific antigen in human seminal fluid. *Clin. Chem.* **41**, 1567-1573 (1995).

72. Takayama,T.K., Fujikawa,K. & Davie,E.W. Characterization of the precursor of prostate-specific antigen. Activation by trypsin and by human glandular kallikrein. *J. Biol. Chem.* **272**, 21582-21588 (1997).

73. Lovgren,J., Rajakoski,K., Karp,M., Lundwall,A. & Lilja,H. Activation of the zymogen form of prostate-specific antigen by human glandular kallikrein 2. *Biochem. Biophys. Res. Commun.* **238**, 549-555 (1997).

74. Takayama,T.K., McMullen,B.A., Nelson,P.S., Matsumura,M. & Fujikawa,K. Characterization of hK4 (prostase), a prostate-specific serine protease: activation of the precursor of prostate specific antigen (pro-PSA) and single-chain urokinase-type plasminogen activator and degradation of prostatic acid phosphatase. *Biochemistry* **40**, 15341-15348 (2001).

75. Michael,I.P. *et al.* Human tissue kallikrein 5 is a member of a proteolytic cascade pathway involved in seminal clot liquefaction and potentially in prostate cancer progression. *J. Biol. Chem.* **281**, 12743-12750 (2006).

76. Takayama,T.K., Carter,C.A. & Deng,T. Activation of prostate-specific antigen precursor (pro-PSA) by prostin, a novel human prostatic serine protease identified by degenerate PCR. *Biochemistry* **40**, 1679-1687 (2001).

77. Carvalho,A.L. *et al.* Crystal structure of a prostate kallikrein isolated from stallion seminal plasma: a homologue of human PSA. *J. Mol. Biol.* **322**, 325-337 (2002).

78. Zaichick,V.Y., Sviridova,T.V. & Zaichick,S.V. Zinc in the human prostate gland: normal, hyperplastic and cancerous. *Int. Urol. Nephrol.* **29**, 565-574 (1997).

79. Costello,L.C. & Franklin,R.B. Novel role of zinc in the regulation of prostate citrate metabolism and its implications in prostate cancer. *Prostate* **35**, 285-296 (1998).

80. Christensson,A. & Lilja,H. Complex formation between protein C inhibitor and prostate-specific antigen in vitro and in human semen. *Eur. J. Biochem.* **220**, 45-53 (1994).

81. Zhang,W.M. *et al.* Characterization and immunological determination of the complex between prostate-specific antigen and alpha2-macroglobulin. *Clin. Chem.* **44**, 2471-2479 (1998).

82. Christensson,A., Laurell,C.B. & Lilja,H. Enzymatic activity of prostate-specific antigen and its reactions with extracellular serine proteinase inhibitors. *Eur. J. Biochem.* **194**, 755-763 (1990).

83. Watt,K.W., Lee,P.J., M'Timkulu,T., Chan,W.P. & Loor,R. Human prostate-specific antigen: structural and functional similarity with serine proteases. *Proc. Natl. Acad. Sci. U. S. A* **83**, 3166-3170 (1986).

84. Malm,J., Hellman,J., Magnusson,H., Laurell,C.B. & Lilja,H. Isolation and characterization of the major gel proteins in human semen, semenogelin I and semenogelin II. *Eur. J. Biochem.* **238**, 48-53 (1996).

85. Lilja,H., Oldbring,J., Rannevik,G. & Laurell,C.B. Seminal vesicle-secreted proteins and their reactions during gelation and liquefaction of human semen. *J. Clin. Invest* **80**, 281-285 (1987).

86. Cohen,P. *et al.* Prostate-specific antigen (PSA) is an insulin-like growth factor binding protein-3 protease found in seminal plasma. *J. Clin. Endocrinol. Metab* **75**, 1046-1053 (1992).

87. Rehault,S. *et al.* Insulin-like growth factor binding proteins (IGFBPs) as potential physiological substrates for human kallikreins hK2 and hK3. *Eur. J. Biochem.* **268**, 2960-2968 (2001).

88. Killian,C.S., Corral,D.A., Kawinski,E. & Constantine,R.I. Mitogenic response of osteoblast cells to prostate-specific antigen suggests an activation of latent TGF-beta and a proteolytic modulation of cell adhesion receptors. *Biochem. Biophys. Res. Commun.* **192**, 940-947 (1993).

89. Dallas,S.L. *et al.* Preferential production of latent transforming growth factor beta-2 by primary prostatic epithelial cells and its activation by prostate-specific antigen. *J. Cell Physiol* **202**, 361-370 (2005).

90. Iwamura,M., Hellman,J., Cockett,A.T., Lilja,H. & Gershagen,S. Alteration of the hormonal bioactivity of parathyroid hormone-related protein (PTHrP) as a result of limited proteolysis by prostate-specific antigen. *Urology* **48**, 317-325 (1996).

91. Ohlsson,K., Bjartell,A. & Lilja,H. Secretory leucocyte protease inhibitor in the male genital tract: PSA-induced proteolytic processing in human semen and tissue localization. *J. Androl* **16**, 64-74 (1995).

92. Heidtmann,H.H. *et al.* Generation of angiostatin-like fragments from plasminogen by prostate-specific antigen. *Br. J. Cancer* **81**, 1269-1273 (1999).

93. Sun,X.Y., Donald,S.P. & Phang,J.M. Testosterone and prostate specific antigen stimulate generation of reactive oxygen species in prostate cancer cells. *Carcinogenesis* **22**, 1775-1780 (2001).

94. Fortier,A.H. *et al.* Recombinant prostate specific antigen inhibits angiogenesis in vitro and in vivo. *Prostate* **56**, 212-219 (2003).

95. Tchetgen,M.B. & Oesterling,J.E. The effect of prostatitis, urinary retention, ejaculation, and ambulation on the serum prostate-specific antigen concentration. *Urol. Clin. North Am.* **24**, 283-291 (1997).

96. Nash,A.F. & Melezinek,I. The role of prostate specific antigen measurement in the detection and management of prostate cancer. *Endocr. Relat Cancer* **7**, 37-51 (2000).

97. Giannelli,G., Falk-Marzillier,J., Schiraldi,O., Stetler-Stevenson,W.G. & Quaranta,V. Induction of cell migration by matrix metalloprotease-2 cleavage of laminin-5. *Science* **277**, 225-228 (1997).

98. Bair,E.L. *et al.* Membrane type 1 matrix metalloprotease cleaves laminin-10 and promotes prostate cancer cell migration. *Neoplasia.* **7**, 380-389 (2005).

99. Grzmil,M., Hemmerlein,B., Thelen,P., Schweyer,S. & Burfeind,P. Blockade of the type I IGF receptor expression in human prostate cancer cells inhibits proliferation and invasion, up-regulates IGF binding protein-3, and suppresses MMP-2 expression. *J. Pathol.* **202**, 50-59 (2004).

100. Scorilas,A. *et al.* Serum human glandular kallikrein (hK2) and insulin-like growth factor 1 (IGF-1) improve the discrimination between prostate cancer and benign prostatic hyperplasia in combination with total and %free PSA. *Prostate* **54**, 220-229 (2003).

101. Habeck,L.L. *et al.* Expression, purification, and characterization of active recombinant prostate-specific antigen in Pichia pastoris (yeast). *Prostate* **46**, 298-306 (2001).

102. Sutkowski,D.M. *et al.* Growth regulation of prostatic stromal cells by prostate-specific antigen. *J. Natl. Cancer Inst.* **91**, 1663-1669 (1999).

103. Corey,E., Brown,L.G., Corey,M.J., Buhler,K.R. & Vessella,R.L. LNCaP produces both putative zymogen and inactive, free form of prostate-specific antigen. *Prostate* **35**, 135-143 (1998).

104. Denmeade,S.R., Litvinov,I., Sokoll,L.J., Lilja,H. & Isaacs,J.T. Prostate-specific antigen (PSA) protein does not affect growth of prostate cancer cells in vitro or prostate cancer xenografts in vivo. *Prostate* **56**, 45-53 (2003).

105. Meyer-Ficca,M.L. *et al.* Comparative analysis of inducible expression systems in transient transfection studies. *Anal. Biochem.* **334**, 9-19 (2004).

106. Wyborski,D.L., Bauer,J.C. & Vaillancourt,P. Bicistronic expression of ecdysone-inducible receptors in mammalian cells. *Biotechniques* **31**, 618-20, 622, 624 (2001).

107. Herrala,A., Kurkela,R., Vihinen,M., Kalkkinen,N. & Vihko,P. Androgen-sensitive human prostate cancer cells, LNCaP, produce both N-terminally mature and truncated prostate-specific antigen isoforms. *Eur. J. Biochem.* **255**, 329-335 (1998).

108. Stenman,U.H. *et al.* Summary report of the TD-3 workshop: characterization of 83 antibodies against prostate-specific antigen. *Tumour. Biol.* **20 Suppl 1**, 1-12 (1999).

109. Frenette,G., Tremblay,R.R., Lazure,C. & Dube,J.Y. Prostatic kallikrein hK2, but not prostate-specific antigen (hK3), activates single-chain urokinase-type plasminogen activator. *Int. J. Cancer* **71**, 897-899 (1997).

110. Denmeade,S.R., Sokoll,L.J., Chan,D.W., Khan,S.R. & Isaacs,J.T. Concentration of enzymatically active prostate-specific antigen (PSA) in the extracellular fluid of primary human prostate cancers and human prostate cancer xenograft models. *Prostate* **48**, 1-6 (2001).

111. Villoutreix,B.O., Getzoff,E.D. & Griffin,J.H. A structural model for the prostate disease marker, human prostate-specific antigen. *Protein Sci.* **3**, 2033-2044 (1994).

112. von Heijne,G. The signal peptide. *J. Membr. Biol.* **115**, 195-201 (1990).

113. Wu,P., Stenman,U.H., Pakkala,M., Narvanen,A. & Leinonen,J. Separation of enzymatically active and inactive prostate-specific antigen (PSA) by peptide affinity chromatography. *Prostate* **58**, 345-353 (2004).

114. Bernice M.Martin. Tissue culture techniques: an introduction. Birkhauser, Boston (1994).

115. Wilding,G., Zugmeier,G., Knabbe,C., Flanders,K. & Gelmann,E. Differential effects of transforming growth factor beta on human prostate cancer cells in vitro. *Mol. Cell Endocrinol.* **62**, 79-87 (1989).

116. Zhang,Q. *et al.* Insensitivity to transforming growth factor-beta results from promoter methylation of cognate receptors in human prostate cancer cells (LNCaP). *Mol. Endocrinol.* **19**, 2390-2399 (2005).

117. Webber,M.M., Bello,D. & Quader,S. Immortalized and tumorigenic adult human prostatic epithelial cell lines: characteristics and applications Part 2. Tumorigenic cell lines. *Prostate* **30**, 58-64 (1997).

118. Kimura,G. *et al.* Insulin-like growth factor (IGF) system components in human prostatic cancer cell-lines: LNCaP, DU145, and PC-3 cells. *Int. J. Urol.* **3**, 39-46 (1996).

119. Whitbread,A.K., Veveris-Lowe,T.L., Lawrence,M.G., Nicol,D.L. & Clements,J.A. The role of kallikrein-related peptidases in prostate cancer: potential involvement in an epithelial to mesenchymal transition. *Biol. Chem.* **387**, 707-714 (2006).

120. Singh,S. *et al.* Overexpression of vimentin: role in the invasive phenotype in an androgen-independent model of prostate cancer. *Cancer Res.* **63**, 2306-2311 (2003).

121. Hekim,C. *et al.* Novel peptide inhibitors of human kallikrein 2. *J. Biol. Chem.* **281**, 12555-12560 (2006).

122. Vaisanen,V. *et al.* Characterization and processing of prostate specific antigen (hK3) and human glandular kallikrein (hK2) secreted by LNCaP cells. *Prostate Cancer Prostatic. Dis.* **2**, 91-97 (1999).

123. Farina,A.R. *et al.* Identification of plasminogen in Matrigel and its activation by reconstitution of this basement membrane extract. *Biotechniques* **21**, 904-909 (1996).